TECHNICAL REPORT H-77-16

TSUNAMI-WAVE ELEVATION FREQUENCY OF OCCURRENCE FOR THE HAWAIIAN ISLANDS

by

James R. Houston, Robert D. Carver, Dennis G. Markle

Hydraulics Laboratory
U. S. Army Engineer Waterways Experiment Station
P. O. Box 631, Vicksburg, Miss. 39180

August 1977
Final Report

Approved For Public Release; Distribution Unlimited

Prepared for U. S. Army Engineer Division, Pacific Ocean
San Francisco, California 96558

Destroy this report when no longer needed. Do not return it to the originator.

REPORT DOCUMENTATION PAGE

READ INSTRUCTIONS BEFORE COMPLETING FORM

1. REPORT NUMBER: Technical Report H-77-16
2. GOVT ACCESSION NO.:
3. RECIPIENT'S CATALOG NUMBER:

4. TITLE (and Subtitle): TSUNAMI-WAVE ELEVATION FREQUENCY OF OCCURRENCE FOR THE HAWAIIAN ISLANDS

5. TYPE OF REPORT & PERIOD COVERED: Final report

6. PERFORMING ORG. REPORT NUMBER:

7. AUTHOR(s): James R. Houston, Robert D. Carver, Dennis G. Markle

8. CONTRACT OR GRANT NUMBER(s):

9. PERFORMING ORGANIZATION NAME AND ADDRESS: U. S. Army Engineer Waterways Experiment Station, Hydraulics Laboratory, P. O. Box 631, Vicksburg, Miss. 39180

10. PROGRAM ELEMENT, PROJECT, TASK AREA & WORK UNIT NUMBERS:

11. CONTROLLING OFFICE NAME AND ADDRESS: U. S. Army Engineer Division, Pacific Ocean, Building 230, Fort Shafter, Honolulu, Hawaii, APO San Francisco, Calif. 96558

12. REPORT DATE: August 1977

13. NUMBER OF PAGES: 109

14. MONITORING AGENCY NAME & ADDRESS (if different from Controlling Office):

15. SECURITY CLASS. (of this report): Unclassified

15a. DECLASSIFICATION/DOWNGRADING SCHEDULE:

16. DISTRIBUTION STATEMENT (of this Report)

Approved for public release; distribution unlimited.

17. DISTRIBUTION STATEMENT (of the abstract entered in Block 20, if different from Report)

18. SUPPLEMENTARY NOTES

19. KEY WORDS (Continue on reverse side if necessary and identify by block number)

Finite element method
Flood frequencies
Hawaiian Islands
Mathematical models
Tsunamis

20. ABSTRACT (Continue on reverse side if necessary and identify by block number)

An investigation was undertaken to establish frequency-of-occurrence curves for tsunami-wave elevations near the shoreline for the Hawaiian Islands. A hybrid finite element numerical model was used to supplement historical data in determining the ten largest tsunami elevations from 1837 to 1976 at locations along the coastline of the islands. The numerical model was verified by comparing tide gage recordings at various locations in the Hawaiian Islands during the 1960 and 1964 tsunamis with numerical model calculations.

(Continued)

20. ABSTRACT (Continued).

Frequency-of-occurrence curves were established using data from the ten largest tsunami-wave elevations along the Hawaiian coastline. Figures and the table presented in the report can be used to calculate tsunami elevations 200 ft shoreward of the coastline for frequencies of occurrence as high as 1-in-10 years for the entire coastline of the Hawaiian Islands (except the coast of the uninhabited U. S. Navy target island of Kahoolawe). Runup nearly equals tsunami elevation at the shoreline for some of the coastline of the islands, but not for areas where flooding is substantial. A recommendation is given for development of a method to calculate land flooding during a tsunami.

THE CONTENTS OF THIS REPORT ARE NOT TO BE USED FOR ADVERTISING, PUBLICATION, OR PROMOTIONAL PURPOSES. CITATION OF TRADE NAMES DOES NOT CONSTITUTE AN OFFICIAL ENDORSEMENT OR APPROVAL OF THE USE OF SUCH COMMERCIAL PRODUCTS.

PREFACE

Authority for the U. S. Army Engineer Waterways Experiment Station (WES) to conduct a tsunami-wave study for the State of Hawaii was contained in a letter from the U. S. Army Engineer Division, Pacific Ocean (POD), dated 27 February 1976.

This study was conducted from March to October 1976 in the Hydraulics Laboratory, WES, under the direction of Mr. H. B. Simmons, Chief of the Hydraulics Laboratory, Dr. R. W. Whalin, Chief of the Wave Dynamics Division (WDD), and Mr. D. D. Davidson, Chief of the Wave Research Branch. Messrs. J. R. Houston, R. D. Carver, and D. G. Markle (WDD) conducted the study. This report was prepared by Messrs. Houston and Carver.

Drs. H. S. Chen and C. C. Mei of the Massachusetts Institute of Technology provided documentation of the hybrid finite element computer program they developed and materials to aid in its use.

Mr. Ronald Pulfrey, Assistant Chief for Flood Plain Management, POD, assisted in formulating the scope of work and approach for the study through valuable ideas presented during a series of meetings with Mr. Houston from 28 to 30 October 1975. Mr. Pulfrey also helped maintain liaison between WES and POD during the course of the study.

Participants in a meeting convened in Honolulu, Hawaii, on 23 and 24 February 1977 for the purpose of discussing a draft of this report are listed below.

Corps of Engineers:
- R. W. Whalin, WES
- J. R. Houston, WES
- D. Jay, POD
- G. Kimura, POD
- R. Pulfrey (Retired), POD

Federal Insurance Administration:
- F. M. Crompton, Washington, D. C.
- L. Magura, Region IX, San Francisco, Calif.

State of Hawaii:
- A. Ching, Department of Land and Natural Resources
- R. Schank, Department of Defense, Civil Defense Division

Tsunami Specialists:

W. M. Adams, University of Hawaii, Hawaii Institute of Geophysics
C. L. Bretschneider, University of Hawaii, Chairman, Ocean Engineering Department
D. C. Cox, University of Hawaii, Environmental Center
H. Loomis, Joint Tsunami Research Effort
G. Pararas-Carayannis, International Tsunami Information Center

Directors of the WES during the investigation and the preparation and publication of this report were COL G. H. Hilt, CE, and COL J. L. Cannon, CE. Technical Director was Mr. F. R. Brown.

CONTENTS

	Page
PREFACE	2
CONVERSION FACTORS, U. S. CUSTOMARY TO METRIC (SI) AND METRIC (SI) TO U. S. CUSTOMARY UNITS OF MEASUREMENTS	5
PART I: INTRODUCTION	6
Background	6
Tsunamis in the Hawaiian Islands	7
Purpose of Study	9
PART II: APPROACH	11
Time Period Analyzed	11
Interpolation of Historical Data	17
Reconstruction of Historical Data	19
Frequency of Occurrence Distribution	22
PART III: NUMERICAL MODEL	25
Description	25
Numerical Grid	29
Verification	31
Model Use	41
PART IV: RESULTS	52
Use of Plots	52
One-in-Ten-Year Heights	53
Discussion	54
Risk Calculation	56
PART V: CONCLUSIONS AND RECOMMENDATIONS	58
Conclusions	58
Recommendations	59
REFERENCES	60
TABLE 1	
PLATES 1-44	
APPENDIX A: NOTATION	A1

CONVERSION FACTORS, U. S. CUSTOMARY TO METRIC (SI) AND METRIC (SI) TO U. S. CUSTOMARY UNITS OF MEASUREMENTS

Units of measurement used in this report can be converted as follows:

Multiply	By	To Obtain
U. S. Customary to Metric (SI)		
feet	0.3048	metres
miles (U. S. statute)	1.852	kilometres
tons (2000 lb, mass)	907.1847	kilograms
miles (U. S. nautical) per hour	1.852	kilometres per hour
square feet per second	0.09290304	square metres per second
feet per second squared	0.3048	metres per second squared
degrees (angular)	0.01745329	radians
Metres (SI) to U. S. Customary		
metres	3.280839	feet
kilometres	0.6213711	miles (U. S. statute)
square kilometres	0.3861021	square miles (U. S. statute)
radians per second	57.29578	degrees (angular) per second
radians	57.29578	degrees (angular)

TSUNAMI-WAVE ELEVATION FREQUENCY OF OCCURRENCE IN THE HAWAIIAN ISLANDS

PART I: INTRODUCTION

Background

1. Of all water waves that occur in nature, one of the most destructive is the tsunami. The term "tsunami," originating from the Japanese words "tsu" (harbor) and "nami" (wave), is used to describe sea waves of seismic origin. Tectonic earthquakes, i.e. earthquakes that cause a deformation of the sea bed, appear to be the principal seismic mechanism responsible for the generation of tsunamis. Coastal and submarine landslides and volcanic eruptions also have triggered tsunamis.

2. Tsunamis are principally generated by undersea earthquakes of magnitudes greater than 6.5 on the Richter scale. While the typical height of a tsunami in the deep ocean may be only a foot or less, the waves have a tremendous amount of energy which is indicated by the long period between crests (5 min to several hours). Tsunamis travel at the shallow-water wave celerity equal to the square root of acceleration due to gravity times water depth even in the deepest oceans because of their very long wavelengths. This speed of propagation can be in excess of 500 mph* in the deep ocean.

3. When tsunami waves approach a coastal region where the water depth decreases rapidly, wave refraction, shoaling, and bay or harbor resonance may result in significantly increased wave heights. The great period and wavelength of tsunami waves preclude their dissipating energy as a breaking surf; instead, they are apt to appear as bores or just rapidly rising water levels.

4. Localized bathymetric and topographic features may cause the

---

* A table of factors for converting U. S. customary units of measurement to metric (SI) units and metric (SI) units to U. S. customary units is presented on page 5.

effect of the same tsunami wave to be drastically different from one point to another. For example, a bay such as Hilo Bay of the island of Hawaii (Figure 1), has a funneling effect that tends to increase the height of the wave. However, an offshore sandbar or reef such as that of Kaneohe Bay on the island of Oahu (Figure 1) allows only a diminished wave height to reach the coast. It is not impossible for the same wave to be 50 ft high at one location and only 5 ft high a few miles distant as a result of local factors.

5. The loss of life and destruction of property due to tsunamis have been immense. The Great Hoei Tokaido-Nanhaido tsunami of Japan killed 30,000 people in 1707. In 1868, the Great Peru tsunami caused 25,000 deaths and carried the frigate *U.S.S. Waterlee* 1,300 ft inland. The Great Meiji Sanriku tsunami of 1896 killed 27,122 persons in Japan and washed away over 10,000 houses. The most recent major tsunami to affect the United States, the 1964 Alaskan tsunami, killed 107 people in Alaska, 4 in Oregon, and 11 in Crescent City, California, and caused over $100 million in damage on the west coast of North America.[1]

Tsunamis in the Hawaiian Islands

6. The Hawaiian Islands, a chain of eight islands as shown in Figure 1, have a history of destructive tsunamis generated both in distant areas and locally. The earliest recording of a severe tsunami in the Hawaiian Islands was in 1837 when a tsunami from Chile reached an elevation of 20 ft at Hilo and killed 46 people in the Kau District of the island of Hawaii (Figure 1). Prior to 1837, a number of severe tsunamis undoubtedly reached the islands, but unfortunately no detailed records were kept. Since 1837, there have been 16 tsunamis that have caused significant damage.[2]

7. Most of the destructive tsunamis in the Hawaiian Islands have been generated along the coast of South America, the Aleutian Islands, and the Kamchatkan Peninsula. Approximately one fourth of all the tsunamis recorded in the Hawaiian Islands have originated along the coast of South America, while more than one half have originated in the

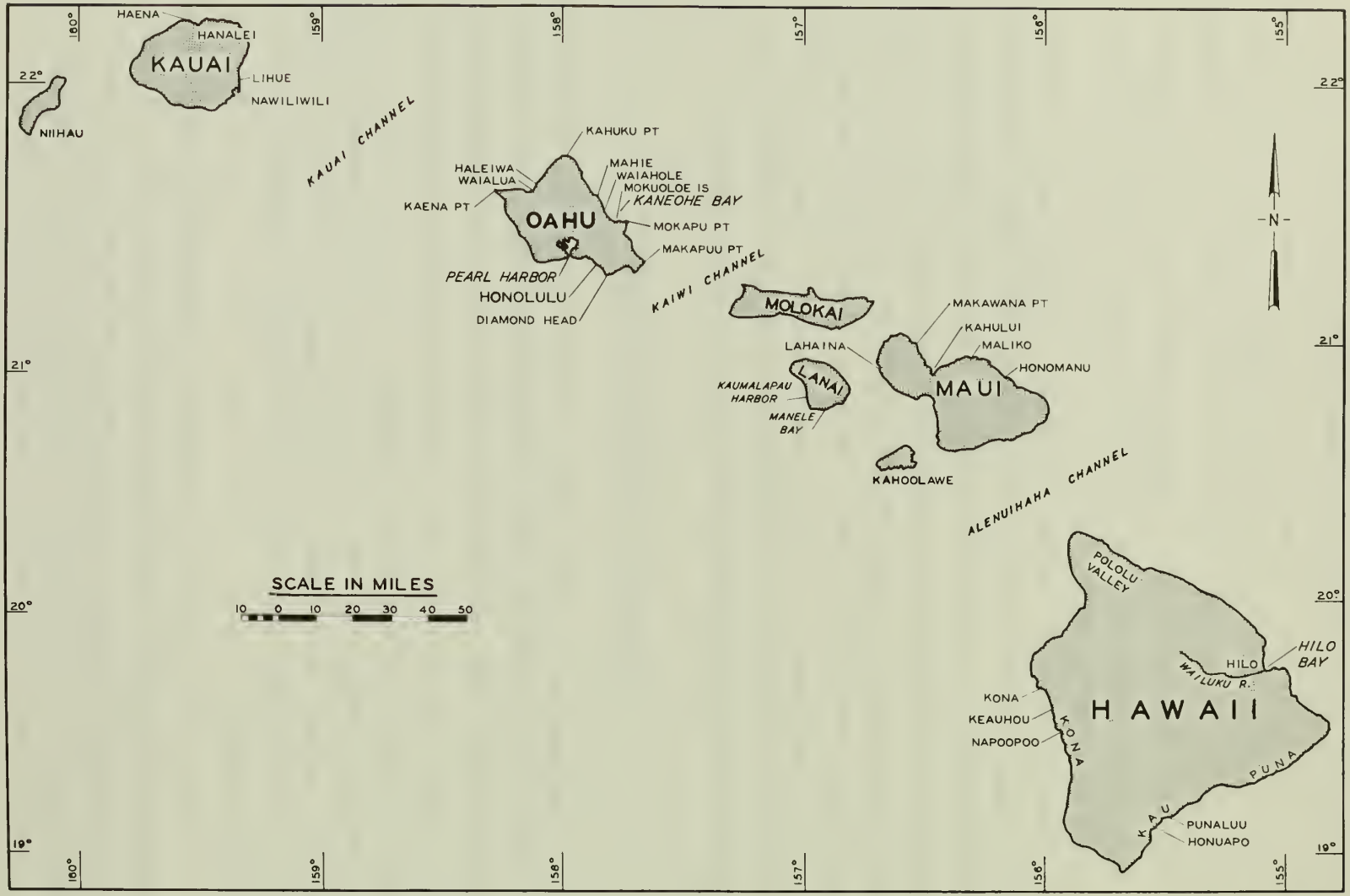

Figure 1. The Hawaiian Islands

Kuril-Kamchatka-Aleutian region of the north and northwestern Pacific.

8. Tsunamis generated by local seismic events have caused large runup in the islands, especially on the southeast coast of the big island of Hawaii. The 1868 tsunami produced the largest waves of record in the Hawaiian Islands with 60-ft waves reported on the South Puna coast of the island of Hawaii. The most recent tsunami in Hawaiian history occurred on 29 November 1975, when waves generated by an earthquake with an epicenter on the South Puna Coast reached elevations as great as perhaps 26 ft along the southeast coast.

9. The most destructive tsunami to ever hit the islands in terms of loss of life and destruction of property was the Great Aleutian tsunami of 1946, which killed 173 people and produced waves over 55 ft in elevation. Hilo incurred $26 million in property damage attributable to this tsunami.

10. The 1960 Chilean tsunami is the most recent distantly generated tsunami that produced major effects in the Hawaiian Islands. Sixty-one lives, all at Hilo, were claimed by the tsunami. Damage throughout the State was estimated to be $23.5 million of which 93 percent occurred at Hilo. Other major damage was restricted to the Kahului area of the island of Maui. Inspection of the damage at Hilo revealed much evidence of the tremendous forces developed by the waves. Twenty-ton boulders had been moved hundreds of feet, asphaltic concrete pavements were peeled from their subbase, and hundreds of automobiles were tossed around and crushed.[3]

Purpose of Study

11. The purpose of this study was to establish tsunami-wave elevation near the shoreline versus frequency-of-occurrence curves for the Hawaiian Islands and to recommend future efforts to determine methods of calculating runup for those areas where substantial flooding of low-lying areas causes runup not to be equal to wave elevation near the shoreline. This information is required by the U. S. Army Engineer Division, Pacific Ocean, for use in tsunami flood hazard evaluations

for floodplain management and flood insurance rate calculations. The *results of this study should not be used to determine evacuation zones based upon 1-in-100-year inundation levels without adding a safety factor through risk calcualtions (Part IV).* The odds that an elevation greater than the general 1-in-100-year elevation will occur within a short time span are not negligible. Any land development that would expose human life to possible danger should be initiated only after an evaluation of the possible risk.

PART II: APPROACH

Time Period Analyzed

12. It is necessary to use historical data of tsunami occurrence covering the greatest possible time span to properly determine frequency of occurrence of tsunami elevations for the Hawaiian Islands. Tsunami activity has not been uniform in these islands during recorded history. For example, the two largest and four of the ten largest tsunamis striking Hilo from 1837 through 1976 occurred during the 15-year period from 1946 through 1960. Two of the tsunamis from 1946 through 1960 originated in the Aleutian Islands, one in Kamchatka, and one in Chile. However, six of the ten largest tsunamis occurred during the 109-year period from 1837 through 1945 with three originating in Chile, two in Kanchatka, and one in Hawaii. Therefore, both the frequency of occurrence and place of origin of tsunamis have been remarkably variable. Any study, such as Reference 4, using a short time span that includes the period from 1946 through 1960 will predict a significantly more frequent occurrence of large tsunamis than is warranted by historical data from 1837 through 1976. Although the quantitative accuracy of the data for tsunamis from 1837 through 1945 may be questionable, there is little doubt that the recorded occurrence of large tsunamis is accurate (i.e., tsunamis noted as being significant were indeed so, and major tsunamis did not occur and go unrecorded).

13. From an analysis of tsunami data for Hilo the errors introduced in frequency-of-occurrence calculations by consideration only of a short period that includes the unrepresentative years from 1946 through 1960 will be greater than the errors resulting from possible observational inaccuracies of the nineteenth century. A calculated 1-in-100-year tsunami elevation for Hilo is 27.3 ft. This was determined by a least-squares fit of the data using the logarithmic frequency distribution discussed later and based upon data compiled by Cox[5] for the ten largest tsunamis in Hilo from 1837 through 1976. (His data were actually through 1964, but no large events have occurred since

1964). Increasing by 50 percent the elevations for five of the ten large tsunamis occurring during the nineteenth century yields a 1-in-100-year elevation of 30.4 ft. The 1-in-100-year elevation that is based just upon the large tsunamis during the period of accurate survey measurements in Hilo from 1946 through 1976 is 44.2 ft. Since the largest elevation in Cox's data for the 140-year period from 1837 through 1976 was 28 ft for the 1960 Chilean tsunami, the 44.2-ft elevation is obviously much too large.

14. Since an overestimate of the frequency of major tsunamis at Hilo, which has the most complete data for tsunamis in the Hawaiian Islands, did result from using an analysis based upon the short period from 1946 through 1960, it was concluded that overestimates will occur at all other locations throughout the islands from analyses based upon similar short periods. The exceptionally frequent occurrence of major tsunamis in Hilo from 1946 through 1960 is a property of the unusual activity of tsunami generation areas and not of special properties of Hilo.

15. The unusual tsunamigenic activity in generation regions is reflected in the most up-to-date catalog of tsunami occurrence in the circumpacific area compiled by Soloviev.[6] This catalog shows, for example, that since 1788 the three tsunamis generated with the greatest intensity in the Aleutian-Alaskan region occurred in 1946, 1957, and 1964. No significant tsunamis were generated during the period from 1837 through 1945 in this region and there also were no reports of significant tsunamis in the Hawaiian Islands which might have originated in this region. However, Pararas-Carayannis[2] reports a minor tsunami arriving in the Hawaiian Islands from the Aleutian-Alaskan region on 10 November 1938 that produced an elevation in Hilo of 0.3 m and in Honolulu of 0.1 m. This tsunami also is reported as a minor one in Soloviev's catalog. Clearly, tsunami generation was much more active in the Aleutian-Alaskan region from 1946 through 1964 than from 1837 through 1945.

16. The 1946 and 1957 tsunamis are the dominant tsunamis for northern coasts of many of the Hawaiian Islands (the 1946 tsunami is

one of the largest tsunamis for most locations even on southern coasts). For example, at Haena, Kauai, the 1957 tsunami elevation was 52.5 ft; the 1946 tsunami elevation, 45.0 ft; and the 1960 Chilean tsunami elevation, 9.2 ft. A least-squares fit of these data using the logarithmic distribution discussed later for the period 1946 through 1976 yields a 1-in-100-year elevation of 97.6 ft. However, since Aleutian-Alaskan tsunamis clearly produce the largest elevations at Haena (and on all of the northern Kauai coast), the 52.5-ft elevation must be the largest tsunami elevation at Haena since at least 1788. As reported by Soloviev,[6] the 1788 tsunami generated in the Aleutian-Alaskan region was quite large but produced unknown consequences to the Hawaiian Islands. A logarithmic distribution fit of the same data for the years 1837 through 1976 yields a 1-in-100-year elevation of 44.5 ft. Therefore, the period from 1946 through 1976 is clearly unrepresentative of long-period tsunami activity in the Hawaiian Islands due to Aleutian-Alaskan generated tsunamis.

17. Soloviev's catalog[6] also lists the 1960 Chilean tsunami as having the largest intensity of any tsunami generated in South America in recorded history (415-year period from 1562 through 1976). Reporting of tsunamis on the west coast of South America is quite good with 105 tsunamis reported during the 415-year period. A recent revision of the Richter scale for measuring earthquake energy by H. Kanamori of the California Institute of Technology* and a consequent revision of Richter magnitude estimates for several important large earthquakes listed a new magnitude of 9.5 for the 1960 Chilean earthquake, thus making this earthquake the largest in recorded history. McGarr[7] recently calculated seismic moments of earthquakes and found that earthquakes much larger than the Chilean earthquake of 1960 do not seem possible in view of the bounds associated with the relative motion of tectonic plates. Earthquakes as large as the 1960 event are probably quite rare. Plafker and Rubin,[8] for example, claim that relative submergence occurred along the Alaskan coast for at least 900 years before the 1964 Alaskan earthquake.

---

* Associated Press news article, March 1977.

The period from 1946 through 1960 certainly cannot be considered as being representative of long-period tsunami activity in South America when the greatest tsunami (and earthquake) in recorded history for this region occurred in 1960.

18. Tsunamis arriving in the Hawaiian Islands from Kamchatka may not be too abnormally concentrated within the period from 1946 through 1960. However, tsunamis from Kamchatka rarely produce the dominant flood elevations for locations in the Hawaiian Islands. Two large tsunamis from Kamchatka arrived in the Hawaiian Islands during the years 1837 through 1945 (return period approximately 55 years) and one during the years 1946 through 1976 (return period approximately 31 years). This difference in return periods may not be significant, but again it points to the 1946 through 1960 period as not being representative of long-term activity. It is interesting to note that Soloviev[6] reports two large tsunamis generated in Kamchatka from 1737 through 1836 (return period approximately 51 years). Thus, the return period for large tsunamis was approximately the same for the periods 1737 through 1836 and 1837 through 1945.

19. Evidence that tsunamis in the Hawaiian Islands were unusually active from 1946 through 1960 also exists at Kahului and Lahaina, Maui. Kahului, Lahaina, Hilo, and Honolulu are the only locations in the islands with historical data as far back as 1837. Four of the five largest tsunami elevations recorded at Kahului occurred during the years 1946 through 1960. Three of the four largest tsunami elevations recorded at Lahaina occurred during the same period. In addition, the 1946, 1957, and 1960 tsunamis produced the three largest elevations recorded anywhere in the Hawaiian Islands since 1837.

20. The main evidence that the period 1946 through 1976 might not be unusual for locations other than Hilo is the tsunami data at Honolulu. The greatest elevation in Honolulu used in Reference 4 is a 2.4-m elevation for the 1837 tsunami from Chile. However, this 2.4 m is not an elevation but a drop in water level. According to Pararas-Carayannis,[2] "at 5:00 the water began receding to 2.4 m leaving Honolulu Harbor partly dry, then slowly returned. Wave action lasted until the

following day." There is no indication of the maximum crest elevation achieved other than the fact that it was less than 2.4 m. The amplitude of troughs is of no importance to study of elevation frequencies and is not comparable to data just composed of crest amplitudes. Indeed, a trough of the 1960 tsunami from Chile measured in Honolulu may have had an amplitude as great as twice the maximum crest amplitude (Figure 9, page 40), yet Reference 4 just used the reported crest amplitude for this tsunami. If the 1837 tsunami is neglected, the largest elevation produced in Honolulu by distantly generated tsunamis occurred during the 1946 Aleutian and the 1960 Chilean tsunami. Again, events during the years 1946 through 1960 dominate the maximum flood elevations.

21. Tsunami data for Honolulu must be carefully considered before wide-ranging conclusions based upon the data are made. Since tsunami elevations are small at Honolulu, the tide level may have a significant influence on maximum elevations. Thus, it is difficult to compare probable tsunami crest amplitudes for historical tsunamis because the reported elevations may have significant tidal components. Also, the elevation used in Reference 4 for the 1841 tsunami is a trough amplitude, and elevations for the 1868 and 1877 tsunamis from Chile are not known for Honolulu.

22. Recently, D. C. Cox* has suggested the possibility of tsunamis generated in the central or western Aleutians having occurred during the period from 1837 through 1945 and produced significant elevations in the Hawaiian Islands at locations other than the populated communities of Hilo, Honolulu, Kahului, and Lahaina. As evidence, Cox cites the wave damage at Haleiwa, Oahu, in 1872 probably resulting from a 10-ft elevation of water. However, he further states that the damage might have been caused by a tsunami from the north, but it was more likely a result of storm waves. A tsunami later in 1872, possibly from the north, resulted in rises of 4 ft at Hilo, 1 ft at Honolulu, 1.5 ft at Nawiliwili, Kauai, and probably about 10 ft at Hanalei, Kauai. An 1878 tsunami, also possibly from the north, resulted in a reported runup of 10 ft at

---

* Personal letter, 7 March 1977.

Waialua, Oahu, and probably about 10 or 15 ft at Maliko, Honomanu, and Halehaku on the island of Maui. Cox believes that these events suggest that Aleutian-Alaskan tsunamis might have been more active at some locations in the Hawaiian Islands from 1837 through 1945 than indicated in this study.

23. The evidence that no major tsunamis originating in the Aleutian-Alaskan area from 1837 through 1945 occurred and went unreported is persuasive. It is true that Hilo is not as strongly responsive to tsunamis generated in the western Aleutians as it is to tsunamis generated in the central Aleutians or the eastern Alaskan area. However, the 1957 tsunami from the western Aleutians, although not large compared with many of the historical tsunamis in Hilo, did produce an elevation only 1 ft less than that of the 1868 Chilean tsunami, which was characterized as having caused "severe damage" in Hilo.[2] During the 1957 tsunami, "buildings along the waterfront were badly damaged;"[2] Coconut Island in Hilo Harbor was covered by 3 ft of water and the bridge to the island was destroyed. Kahului, Maui, also is sensitive to Aleutian-Alaskan tsunamis (since it faces north, as does Hilo) and has historical data back to 1837. The 1946 Aleutian tsunami was very destructive in Kahului, and even the 1957 tsunami produced an elevation the same as that of the 1868 Chilean tsunami, which caused considerable damage in Kahului. Yet, like Hilo, there is no report of a significant Aleutian-Alaskan tsunami during the period 1837 through 1945. Furthermore, Honolulu and Lahaina were sufficiently active ports in the nineteenth century to notice water level changes of only 1 m during the 1841 Kamchatkan tsunami (one of the smallest major tsunamis in the Hawaiian Islands during the nineteenth century). Again, no significant Aleutian-Alaskan tsunamis during the years 1837 through 1945 were reported at these locations.

24. There also is evidence from the Aleutian-Alaskan area that the possible events of 1872 and 1878 were not tsunamis generated in this area. George Davidson, U. S. Coast and Geodetic Survey, was sent to Alaska in the summer of 1867 to lead a survey team.[9] The party established a tide gage at Kodiak, which was sensitive enough to record the

1868 tsunami from Chile and the 1883 blast waves from Krakatoa, Indonesia. (The 1883 event was recorded by a tide gage in Honolulu as having a height of 0.2 m.) Apparently, Davidson made no report of tsunamis generated in 1872 or 1878 in the Alaskan area.

25. The elevations reported by Cox for the possible tsunamis of 1872 and 1878 are not particularly large compared with other historical events at the indicated locations. For example, at least four tsunamis at Haleiwa, Oahu, just during the 19-year period from 1946 through 1964 had elevations greater than the possible tsunami of 1872. Actually, if the possible tsunamis of 1872 and 1878 are added to the analysis described later in this report at the indicated locations, the 1-in-100-year elevations are only changed by fractions of a foot. Since these possible events do not significantly influence the 1-in-100-year elevations for locations on Kauai, Oahu, Maui, or for Hilo, Hawaii, they are probably not significant for elevation calculations elsewhere in the Hawaiian Islands. Furthermore, the possible occurrence of these events is not an indication that the Aleutian-Alaskan tsumanis were active enough at locations in the Hawaiian Islands during the years 1837 through 1945 for the period from 1946 through 1960 to be representative of long-period Aleutian-Alaskan tsunami activity.

Interpolation of Historical Data

26. Historical data of tsunami activity in the Hawaiian Islands are, of course, often limited to certain locations. Information on tsunami activity in the islands prior to the 1946 tsunami is concentrated in Hilo, Hawaii, and Honolulu, Oahu, and to a lesser extent in cities such as Kahului and Lahaina on the island of Maui. Even data for tsunamis from 1946 through 1976 are absent or fragmentary (i.e., data exist only for certain of the events) for much of the coastline of the islands. Therefore, it is necessary to rely on more than just available historical data to determine tsunami occurrence frequencies. In this study, a hybrid finite element numerical model was used to supplement historical information by allowing for interpolation between historical

data. The model is described in Part III and verified by a comparison of the numerical model calculations and historical data recorded during the 1960 and 1964 tsunamis.

27. The numerical model is used to fill in historical data gaps for tsunamis from 1946 through 1964 by providing relative responses of the Hawaiian Islands to tsunamis. Although the deepwater wave form of a tsunami such as that of 1946, for example, is not known, the direction of approach of this tsunami and its range of wave periods are known. By inputting sinusoidal waves of unit amplitude from the same direction as the 1946 tsunami into the numerical model over a band of wave periods, the average relative response of the islands to a tsunami similar to the 1946 tsunami is determined. If historical data exist at one location, wave elevations at a nearby location for which historical data do not exist are determined by multiplying the historical data at the first location by the ratio of the response calculated by the numerical model at the second location and the response calculated at the first. The numerical model takes into account the major processes that would cause different wave elevations at the two locations. That is, the model calculates shoaling, refraction, diffraction, reflection, resonance, shielding of the back side of an island by the front side, and interactions between islands. Historical data from 1946 through 1964 were taken from the most recent compilation of these data.[10] Part III describes the use of the numerical model for interpolation in detail.

28. As an example of the use of the numerical model to fill historical data gaps for tsunamis from 1946 through 1964, consider the 1946 tsunami that was recorded on the island of Lanai only at Kaumalapua Harbor and Manele Bay. Wave elevations can be calculated for the 1946 tsunami at other locations on the coastline of Lanai by multiplying these historical values by the ratio of the response calculated at locations on the coastline by the numerical model and the response calculated at Kaumalapua Harbor and Manele Bay by the numerical model. Thus, wave elevations for the 1946 tsunami can be calculated for all of Lanai.

29. Some islands lack any historical data on a particular tsunami. For example, there are no data for the 1960 tsunami on Lanai.

Historical data for such cases can be reconstructed by using historical data from areas of nearby islands in conjunction with the numerical model. For example, the west coast of Maui (near Lahaina) is less than 10 miles from the east coast of Lanai and has historical data for the 1960 tsunami. Wave elevations can be calculated on Lanai for the 1960 tsunami by multiplying the historical wave elevations on the west coast of Maui by the ratio of the response calculated on Lanai by the numerical model and the response calculated on the west coast of Maui by the numerical model. The wave elevations calculated for the 1960 tsunami on Lanai using this approach are consistent with the qualitative reports on tsunami activity during the 1960 tsunami. Damages on Lanai during the 1960 tsunami were slight ($2000) and confined to Kaumalapau Harbor where three small boats were sunk. One beach house was damaged on the island. The reconstructed wave elevations for the 1960 tsunami on Lanai were fairly small. They were smaller than the elevations recorded on the west coast of Maui where the 1960 tsunami caused damage at Lahaina[3] amounting to $17,000.

Reconstruction of Historical Data

30. Tsunamis originating near the Aleutian Islands, Kamchatka, and Chile occurred from 1946 to 1964. Therefore, the response is known of many areas in the Hawaiian Islands to tsunamis originating in the three main locations where tsunamis of destructive power in these islands have historically been generated. It is assumed in this study that tsunamis generated in a single source region (Kamchatka or Chile but not the Aleutians) approach the islands from approximately the same direction and have energy lying in the same band of wave periods. The difference in wave elevations at the shoreline in the Hawaiian Islands produced by tsunamis generated at different times in the same region is attributed mainly to differences in deepwater wave amplitudes. For example, the 1841 tsunami from Kamchatka produced a wave elevation in Hilo that was approximately 25 percent greater than that of the 1952 tsunami from Kamchatka.[2] The same relative magnitude of the two tsunamis is used for all of the islands to determine the elevation that must have

occurred in 1841 at some location, knowing the elevation which did occur in 1952. Therefore, knowing the elevations of tsunamis at a location from 1946 to 1960 and the response of Hilo to tsunamis from 1837 to 1960 allows a reconstruction of the elevations of tsunamis that occurred prior to 1946 but were not recorded.

31. The assumption that tsunamis generated in Kamchatka and Chile approach the Hawaiian Islands from nearly the same direction is justified by the small spatial extent of the known generation areas in Kamchatka and results of a study[11] that considered the propagation of tsunamis from Chile using a finite difference numerical model. This study indicated that the directional effects for tsunamis originating along the Chilean coast are small in the Hawaiian Islands (probably because the generation areas in Chile subtend a relatively small angle with respect to the islands). The position of the Aleutian-Alaskan Trench relative to the Hawaiian Islands does introduce important directional efforts for tsunamis generated in the Aleutian-Alaskan area. However, these effects are known from historical observations for tsunamis generated in the western Aleutians (1957 tsunami), central Aleutians (1946), and eastern Alaskan area (1964).

32. Many observers have noted that wave elevations produced at a location by "tsunamis of diverse geographic origin are strikingly different, whereas those from nearly the same origin are remarkably similar."[12] A recent study[13] shows that the normalized frequency distribution for tsunamis of the same origin have the same distribution. Therefore, the assumption is quite reasonable that heights of past tsunamis for which no data exist can be estimated by considering tsunamis of the same origin for which data do exist.

33. In his report, Cox[5] noted the problem of selecting elevations measured during surveys of runup and inundation for tsunamis from 1946 through 1964 in Hilo Bay that are comparable with the earlier visual elevations recorded there from 1837 to 1946. He claimed that it could be assumed that the reporters of early tsunamis did not record the minimum level reached, nor even an average. Furthermore, he believed that it could not be assumed that they identified the absolute maximum in the

absence of surveys comparable with the ones from 1946 through 1964. Therefore, in order to make the recorded values from 1946 through 1964 comparable with earlier historical tsunamis, he chose as the "normal maximum" elevation the upper decile value for each of the tsunamis from 1946 through 1964 from inundation heights measured along the shores of Hilo Bay between the west bank of the Wailuku River and the root of the breakwater. His compilation of historical data and comparable adjusted values were used to determine the ratios needed to reconstruct the elevation of tsunamis that occurred prior to 1946 at locations lacking such historical data.

34. Tsunami elevations along the coasts of the Hawaiian Islands can be calculated for the ten largest tsunamis in Hilo from 1837 through 1976 by using the finite element numerical model to fill in data gaps for those tsunamis of the ten that occurred from 1946 through 1964 and then taking these results and the ratios from Cox's study to reconstruct the elevations of those tsunamis that occurred prior to 1946. For much of the coast of the Hawaiian Islands, the ten largest tsunamis since 1837 would be the same as the ten largest tsunamis in Hilo. That is, the ten largest would be the 1960, 1946, 1923, 1837, 1877, 1841, 1957, 1952, and the two in 1868. Of course, the order of the ten largest would vary from location to location. For example, the largest tsunami on the South Puna coast of the island of Hawaii was the locally generated tsunami of 1868. There are some locations where one or more of the ten largest tsunamis to have occurred are not among the ten largest in Hilo from 1837 through 1976. For example, the 1896 tsunami generated near Japan is the largest to hit Keauhau on the Kona coast of the big island of Hawaii. The ten largest tsunamis at each location are determined by adding such historical tsunamis and eliminating a corresponding number of the smallest tsunamis from the initial compilation at each location of the ten that were the largest at Hilo. The following tabulation lists the sixteen tsunamis considered in determining the ten largest tsunamis for locations along the Hawaiian coastline, the source location of the tsunami, and the islands experiencing significant wave elevations:

Data	Source	Island(s) Affected
7 November 1837	Chile	All
17 May 1841	Kamchatka	All
2 April 1868	Hawaii	Hawaii
13 August 1868	Chile	All
10 May 1877	Chile	All
15 June 1896	Japan	Hawaii
16 August 1906	Chile	Maui
30 April 1919	Tonga Island	Hawaii
3 February 1923	Kamchatka	All
2 March 1933	Japan	Hawaii
1 April 1946	Aleutian Islands	All
4 November 1952	Kamchatka	All
9 March 1957	Aleutian Islands	All
23 May 1960	Chile	All
27 March 1964	Alaska	All
29 November 1975	Hawaii	Hawaii

35. Historical data for the tsunamis prior to 1946 listed above were taken from Reference 2. Tsunamis listed as being questionable in Reference 2 are not listed. Data for the 29 November 1975 tsunami were taken from Reference 14. These data were used in conjunction with data from Reference 2 on the 2 April 1868 tsunami to fill in data gaps for the 1868 tsunami. Both the 1868 and 1975 tsunamis were generated on the southeastern coast of the island of Hawaii. Wave elevations in the Kau District at cities such as Honuapo and Punaluu were similar for the two tsunamis. Wave elevations along the South Puna coast, however, were much larger for the 1868 tsunami than the 1975 tsunami. The 1868 wave elevations were reconstructed for the South Puna coast by multiplying the 1975 elevations by ratios determined at locations such as Keauhau Landing on the South Puna coast where data exist for both the 1868 and 1975 tsunamis.

Frequency of Occurrence Distribution

36. Cox found that the logarithm of tsunami frequency of occurrence is linearly related to tsunami elevations for the ten largest tsunamis occurring from 1837 to 1964 in Hilo.[5] This result is not

unexpected considering the fact that Soloviev of the Soviet Union has shown a similar relationship between tsunami frequency of generation and the intensity of the tsunamis near the generation area for moderate to large tsunamis.[15] Also, earthquake intensity and frequency of occurrence have been similarly related by Gutenberg and Richter.[16] Furthermore, Wiegel[17] found the same relationship for historical tsunamis at Hilo, Hawaii; San Francisco, California; and Crescent City, California; and Adams,[18] for tsunamis at Kahuku Point, Oahu. A recent study by Rascón and Villarreal[19] revealed this same relationship for historical tsunamis on the west coast of Mexico (data from 1732) and on the Pacific West coast of America, excluding Mexico.

37. After the ten largest tsunamis from 1837 through 1976 are determined at locations all along the coasts of the Hawaiian Islands, elevation versus frequency of occurrence is fit at each location using the least-squares techniques by curves that can be represented by the equations

$$h = -B - A \log_{10} F \qquad (1)$$

where

h* = elevation of maximum tsunami-wave crest above mean sea level 200 ft shoreward of the coastline

F = frequency per year of occurrence

According to Cox,[20] unless there is evidence to the contrary, recorded historical runup heights may reasonably be considered to have been measured 200 ft inland of the coastline. Since the coefficients of Equation 1 are based ultimately on recorded historical data, the values of h determined from this equation are elevations 200 ft shoreward of the coastline. He fit his Hilo data by a curve that can be represented by a similar equation. Plots of the coefficients A and B versus location along the coasts of all the islands are shown in Part IV. The negative signs in Equation 1 were used so that these coefficients would be positive. Furthermore, these coefficients can be found for any locality of the Hawaiian Islands and used in Equation 1 to calculate

---

* For convenience, symbols and unusual abbreviations are listed and defined in the Notation (Appendix A).

"h" for any desired "F" within a certain range of frequencies.

38. Cox found that the linear relation between the logarithm of tsunami frequency of occurrence and tsunami elevations at Hilo was valid for frequencies of occurrence as high as 0.1 per year (1-in-10-year tsunami). He found that the frequency-elevation relation for higher frequencies followed approximately a power law. Equation 1 should, therefore, be used only for frequencies of occurrence lower than 0.1 per year. There are some locations, however, where the linear relation is valid only for frequencies of occurrence lower than 0.05 (1-in-20-year tsunami) per year. This problem is discussed in Part IV, and a table (Table 1) is presented that gives 0.1-per-year elevations for the entire coastline of the Hawaiian Islands. It is recommended that Table 1 be used for the 0.1-per-year elevations and Equation 1 for frequencies lower than or equal to 0.05 per year.

39. Equation 1 was used as a frequency of occurrence distribution because it has been found to agree with historical data at several locations, as discussed earlier. Other distributions may agree with historical data equally well. For example, the Gumbel distribution has been used in the past to study annual streamflow extremes.[21] Borgman and Resio[22] illustrate the use of this distribution to determine frequency curves for nonannual events in wave climatology. To investigate the sensitivity of calculations of 1-in-100-year elevations on the assumed frequency distribution, the approach of Borgman and Resio was applied to the Hilo data of Cox.[5] The Gumbel distribution yields a 1-in-100-year elevation of 28.8 ft for data from 1837 through 1976 and an elevation of 42.5 ft for data from 1946 through 1976. This compares with the elevations of 27.3 and 44.2 ft calculated for the same time periods using the logarithmic distribution. Clearly, the arguments used earlier concerning the period of time that must be considered for a valid analysis are not dependent upon the assumed frequency distribution. Since ample precedents exist for using the logarithmic distribution for analyzing tsunami frequency of occurrence, this distribution was used in this report.

PART III: NUMERICAL MODEL

Description

40. The interaction of tsunamis with the Hawaiian Islands was determined by using a hybrid finite element numerical model developed recently for harbor oscillation and wave scattering problems by Chen and Mei[23] at Massachusetts Institute of Technology. The model solves the following generalized Helmholtz equation:

$$\nabla[d(x,y)\nabla\phi(x,y)] + \frac{\omega^2}{g}\phi(x,y) = 0 \qquad (2)$$

where

∇ = gradient operator, ft^{-1}

x,y = Cartesian coordinates, ft, of the location

$d(x,y)$ = water depth at the location

$\phi(x,y)$ = total velocity potential at the location with $U(x,y)$, a two-dimensional vector, equal to $-\nabla\phi(x,y)$

ω = angular frequency

g = acceleration due to gravity

Equation 2 governs small amplitude undamped long waves in a region with land masses of arbitrary shape and water of variable depth. It has further been assumed that the flow is irrotational.

41. The Helmholtz equation expressed as

$$\nabla^2\phi(x,y) + \frac{\omega^2}{gd}\phi(x,y) = 0 \qquad (3)$$

is the governing equation for a constant-depth ocean region outside the region containing the islands.

42. Waves incident upon islands in an infinite ocean produce a scattered wave having a velocity potential ϕ_S given by

$$\phi_S = \sum_{n=0}^{\infty} H_n(kr)(\alpha_n \cos n\,\theta + \beta_n \sin n\,\theta) \qquad (4)$$

where

H_n = Hankel function of the first kind of order n

k = wave number

r = spherical coordinate, ft

α_n = unknown coefficient

θ = spherical coordinate, radians

β_n = unknown coefficient

43. The symbol ϕ_S satisfies the Sommerfeld radiation condition that the scattered wave must behave as an outgoing wave at infinity and may be expressed mathematically as

$$\lim_{r\to\infty} \sqrt{r}\left(\frac{\partial}{\partial r} - ik\right)\phi_S = 0 \tag{5}$$

where i equals $\sqrt{-1}$.

44. Chen and Mei used a calculus of variations approach and obtained a Euler-Lagrange formulation of the boundary value problem. The following functional with the property that it is stationary with repect to arbitrary first variations of $\phi(x,y)$ was constructed by Chen and Mei:

$$F(\phi) = \iint \frac{1}{2}\left[h(\nabla\phi)^2 - \frac{\omega^2}{g}\phi^2\right] dR + \frac{1}{2}\S\left[h(\phi_R - \phi_I)\frac{\partial(\phi_R - \phi_I)}{\partial n_a}\right] da - \S\left[h\phi_a \frac{\partial(\phi_R - \phi_I)}{\partial n_a}\right] da - \S\left(h\phi_a \frac{\partial\phi_I}{\partial n_a}\right) da + \S\left[h\phi_I \frac{\partial(\phi_R - \phi_I)}{\partial n_a}\right] da \tag{6}$$

where

R = region containing the islands

§ = line integral

ϕ_R = far-field velocity potential

ϕ_I = velocity potential of incident wave

n_a = unit normal vector outward from region R

a = boundary of region R

ϕ_a = total velocity potential evaluated on boundary a

45. Proof was given by Chen and Mei that the stationarity of this functional is equivalent to the original boundary value problem.

46. The integral equation obtained from extremizing the functional is solved by using the finite element method. This method is a technique of numerical approximation that involves dividing a domain into a number of nonoverlapping subdomains, which are called elements.

47. The solution of the problem is approximated within each element by suitable interpolation functions in terms of a finite number of unknown parameters. These unknown parameters are the values of the field variable $\phi(x,y)$ at a finite number of points, which are called nodes. The relations for individual elements are combined into a system of equations for all unknown parameters.

48. In the constant depth region outside the region containing the islands, the velocity potentials are solved analytically in terms of unknown coefficients. The region is considered to be a single element with an "interpolation function" given by Equation 4. The infinite series is terminated at some finite value such that the addition of further terms does not significantly influence the calculated values of $\phi(x,y)$. The resulting equation is combined with the system of equations for unknown parameters at nodal points within the region containing the islands, and this complete system is solved using Gaussian elimination matrix methods.

49. The relation of $\eta(x,y)$ to $\phi(x,y)$ through the linearized dynamic free surface boundary condition is expressed as

$$\eta(x,y) = -\frac{1}{g}\left[\frac{\partial\phi(x,y)}{\partial t}\right] \tag{7}$$

where

η = wave amplitude

t = time

50. The hybrid finite element method (so named by Chen and Mei because the method involves the combination of analytical and finite element numerical solutions) is a steady-state solution of the boundary value problem. The response of a group of islands to an arbitrary

tsunami can be easily determined within the framework of a linearized theory. For example, an arbitrary tsunami in the deep ocean can be Fourier decomposed as follows:

$$b_o(t) = \int_{-\infty}^{\infty} b(\omega) e^{-i[\omega t + \rho(\omega)]} \, d\omega \tag{8}$$

where

b_o = incident wave amplitude

$b(\omega)$ = amplitude of frequency component ω

$\rho(\omega)$ = phase angle

If $\eta(x,y,\omega)$ is the response amplitude at any point (x,y) along the island coasts due to an incident plane wave of unit amplitude and frequency ω, then the response of the islands to the arbitrary tsunami time history $b_o(t)$ is given by

$$\xi(x,y,t) = R_e \left\{ \int_{-\infty}^{\infty} b(\omega) \eta(x,y,\omega) e^{-i[\omega t + \rho(\omega)]} \, d\omega \right\} \tag{9}$$

where the operation $R_e\{\}$ takes the real part of the braced quantity. Therefore, as soon as $\eta(x,y,\omega)$ is known for all ω, the island response to an arbitrary tsunami can be calculated.

51. Chen and Mei verified their finite element numerical model by comparing the model's calculations with analytical and experimental results for simple wave problems. Figure 2 shows a comparison of analytical and numerous results of wave diffraction off a vertical circular cylinder.

52. The computer program of Reference 23 was modified before calculations were made for tsunami response of the Hawaiian Islands. Slight modifications were necessary to allow the model to handle problems with variable depths, since Chen and Mei had applied their original numerical model only to constant depth problems. The subroutine that solves the large system of algebraic equations arising from finite elements was modified to be more efficient by taking advantage of the sparseness (many zero terms) of the system of equations. This modification resulted in a decrease in the computational time of the numerical

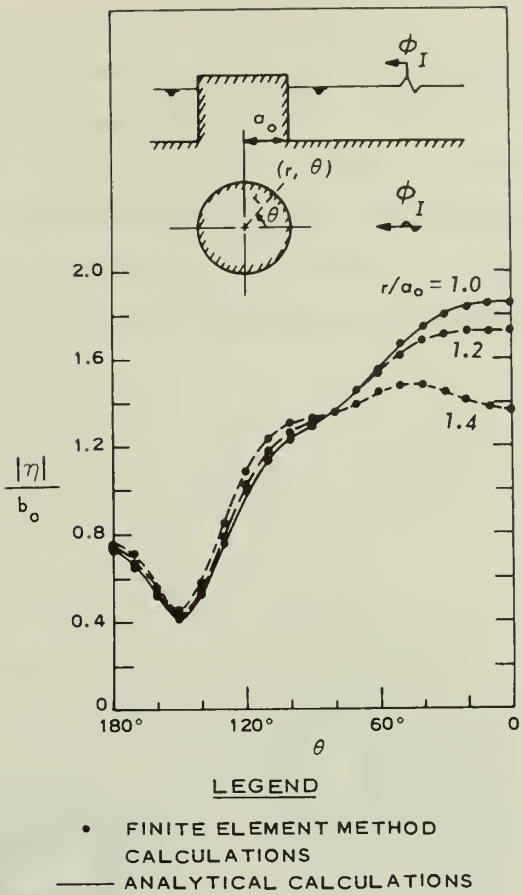

Figure 2. Comparison of numerical and analytical results for wave scattering off a vertical circular cylinder[23]

model by a factor of approximately six for the grid shown in the next section. The solution of the system of algebraic equations also had to be modified so that calculations involved only small blocks of equations at a time since there were more than 800,000 terms in the system of equations.

Numerical Grid

53. The finite element model has great advantages relative to finite difference numerical models in accuracy representing land shapes and ocean bathymetry since finite element techniques allow dramatic changes in element sizes and shapes. Element sizes can be large in deep water because wavelengths are large and, therefore, adequately resolved by a crude grid. As a wave enters shallower water, its wavelength decreases and the elements of the grid can be telescoped to smaller sizes with no loss of resolution.

54. The finite element grid in Figure 3 shows elements of the grid telescoping from large sizes in the deep ocean to triangles with areas as small as 0.5 sq km in shallow coastal waters. For comparison, a recent study by Bernard[24] used a finite difference grid that included the major islands of Hawaii and had grid cells with areas of approximately 30 sq km (square cells 5.5 km on a side). Since the islands of Hawaii have small surface areas and are surrounded by waters of rapidly

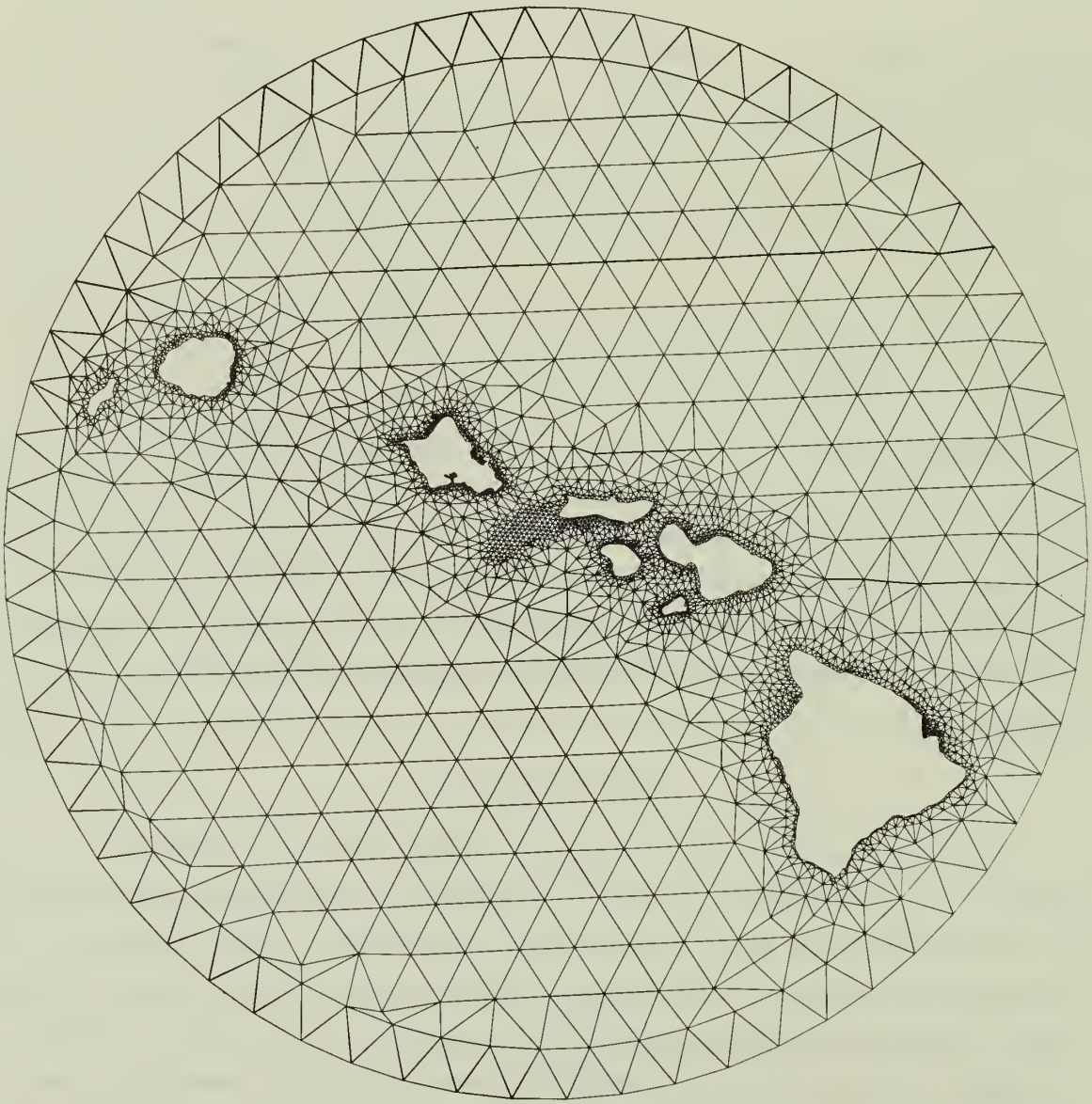

Figure 3. Finite element grid

varying bathymetry, an accurate representation of the islands in a numerical model requires the small grid units that are feasible (from an economic viewpoint) for a finite element model only.

55. The geometric shapes of the eight islands comprising the Hawaiian Island chain are obviously modeled very precisely by the finite element grid (Figure 3). Extremely rapid bathymetry changes also are very accurately modeled by the grid. Furthermore, the number of node points (corner points of the triangles) along the shoreline of the islands is very dense. Since wave amplitudes are calculated at node points by the finite element model, the model can adequately resolve the rapid wave height variations along coastlines that are known to occur during tsunami activity.

56. The finite element model calculations for the grid (Figure 3) are extremely rapid. The main calculation time involves the solution of a very large matrix with over 800,000 terms, yet the computational time for the model to solve the response of the islands to waves of a particular period is less than 1 min of computer time on a Control Data Corporation 7600. This rapid calculation time makes it economically feasible to determine the response of the islands to arbitrary tsunamis, as discussed in the following section. One reason that the computational time required by the finite element model is so much less than that required by finite difference models is that the finite element model uses small elements only in areas where they are necessary. The grid in Figure 3 has approximately 2,500 nodal points, whereas the finite difference grid of Bernard[24] had 26,000 grid points. Even so, some of the elements of the finite element grid are up to 60 times smaller than the finite difference grid cells.

Verification

57. The finite element numerical model is verified in this study by comparing numerical model calculations with tide gage recordings of the 1960 and 1964 tsunamis. The 1960 Chilean and 1964 Alaskan tsunamis are the only major tsunamis for which some reliable information

regarding source-generating characteristics exists, with much more information existing for the Alaskan source than the Chilean source.

58. A deepwater recording of a tsunami far from the perturbing influences of a coastal area has never been made. Therefore, a prototype wave record in deep water of the 1960 Chilean and 1964 Alaskan tsunamis is not available for use as input to verify the finite element model. However, finite difference numerical models have been used in previous studies[11,25,26,27] to simulate the uplift deformation of the ocean water surface caused by the permanent vertical displacement of the ocean bottom during an earthquake and the subsequent propagation of the tsunami across the deep ocean. The permanent deformation (permanent in the sense that the time scale associated with it is much longer than the period of the tsunami) is considered to be the important parameter in tsunami generation and not the transient movements within the time history of the ground motion. These transient movements occur over periods of time of the order of seconds, whereas tsunami wave periods are of the order of tens of minutes. Reference 28 confirms the fact that the permanent ground displacement of the source region and not the transient ground movements determines the characteristics of the resulting tsunami.

59. Figures 4 and 5 show time histories of the 1960 Chilean and 1964 Alaskan tsunamis in deep water near the Hawaiian Islands calculated by finite difference models in previous studies.[11,27] The permanent deformation of the ocean's bottom at the source as a function of spatial location was taken from Reference 29 for the Alaskan source and References 30 and 31 for the Chilean source. Grids measuring 1/3 by 1/3 deg were used for the calculations.

60. The hybrid finite element method is a steady-state solution of the boundary value problem. As described in paragraphs 40-52, the response of a location in the Hawaiian Islands to any tsunami can be calculated by the finite element model once the response amplitude $\eta(x,y,\omega)$ due to an incident plane wave of unit amplitude and frequency ω is known at the location (x,y) for all frequencies. Of course, it is not feasible to calculate the integrals of Equations 8 and 9 over all

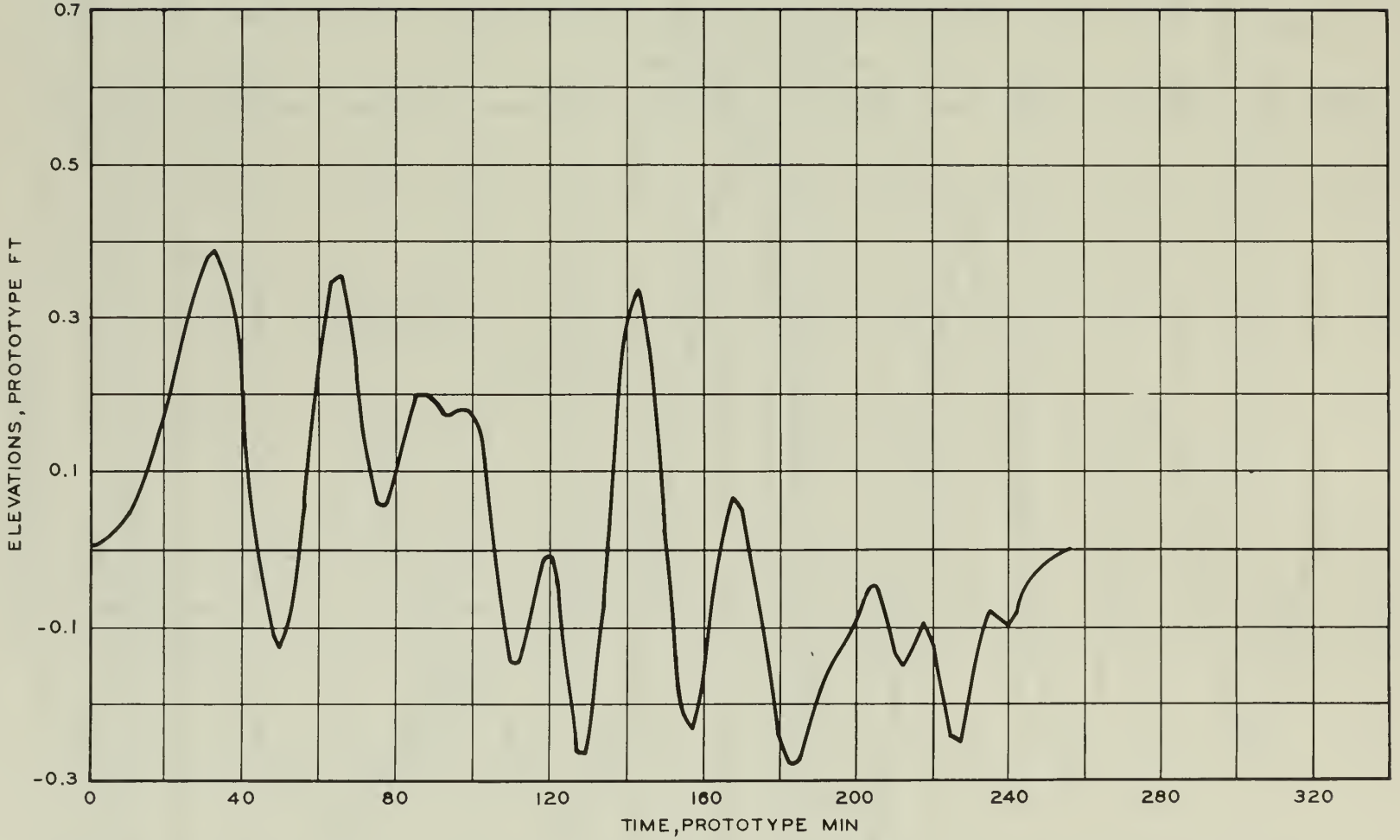

Figure 4. Numerical model calculations of the 1964 Alaskan tsunami in deep water near Hawaii

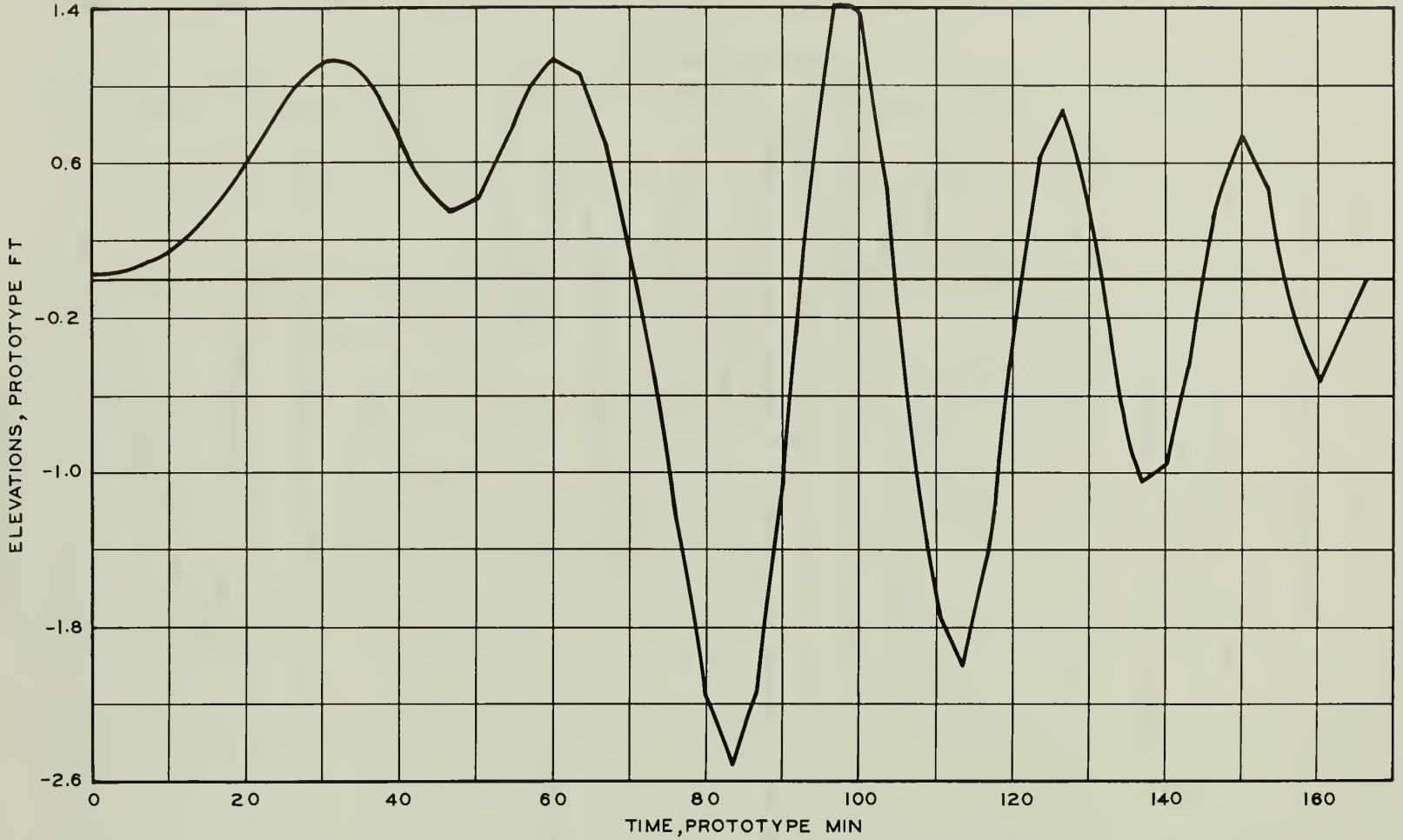

Figure 5. Numerical model calculations of the 1960 Chilean tsunami in deep water near Hawaii

frequencies. Instead the frequency range is discretized, and the integrals replaced by sums over a frequency range containing most of the energy of the tsunami.

61. Equation 8 involves a Fourier decomposition of a time series. This decomposition was accomplished for the time histories of the 1960 Chilean and 1964 Alaskan tsunamis (Figures 4 and 5) by using a least-squares harmonic fitting procedure. The time history of the Alaskan tsunami in deep water was decomposed into 18 components with periods ranging from 14.5 min to the time length of the record. The variance of the residual (difference between the actual record and a recomposition of the 18 components) was approximately 0.2 percent of the variance of the record. Therefore, virtually all the energy in the wave record was contained in the 18 components. The time history of the Chilean tsunami in deep water was decomposed into 11 components with periods ranging from 15.5 min to the time length of the record. The variance of the residual was less than 0.1 percent of the variance of the record. For both cases, the original time history and a time history constructed from a recomposition of the components were virtually indistinguishable visually.

62. Equations 8 and 9 take the following form when discretized:

$$b_o(t) = \sum_{\eta=1}^{m} b(\omega_\eta) e^{-i[\omega_\eta t + \rho(\omega_\eta)]} \tag{10}$$

and

$$\xi(x,y,t) = R_e \left\{ \sum_{\eta=1}^{m} b(\omega_\eta) \eta(x,y,\omega_\eta) e^{-i[\omega_\eta t + \rho(\omega_\eta)]} \right\} \tag{11}$$

where

m = number of components

ω_η = frequency of ηth components

63. The $b(\omega_\eta)$ term is determined by the least-squares harmonic fitting procedure, and $\eta(x,y,\omega_\eta)$ is determined by the finite element numerical model for each frequency ω_η and at each location (x,y). Therefore, the time history $\xi(x,y,t)$, which represents the response

of location (x,y) to the deepwater tsunami time history represented by $b_o(t)$, can be simply calculated for any location along the coastline of the Hawaiian Islands.

64. Figures 6 through 8 present a comparison between tide gage recordings of the 1964 tsunami at Kahului (Maui), Honolulu (Oahu), and Hilo (Hawaii), respectively, and the numerical model calculations. The largest waves recorded at each of these sites are shown, but the smaller waves arriving at later times and thus of little interest to this study are not. Whenever gage limits were encountered, the tide gage recordings were linearly extended. Of course, a tide gage is a nonlinear device with a response depending both upon the period and amplitude of the disturbance measured. However, based upon the work of Noye,[32] the distortion of the tsunami shown in Figures 6 through 9 by a standard tide gage is not significant.

65. The comparisons shown in Figures 6 through 8 are in remarkable agreement, especially considering the fact that the ground displacement of the 1964 earthquake was not precisely known. Since the Hilo breakwater was not included in the numerical model grid, the numerical model calculations for Hilo are too large. This breakwater was undoubtedly highly permeable to the 1964 tsunami. However, it probably did cause some energy dissipation and reflection, although how much is not known. The numerical model results appear to be too large in Hilo by some constant factor, since the tide gage recording and the numerical model calculations have the same form with the first wave crest and trough having approximately the same amplitude and being proportionately smaller than the second crest.

66. Figure 9 shows a comparison between the tide gage recording of the 1960 tsunami at Honolulu and the numerical model calculations. The Honolulu gage was the only tide gage in the Hawaiian Islands not seriously damaged by this tsunami. Again the largest waves recorded are shown. The agreement indicated in Figure 9 is quite good considering the fact that the ground displacement of the 1960 earthquake was not known precisely. Figure 9 is the first comparison ever published of a recording of the 1960 tsunami and a numerical model calculation.

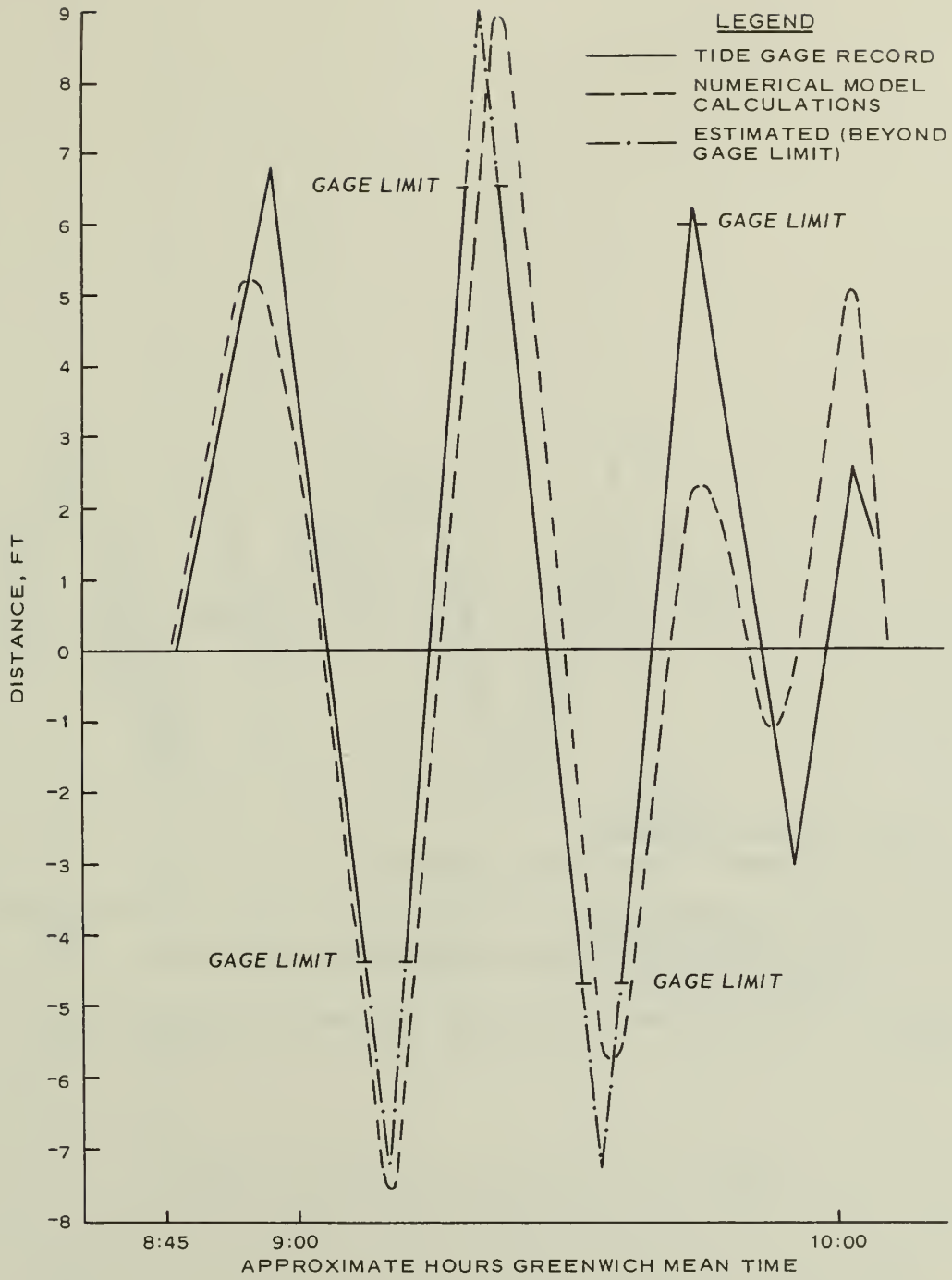

Figure 6. 1964 tsunami from Alaska recorded at Kahului, Maui

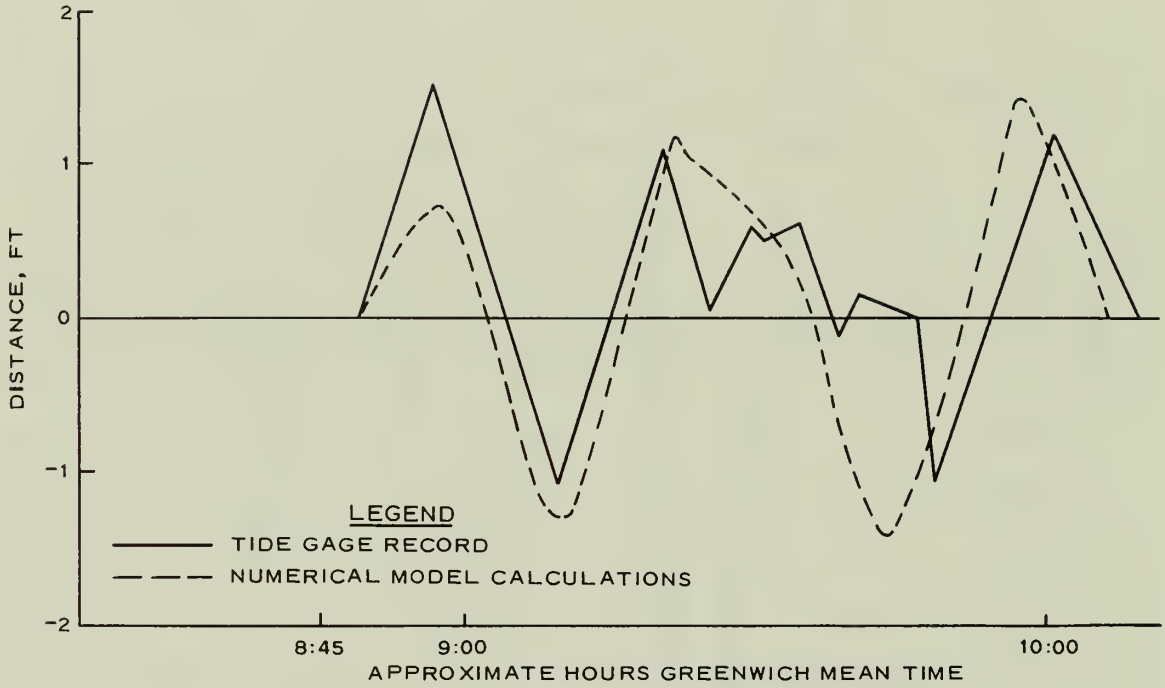

Figure 7. 1964 tsunami from Alaska recorded at Honolulu, Oahu

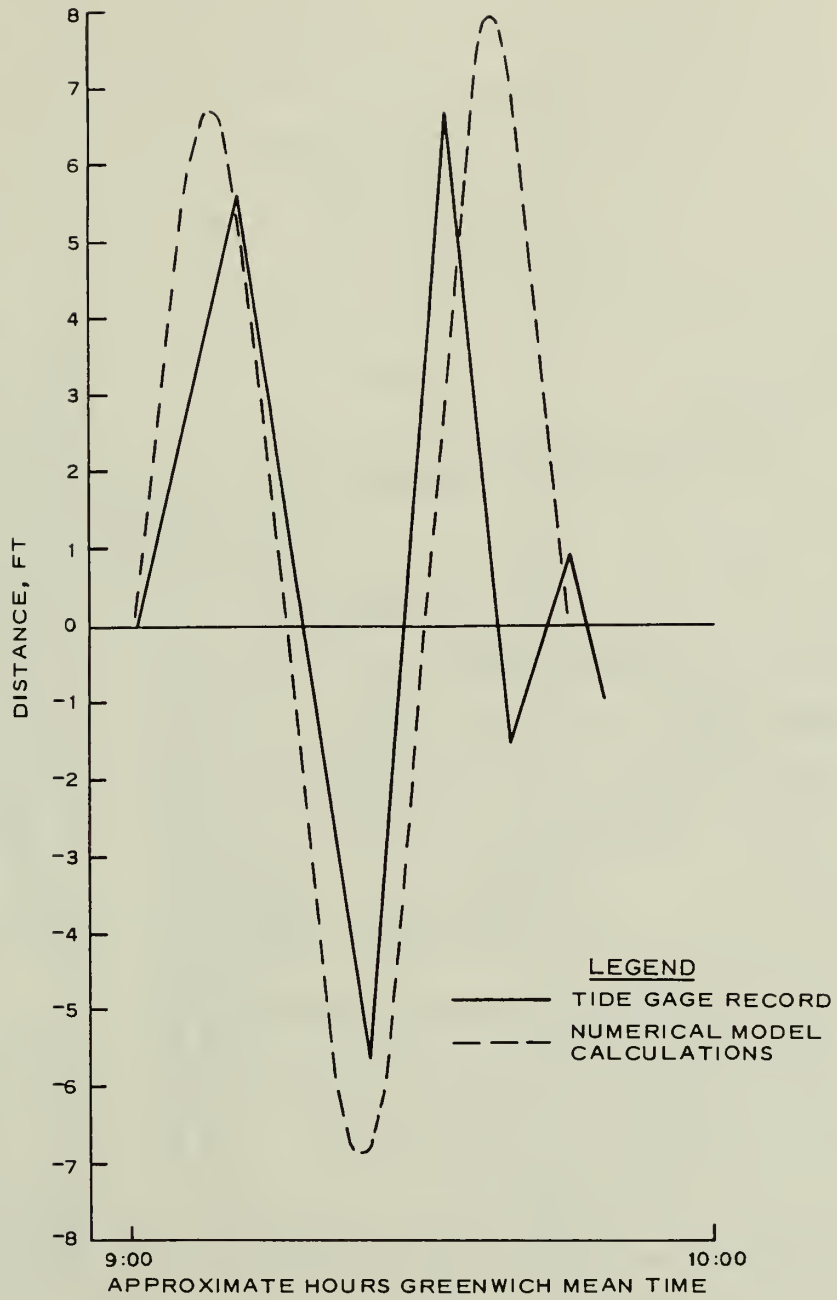

Figure 8. 1964 tsunami from Alaska recorded at Hilo, Hawaii

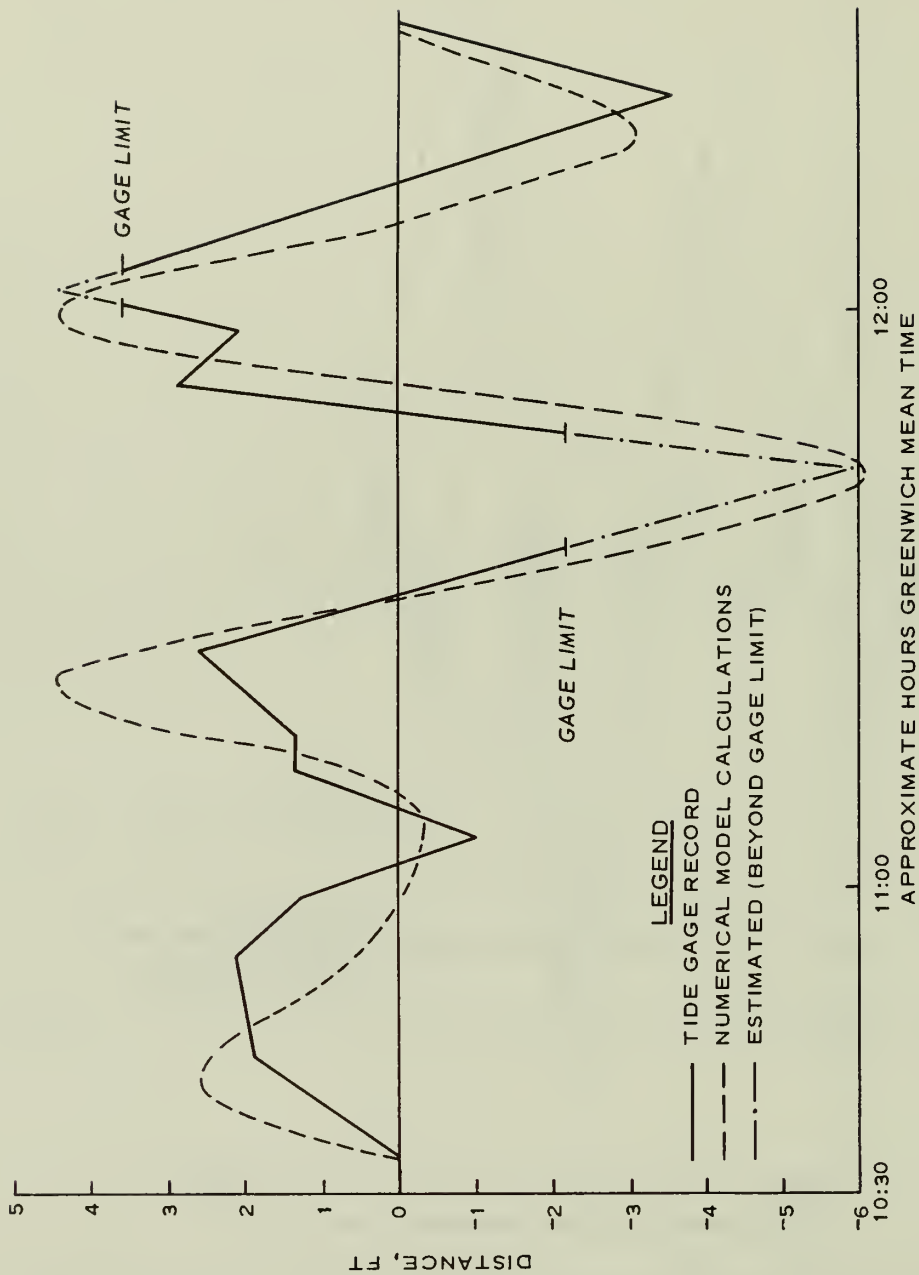

Figure 9. 1960 tsunami from Chile recorded at Honolulu, Oahu

67. The comparisons displayed in Figures 6 through 9 are also the first close comparisons of tide gage recordings of tsunamis in shallow water and numerical model calculations. Numerical model calculations have been compared with a recording of the 1964 tsunami by Van Dorn's gage at Wake Island which was located at a depth of approximately 800 ft.[33] Only the first wave of the tsunami was in good agreement in the comparison, however. A comparison also has been previously made for the 1964 tsunami at Hilo.[34] However, this comparison took a time history of the 1964 tsunami calculated over 100 miles from Hilo in a water depth of approximately 15,000 ft and used it as input to a fine finite difference grid covering only the immediate Hilo area with an input boundary approximately 6 to 7 miles from Hilo in about 1,000 ft of water. The wave period and phase of the waves in the comparison were not in good agreement, but the amplitudes of the largest waves were in reasonable agreement. The amplitudes of the computed waves depend upon the water depth at the input boundary of the grid, however, and can be changed by varying this depth. No explanation was given in Reference 34 for the depth used; however, it seems likely that it was chosen because the computed waves had reasonable amplitudes when this depth at the input boundary was tried and not when others were tried.

Model Use

68. The use of a numerical model as an aid for interpolation between historical data points can be illustrated for the 1960 tsunami from Chile (there were too few measurements of the 1964 tsunami from Alaska to be illustrative). Figure 10 shows a comparison on Oahu of the shoreline elevations calculated by the numerical model with historical measurements for the 1960 tsunami. The numerical and historical elevations do not compare as favorably as the comparison shown in Figure 9 for several reasons. First, the historical measurements are not at the shoreline. As discussed in Part II, these measurements occurred on an average of 200 ft from the shoreline. The water depths in elements of the numerical grid touching land also are variable around the island.

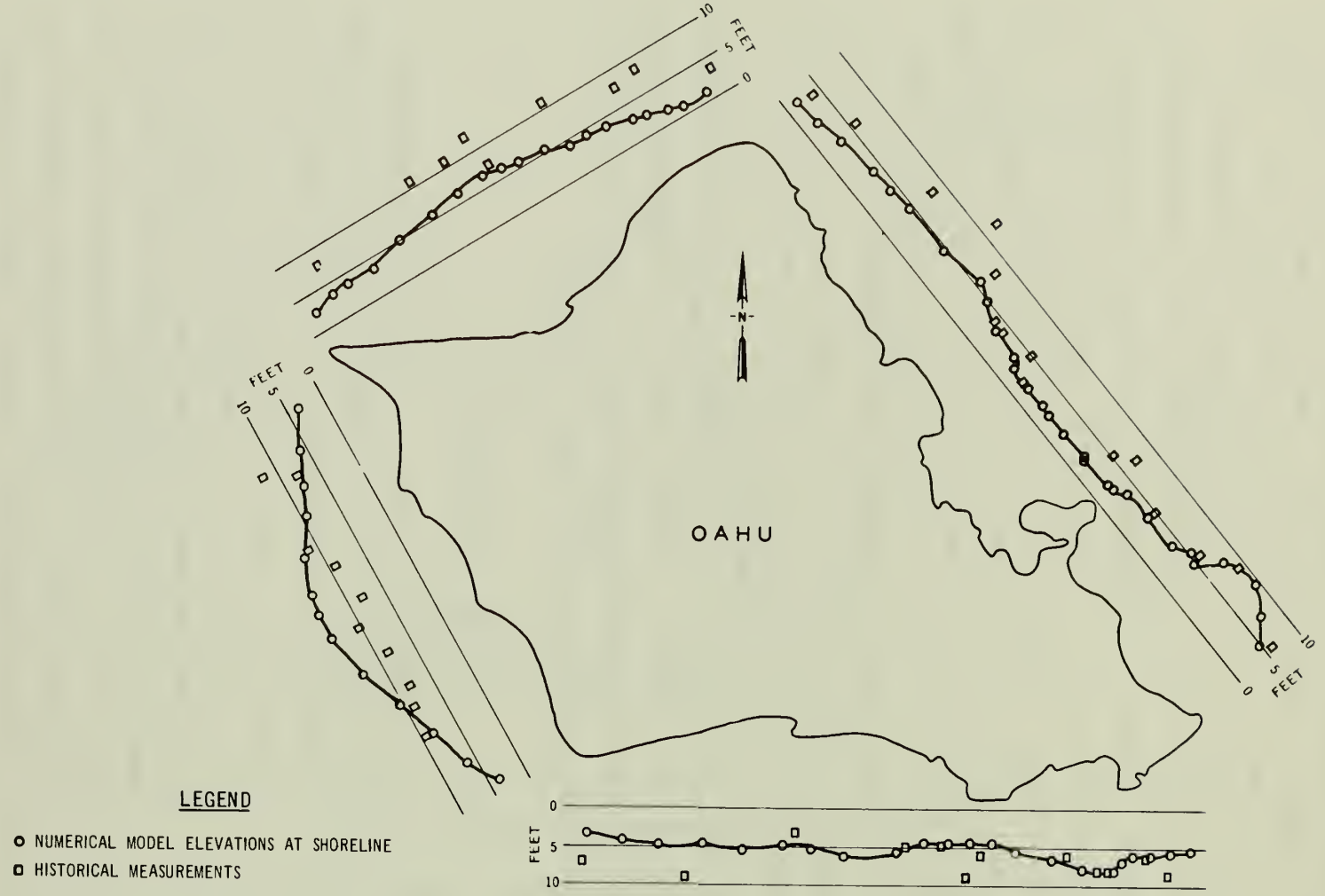

Figure 10. Comparison of numerical model shoreline elevations with historical measurements for the 1960 Chilean tsunamis

The depths cannot approach zero and, therefore, the shoaling process may not be complete. The tide gage recording shown in Figure 9 was in a depth of water well represented in the numerical grid. Furthermore, some parts of Oahu have reefs that may significantly influence tsunamis and may not be well simulated by the numerical model (especially if they are relatively narrow). Only the effect on the 1960 tsunami of the reefs of Kaneohe Bay are known from historical data. A tide gage at Mokuoloe Island in Kaneohe Bay[35] clearly shows that the reefs of the bay act like a low-pass filter, filtering out wave periods below approximately 1 hr. Thus, only components with periods above 1 hr were recomposed to give the elevations in Kaneohe Bay shown in Figures 10 through 16.

69. Figure 11 shows a comparison of the numerical model elevations of Figure 10 multiplied by correction factors with historical measurements for the 1960 tsunami from Chile. The correction factor for a point is determined by taking the ratio of the nearest historical measurement elevation and the numerical model elevation at the historical measurement location. This correction factor is then multiplied by the numerical model elevation at the point of interest. The final step is to require that the curve through the corrected numerical model elevations also pass through any historical measurements through which it does not already pass. Figure 12 shows elevations of the 1960 tsunami from Chile determined by this process. The correction factor determines all of the local factors not already determined by the numerical model. These local factors include the effects of land flooding to the point of the historical measurement, final shoaling near the shoreline, and effects of reefs. Figure 12 is, therefore, a reconstruction of elevations for the 1960 tsunami from Chile on the island of Oahu.

70. Figure 13 shows a comparison on Oahu of normalized numerical model shoreline elevations for a generalized tsunami from Kamchatka with normalized historical measurements for the 1952 tsunami from Kamchatka. Since the vertical uplift of the ground in the source region is not known for this tsunami, the deepwater form of the tsunami cannot be determined using a numerical model, as was done for the 1960 and 1964

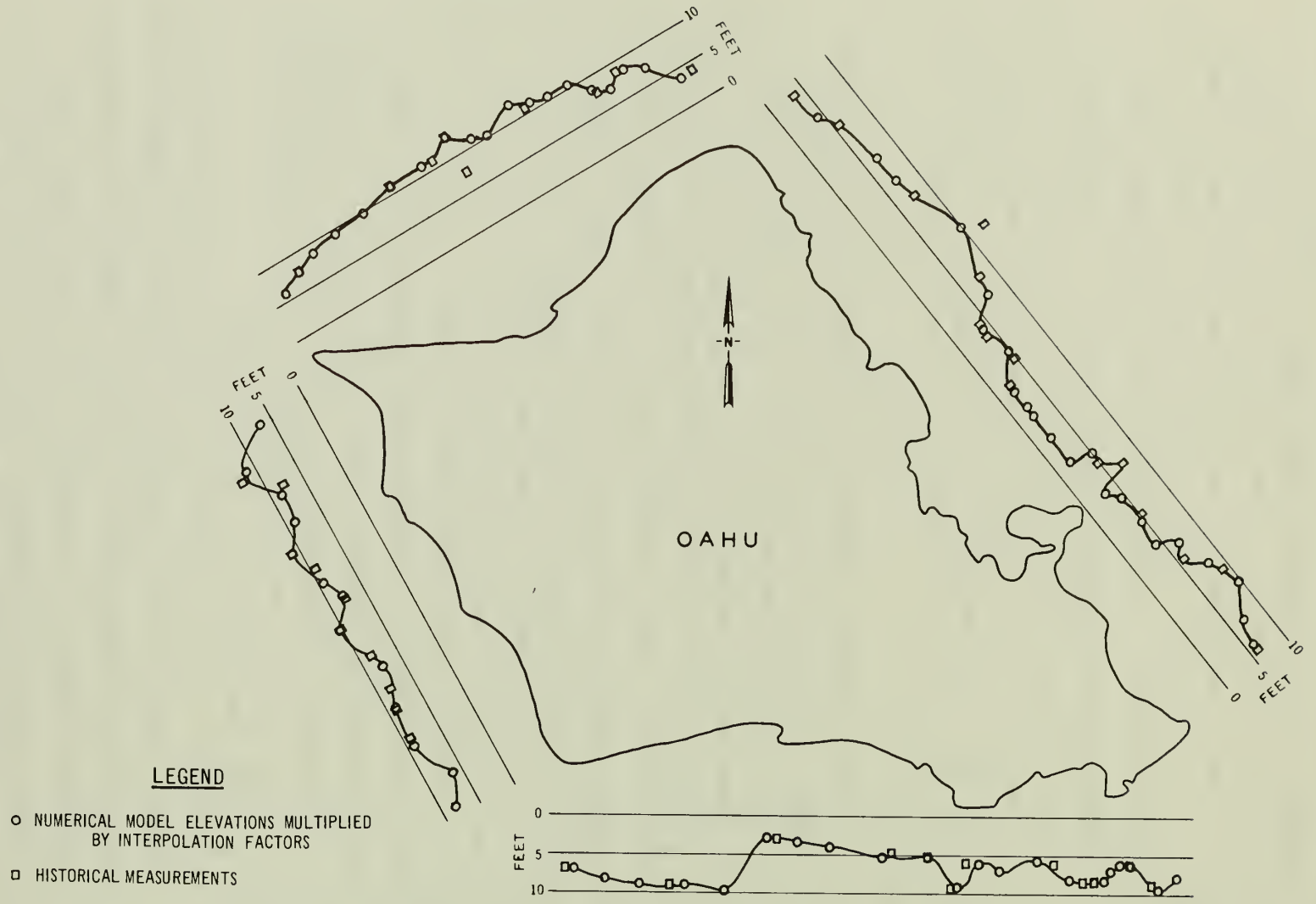

Figure 11. Comparison of numerical elevations multiplied by correction factors with historical measurements for the 1960 Chilean tsunami

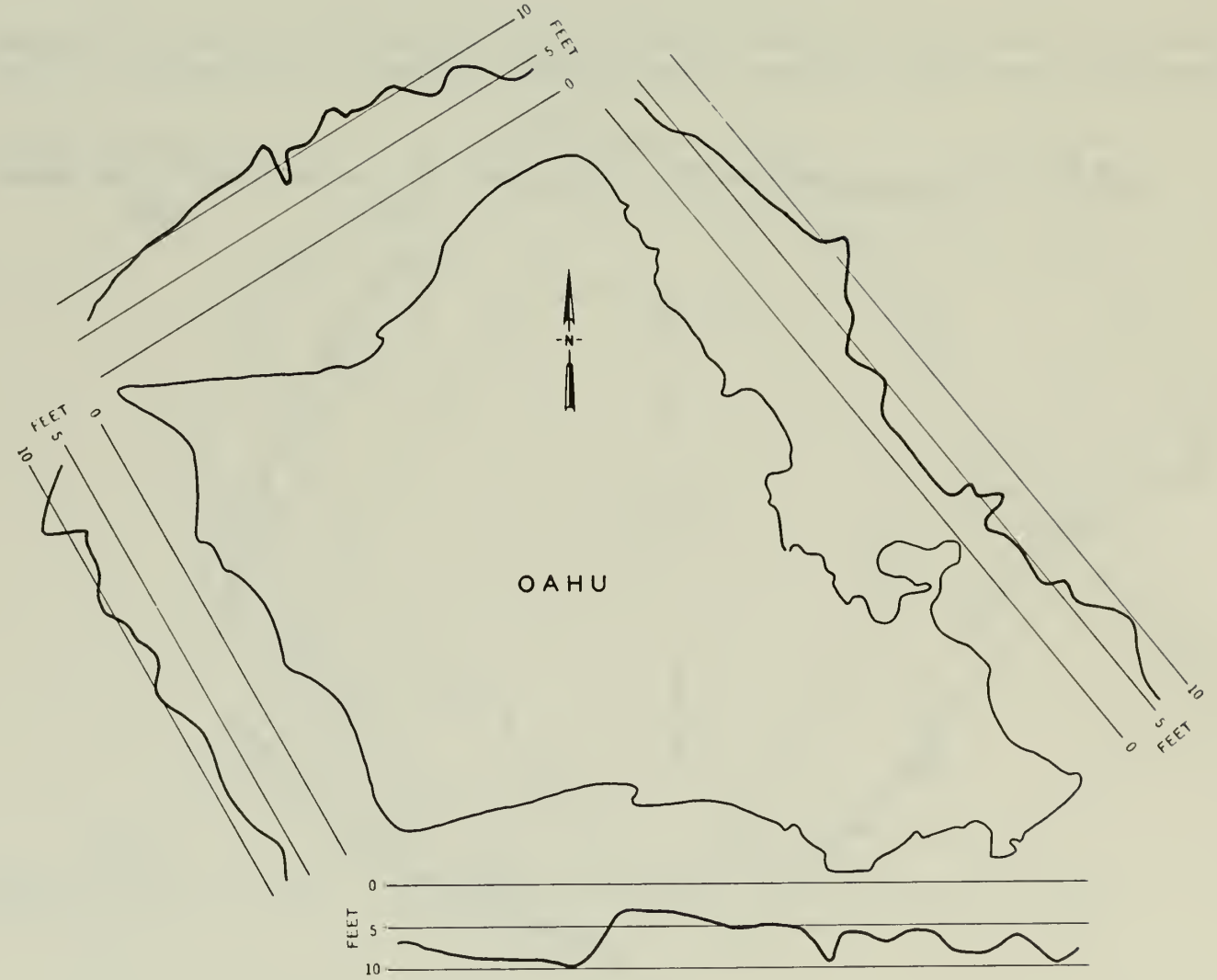

Figure 12. Elevations of 1960 Chilean tsunami from historical data and corrected numerical model elevations

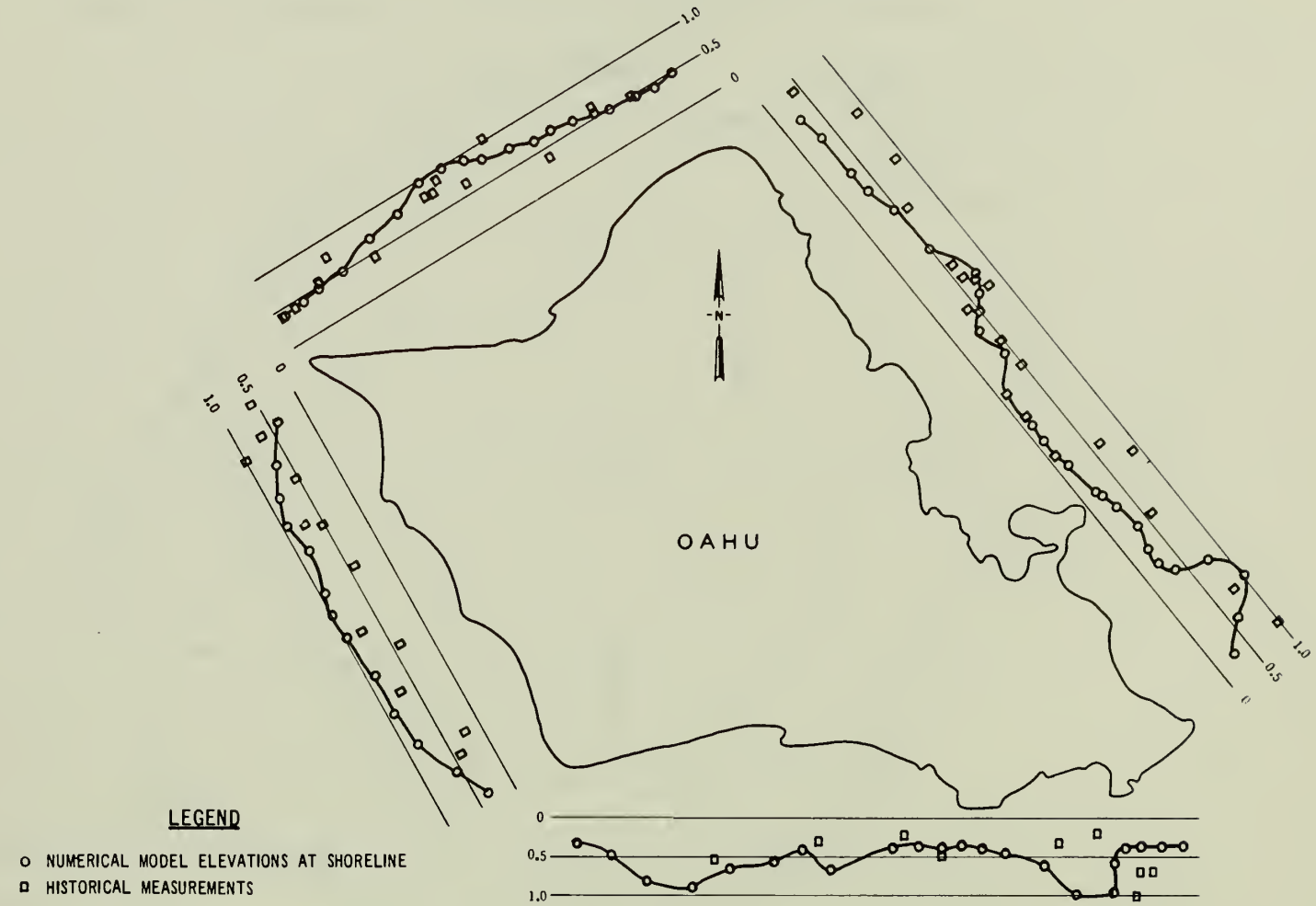

Figure 13. Comparison of normalized numerical model shoreline elevations for generalized Kamchatkan tsunami with normalized historical measurements for 1952 Kamchatkan tsunami

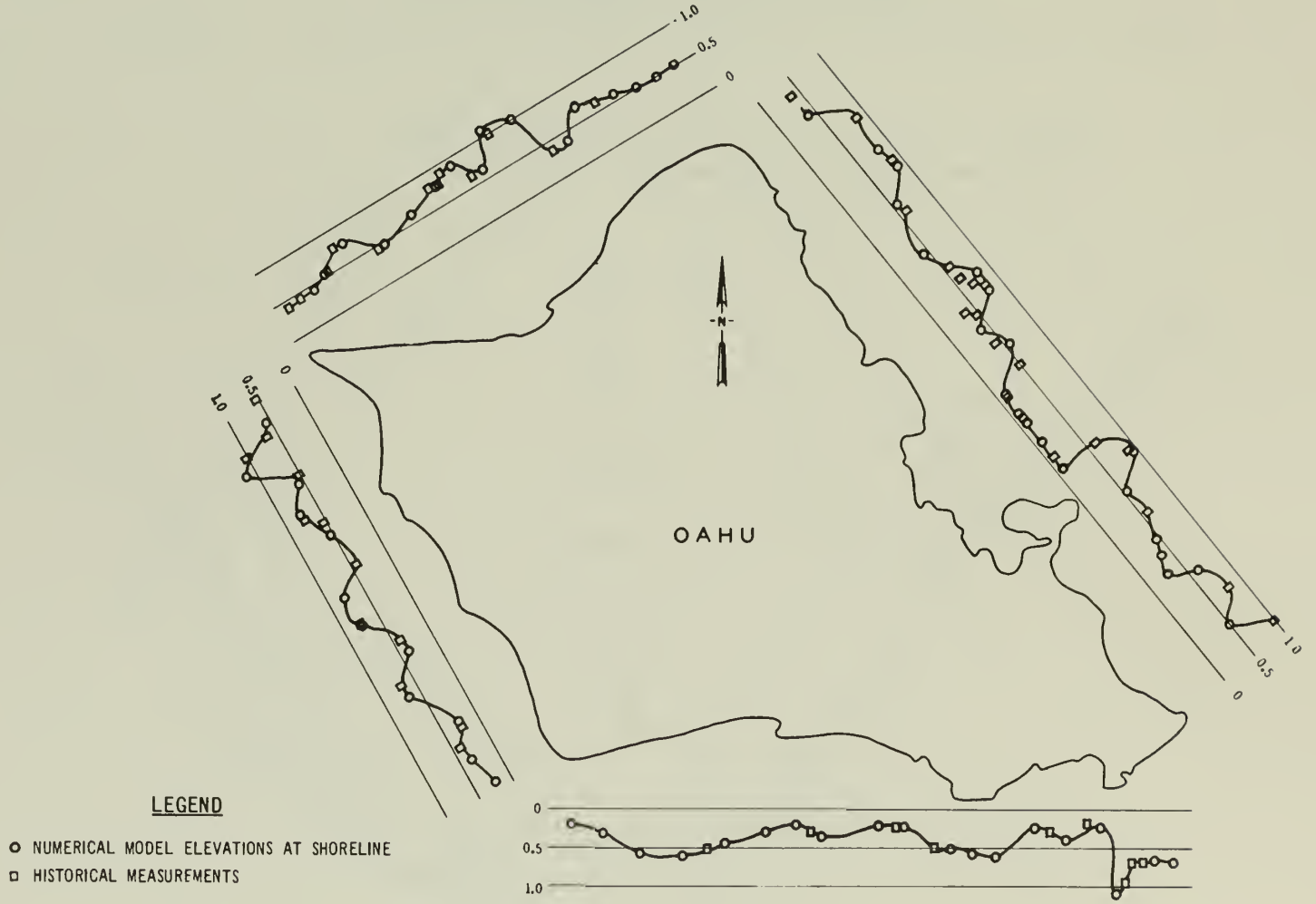

Figure 14. Comparison of numerical model elevations multiplied by correction factors for generalized Kamchatkan tsunami with normalized historical measurements for 1952 Kamchatkan tsunami

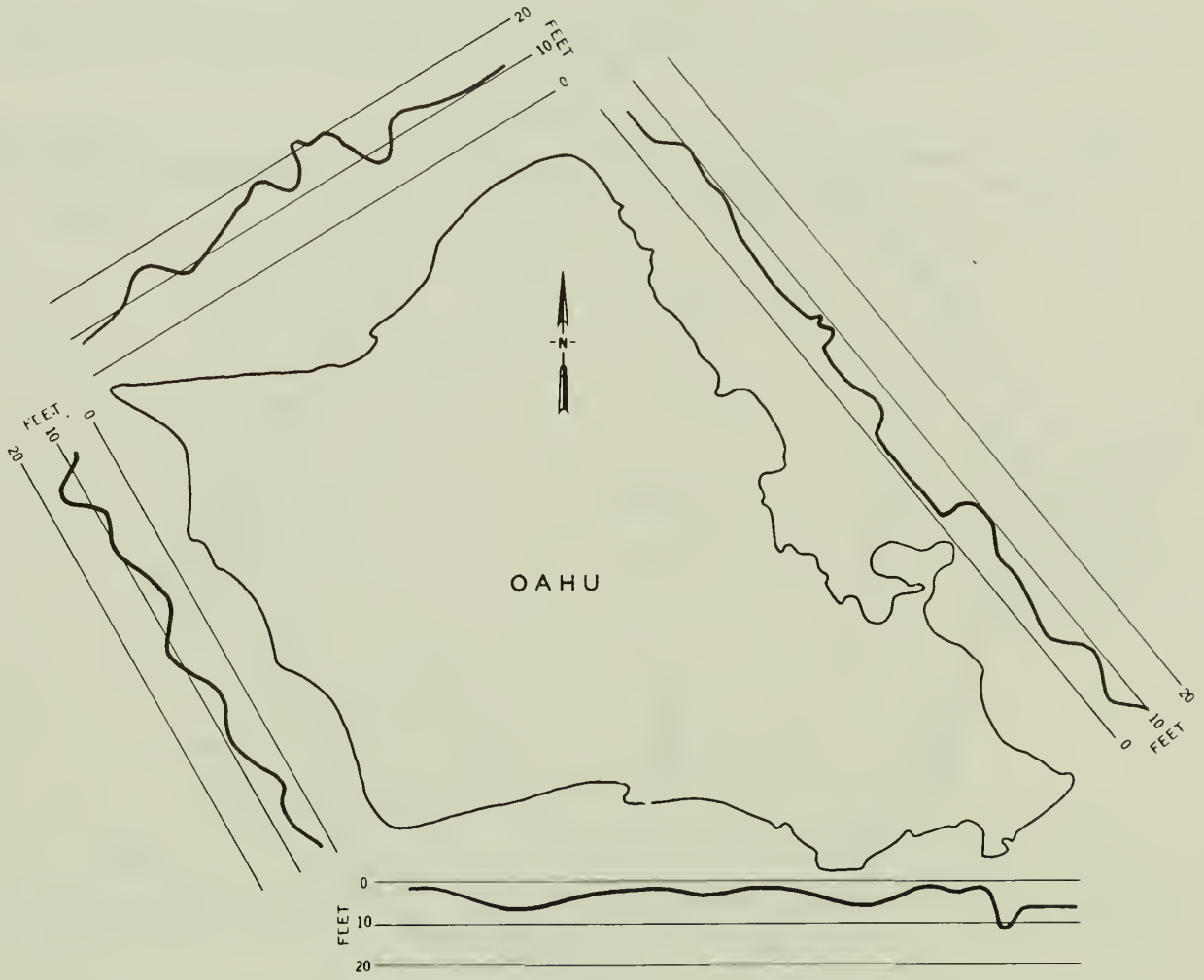

Figure 15. Elevations of 1952 Kamchatkan tsunami from historical data and corrected numerical model elevations

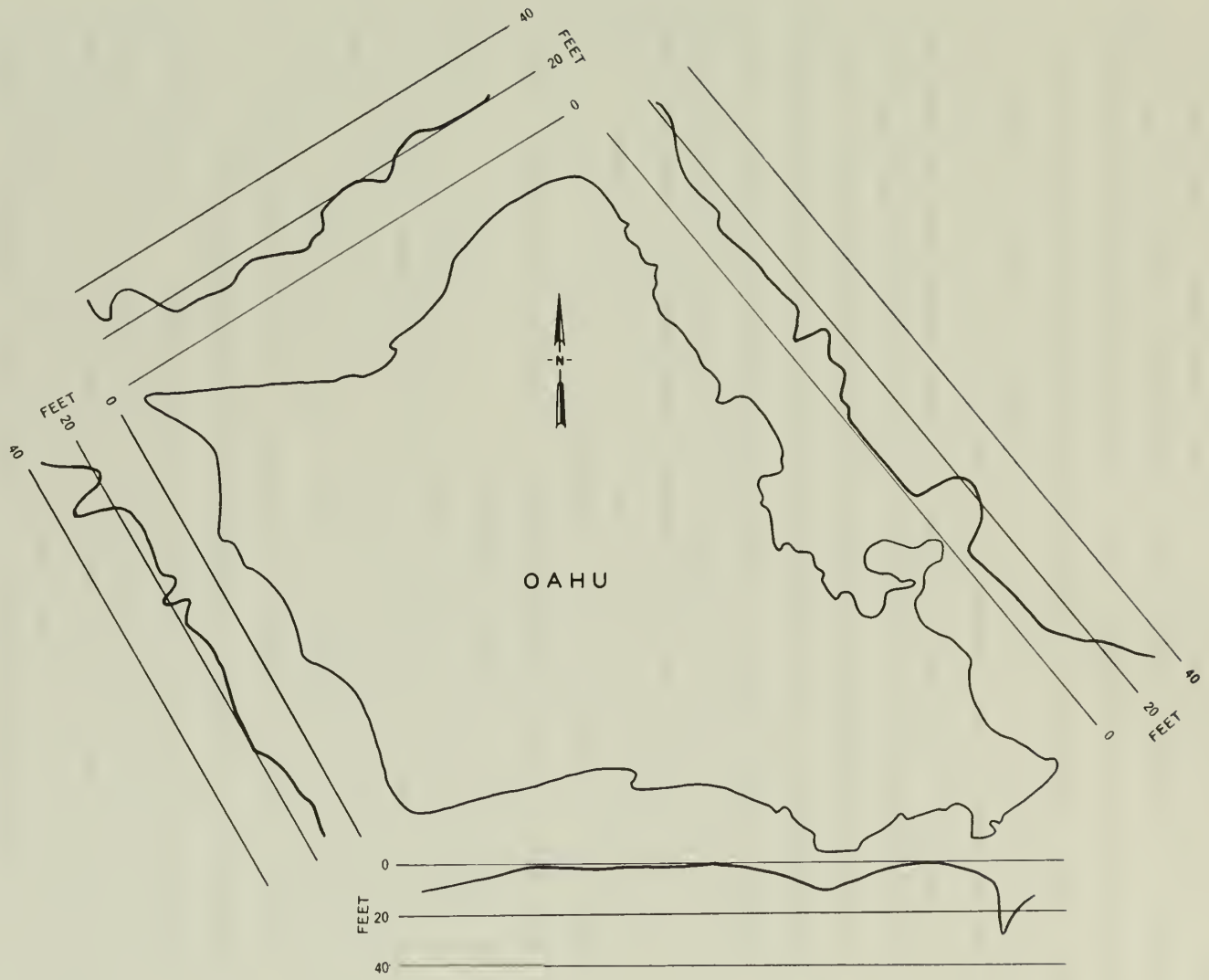

Figure 16. Elevations of 1946 Aleutian tsunami from historical data and corrected numberical model elevations

tsunamis. Therefore, an average or generalized Kamchatkan tsunami must be used as input to the numerical model, as discussed in Part II. Since a deep ocean height of the 1952 tsunami or a generalized Kamchatkan tsunami is not known, normalized elevations are shown. Both the numerical model elevations and the historical data have been normalized on each of the four sides of Oahu by the largest corresponding elevation on that particular side. Figures 14 and 15 show comparisons for the Kamchatkan tsunami analogous to Figures 11 and 12 for the 1960 tsunami. The normalization has been eliminated in Figure 15 by multiplying the elevations on each island side by the inverse of the factor used to normalize the historical data. Figure 16 shows elevations of the 1946 tsunami from the Aleutians determined from the historical data and the numerical model calculations. Again, a generalized tsunami had to be used to represent the 1946 tsunami because the source characteristics and consequently the deepwater form of this tsunami are unknown.

71. Figures 12, 15, and 16 can be used to determine elevations on Oahu for the 1960, 1952, and 1946 tsunamis, respectively, even for locations not having historical data for any or all of these tsunamis. Similar curves for the 1957 and 1964 tsunamis were derived. The same techniques were used to allow the prediction of elevations for these five tsunamis on all of the islands of Hawaii.

72. Reference 36 also used a numerical model (the finite difference model developed by Bernard[24]) to interpolate between estimated (from historical data) elevations produced on five islands by a tsunami from the north with a magnitude of four. This finite difference model had a grid size much too crude to adequately resolve island shapes, ocean bathymetry, or tsunami wavelengths (see paragraphs 54-56). A single Gaussian wave crest is inputted into the model. If a resolution of four grid cells per crest wavelength is maintained, this model cannot propagate waves in water with a depth less than about 500 ft. The main processes involved in the transformation of the form of a tsunami probably occur in the region over the continental shelf (depths less than 600 ft). Consequently, this model calculates elevations much smaller than historical data. The effects of propagation over the continental

shelf are determined by multiplying the numerical model elevations by a single factor for each island (two factors for the island of Hawaii), which results in the best agreement between the historical data and the corrected numerical model elevations.

73. The agreement is poor between historical data and the corrected numerical model elevations presented in Reference 36. For example, on the northeast side of Oahu, from Kahuku Point to Makapuu Point, the elevations for a magnitude four tsunami from the north vary from 7 to 10.7 ft. This remarkable lack of variation is undoubtedly a result of using a single factor for Oahu to represent the effects of propagation over the continental shelf. For a magnitude five tsunami, such as the 1946 Aleutian tsunami, these elevations must be multiplied by a factor of two, resulting in an elevation range from 14 to 21.4 ft. Reference 10 presents 36 historical elevations for the 1946 Aleutian tsunami on the northeast coast of Oahu from Kahuku Point to Makapuu Point, and only 7 fall within this range of elevations. The historical elevations actually vary from 1 to 37 ft on this coast.

PART IV: RESULTS

Use of Plots

74. Plates 1-8 show the location numbers that are plotted along the location axis in Plates 9-44. Plate 2 shows the location numbers for the Hilo area. The location numbers are equidistantly plotted in Plates 9-44 even though the distance between them shown in Plates 1-8 is not equidistant. *Plates 9-44, therefore show location and not distance along the coast. However, distances are true between integer numbers plotted along the location axis.* That is, if a place of interest is located halfway between two location numbers shown on one of the plots of Plates 1-8, it is also located halfway between the corresponding location numbers of Plates 9-44.

75. Plots displaying the A and B coefficients are shown in Plates 9-44. An island by island (plus the Hilo area) breakdown of the A- and B-coefficient plots is as follows (the uninhabited U. S. Navy target island of Kahoolawe (Figure 1) is not included):

Island	Coefficient A	Coefficient B
Hawaii	Plates 9-14	Plates 15-20
(Hilo)	Plates 12	Plate 18
Oahu	Plates 21-23	Plates 24-26
Maui	Plates 27-29	Plates 30-32
Kauai	Plates 33-34	Plates 35-36
Molokai	Plates 37-38	Plates 39-40
Lanai	Plate 41	Plate 42
Niihau	Plate 43	Plate 44

76. To illustrate how A and B are determined using Plates 1-44, the city of Waiahole in Kaneohe Bay on the island of Oahu has a location number of 31 (Plate 3). Plate 21 gives a value of 2.0 for coefficient A , and Plate 24 yields a B coefficient of 1.5. Then, these values of A and B plus F , which equals 0.05 for a 1-in-20-year event, are substituted into Equation 1 (see paragraph 37) as follows:

$$h_{20} = -1.5 - 2.0 \log_{10}(0.05)$$

$$= -1.5 - 2.0(-1.3)$$
$$= 1.1 \text{ ft}$$

77. If F equals 0.01 for a 1-in-100-year event, substituting in Equation 1 results in

$$h_{100} = -1.5 - 2.0 \log_{10}(0.01)$$
$$= -1.5 - 2.0(-2)$$
$$= 2.5 \text{ ft}$$

78. The tsunami elevations in Kaneohe Bay are very small as a result of an extensive reef protecting the bay from tsunamis.

79. Another example is a calculation for Makawana Point on the island of Maui. Plate 4 shows Makawana Point lying one third of the way between points 34 and 35. The values, A = 22 and B = 22.5 , come from Plates 28 and 31, respectively. Substituting these values in Equation 1 with a 1-in-20-year frequency yields

$$h_{20} = -22.5 - 22 \log 0.05$$
$$= -22.5 - (22)(-1.3)$$
$$= 6.1 \text{ ft}$$

and with a 1-in-100-year frequency gives

$$h_{100} = -22.5 - 22 \log 0.01$$
$$= -22.5 - (22)(-2)$$
$$= 21.5 \text{ ft}$$

One-in-Ten-Year Heights

80. Part II discusses the fact that the linear relation between the logarithm of tsunami frequency of occurrence and tsunami elevations at Hilo is valid for frequencies of occurrence lower than 0.1 per year only. There are some locations where this linear relation is valid for

frequencies of occurrence equal to or lower than 0.05 per year only. It is, therefore, recommended that Equation 1 and Plates 9-44 be used for frequencies of occurrence equal to or lower than 0.05 per year. The one-in-ten-year frequency of occurrence for the entire Hawaiian coastline can be determined by using Table 1. The elevations presented in this table were estimated by multiplying the elevation of the tenth largest tsunami at a location (return period of 140 years divided by ten, i.e. 14 years) by 0.7. The value of 0.7 is the ratio of the return period of the frequency 0.1 tsunami (10 years) and the return period of the tenth largest tsunami (14 years). Frequencies of occurrence between 0.1 and 0.05 can be linearly interpolated between the 0.1 values from Table 1 and calculations using Equation 1 for a 1-in-20-year frequency of occurrence.

Discussion

81. Since the plots in Plates 9-44 are strongly based upon historical data, they should show trends similar to those in the historical data. Of course, frequency of occurrence depends upon both the absolute and relative magnitudes of the A and B coefficients. It is difficult to make generalizations involving only one of these coefficients. However, it is true that the elevations calculated for tsunamis with a low frequency of occurrence are usually large when A is large.

82. Plates 9-14 show the A coefficient for the big island of Hawaii. The coefficient is fairly small all along the west coast of Hawaii except for moderate values from Napoopoo to Keauhau resulting from the fairly large tsunami that struck this area in 1896. However, A is large along the northeast coast of Hawaii with a very large peak near the Pololu Valley caused by the large tsunami elevations that occurred during the 1946 and 1960 tsunamis. In the Hilo Bay area, the A value is fairly large but not in comparison with the A values along the northeast coast. Extensive damage and great loss of life occurs in Hilo but not along the northeast coast because Hilo is the most populous city on the island of Hawaii and has a low-lying waterfront area,

whereas the northeast coast is sparsely settled with villages on high cliffs. Plates 13 and 14 show large A values on the South Puna coast due to the local tsunamis of 1868 and 1975.

83. Plates 21-23 show A values for the island of Oahu. The largest A values for Oahu are generally at the corners or tips of the island. For example, there are peaks in the A-coefficient plots at Kaena Point, Kahuku Point, Mahie Point, Mokapu Point, Makupuu Point, and Diamond Head (Figure 1). Other islands of the Hawaiian Islands often display a similar trend of large A values on island tips. The A coefficient values are small on Oahu in reef-protected Kaneohe Bay and in Pearl Harbor.

84. The 1-in-100-year elevations for Oahu that can be calculated using the information presented in this report are in general less than the 1-in-100-year elevations calculated in an earlier tsunami study (Reference 4) except at Honolulu. However, Reference 4 used data for the period 1946 through 1964 only, except for Honolulu, where data dating back to 1837 were used.

85. Values of A for the island of Maui are shown in Plates 27-29. The A coefficient is fairly small on the south coast of the island and large on the north coast. This difference in A values between the north and south coasts of the island is due to the fact that the 1946 tsunami from the Aleutian Islands produced the largest historical elevations on the island. The north coast is directly exposed to tsunamis generated in the Aleutians, whereas the south coast is shielded. This same effect of wave elevations on the back side of an island being less than elevations on the side of the island facing the tsunami-generating area occurs on Kauai, Molokai, and Niihau. The 1946 and 1957 tsunamis from the Aleutian Islands were the largest to strike all three of these islands. The south coast of Molokai is also reef protected, and this partially accounts for its exceptionally low values of A.

86. Since data were taken from a 140-year period of time (1837-1976), the 1-in-140-year tsunami elevation at a location should be similar to the largest value during the 140-year period at the

location. This is usually the case, of course. For example, the 1-in-140-year elevation near Mooheau Park in Hilo (Plate 2) is approximately 28 ft according to Equation 1 and Plates 12 and 18. The largest historical elevation above mean sea level was 26 ft during the 1946 tsunami. The 1-in-140-year elevation at Lahaina, Maui, is 10 ft according to Equation 1 and Plates 27 and 30. The largest historical elevation was 9 ft during the 1960 tsunami.

Risk Calculation

87. The average frequency of occurrence F is a mean exceedance frequency, i.e. an average frequency per year of tsunamis of equal or greater elevation. It is also possible to calculate the chance of a given elevation being exceeded in a certain period of time. Such a calculation is a risk calculation.

88. Tsunamis are usually caused by earthquakes, and earthquakes are often idealized as a generalized Poisson process.[37,38] Many investigators have assumed that tsunamis also follow such a stochastic process.[19,39] The probability that a tsunami with an average frequency of occurrence of F is exceeded in D years, assuming that tsunamis follow a Poisson process, is given by the following equation:

$$P = 1 - e^{-FD} \tag{12}$$

89. For example, the probability that the 1-in-100-year elevation of 21.5 ft at Makawana Point, Maui (Plate 4), will occur in a 50-year period is

$$\begin{aligned} P &= 1 - e^{-(0.01)(50)} \\ &= 1 - e^{-0.05} \\ &= 1 - 0.61 \\ &= 0.39 \end{aligned}$$

and in a 10-year period is

$$P = 1 - e^{-(0.01)(10)}$$
$$= 1 - e^{-0.1}$$
$$= 1 - 0.9$$
$$= 0.1$$

90. As mentioned in the introductory section of Part I, an evaluation of risk is important whenever human life may be exposed to possible danger as a result of land development. For example, it would certainly be extremely foolhardy to base tsunami evacuation zones simply on something like the 1-in-100-year elevations given in this report. As shown in the previous paragraph, the odds that a 1-in-100-year event will occur during a 10-year period are not insignificant.

91. Risk calculations can be used to add a safety factor when evaluating whether or not it is prudent to develop land at some elevation that might expose human life to possible danger. First, it is necessary to decide on some acceptable risk. For example, perhaps a one chance in 10,000 that an elevation be exceeded during a 10-year period is an acceptable risk. (This risk is used only for illustration and not to suggest that such a risk is or is not acceptable.) Then D of Equation 12 equals 10 and P equals 0.0001. Substituting these values of D and P in Equation 12 yields an F equal to approximately 0.00001. Therefore, the elevation for which there is only one chance in 10,000 that the elevation will be exceeded during a 10-year period is the 1-in-100,000-year elevation. For Makawa Point, Maui, this elevation would be 87 ft (substituting $F = 0.00001$ and A and B values from Plates 28 and 31 into Equation 1). Of course, Equation 1 may not be valid for the 1-in-100,000-year tsunami, since the linear relationship between h and the logarithm of F may not be valid for arbitrarily small values of F. However, there is not sufficient historical data at this time to determine any other relationship between h and F.

PART V: CONCLUSIONS AND RECOMMENDATIONS

Conclusions

92. The hybrid finite element numerical model was shown to be an excellent numerical method for determining the interaction of tsunamis with the Hawaiian Islands. The comparisons presented between the numerical model calculations and historical tide gage recordings for the 1960 and 1964 tsunamis were the first close comparisons for tsunamis in shallow water. This accurate modeling of tsunamis by a numerical model is a significant breakthrough in tsunami research. Future studies using this numerical model may develop a greater understanding of the processes that lead to large tsunami elevations at one location along a coast and small elevations at a nearby location. Understanding a problem is the first step toward alleviating it. Furthermore, sound floodplain management involves not only understanding possible hazards to an area that may be developed, but also the effect the development itself may have on the hazard. The finite element model can be used to test the effect on tsunami elevations of topographic or bathymetric modifications in an area.

93. This report presents a simple method to determine the frequency of occurrence of tsunami elevations above mean sea level at the shoreline for frequencies equal to or lower than 1-in-10 years for the entire coastline of the Hawaiian islands (except for the uninhabited U. S. Navy target island of Kahoolawe). For some of the coastline of the Hawaiian Islands, runup above mean sea level can be shown to nearly equal wave elevation above mean sea level at the shoreline both for tsunamis producing water-surface changes similar to rapidly rising tides and for borelike waves. Thus, the elevations calculated using the methods presented also are often runup elevations. However, there are places, such as low-lying or estuarine areas, or areas with large elevations at the shoreline, where the wave elevation decreases as the wave moves across the land so that runup is less than the elevation at the shoreline. Such an effect probably occurs whenever there is significant flooding during a tsunami.

Recommendations

94. Bretschneider and Wybro[40] have developed a one-dimensional (1-D) approach to estimate flooding that neglects time-dependent effects but does include dissipative effects. Since the method is 1-D, it neglects flow convergence and divergence; thus, it is valid only for straight coastlines where land elevation contours are parallel to the coast, and there are no natural or man-made barriers (large rock outcropping, buildings, or elevated roads) or land roughness variations along the coastline (e.g. due to elimination of homogeneous natural vegetation or topography by development and replacement by partial grass plantings and land grading). Since the method allows no time dependence, it is not valid for large low-lying areas where there would be insufficient time for complete flooding or areas where coastline restrictions (e.g. harbors) or sand dune barriers limit the rate of flooding and thus make the time dependence of the flooding important. This method is not completely adequate for bays, harbors, land points, developed areas such as cities, large low-lying areas, some sand-dune protected areas, and other areas where there are topographical, roughness, or coastline variations. There are many sections of coast in the Hawaiian Islands where assumptions of this method are approximately satisfied. The method is suitable for application on these largely unpopulated open coasts.

95. There is not a numerical model at this time that includes two-dimensional and time-dependent effects of land flooding during a tsunami. However, the WES has developed an implicit finite difference numerical model for simulating the tidal hydrodynamics of an inlet, bay, or harbor.[41] This model includes variable bottom roughness, nonlinear advective terms in the momentum equations, treatment of regions that are inundated during a portion of the tidal cycle, exposed and submerged barriers, and other physical features of the region to be modeled. It is recommended that the WES model[41] be modified so that it can be used in conjunction with results of this study to determine actual runup for areas where runup may not be equal to elevation at the shoreline and where Bretschneider's method is not completely satisfactory.

REFERENCES

1. Iida, K., Cox, D. C., and Pararas-Carayannis, G., "Bibliography to the Tsunamis Occurring in the Pacific Ocean," HIG-67-25, Dec 1967, Hawaii Institute of Geophysics, University of Hawaii, Honolulu, Hawaii.

2. Pararas-Carayannis, G., "Catalog of Tsunamis in the Hawaiian Islands," WDCA-T-69-2, May 1969, Environmental Science Services Administration, Coast and Geodetic Survey, Washington, D. C.

3. U. S. Army Engineer District, Honolulu, CE, "The Tsunami of 23 May 1960 in Hawaii," Final Post Flood Report, 25 Apr 1962, Honolulu, Hawaii.

4. R. M. Towill Corporation, "Tsunami Studies for Oahu, Hawaii," May 1975, Honolulu, Hawaii.

5. Cox, D. C., "Tsunami Height-Frequency Relationship of Hilo," Unpublished Paper, Nov 1964, Hawaii Institute of Geophysics, University of Hawaii, Honolulu, Hawaii.

6. Soloviev, S. L. and Go, N., "Catalog of Tsunamis in the Pacific (Main Data)," 1969, Union of Soviet Socialist Republics, Moscow.

7. McGarr, A., "Upper Limit to Earthquake Size," Nature, Vol 262, No. 5567, 29 Jul 1976, pp 378-379.

8. Plafker, G. and Rubin, M., "Vertical Tectonic Displacements in South-Central Alaska During and Prior to the Great 1964 Earthquake," Journal of Geoscience of Osaka City University, Vol 10, No. 53, 1967.

9. Cox, D. C. and Pararas-Carayannis, G., "Catalog of Tsunamis in Alaska, Revised 1976," World Data Center A, Report SE-1, 1976, for Solid Earth Geophysics, National Aeronautics and Atmospherical Administration, Washington, D. C.

10. Loomis, H. G., "Tsunami Wave Runup Heights in Hawaii," HIG-76-5, May 1976, Hawaii Institute of Geophysics, University of Hawaii, Honolulu, Hawaii.

11. Garcia, A. W., "Effect of Source Orientation and Location in the Peru-Chile Trench on Tsunami Amplitude Along the Pacific Coast of the Continental United States," Research Report H-76-2, Sep 1976, U. S. Army Engineer Waterways Experiment Station, CE, Vicksburg, Miss.

12. Eaton, J. P., Richter, D. H., and Ault, W. U., "The Tsunami of May 23, 1960, on the Island of Hawaii," Bulletin, Seismological Society of America, Vol 51, No. 2, Apr 1961, pp 135-157.

13. Wybro, P. G., "M. S. Plan B" (to be published), University of Hawaii, Honolulu, Hawaii.

14. Loomis, H. G., "The Tsunami of November 29, 1975 in Hawaii," HIG-75-21, Dec 1975, Hawaii Institute of Geophysics, University of Hawaii, Honolulu, Hawaii.

15. Soloviev, S. L., "Recurrence of Tsunamis in the Pacific," Proceedings, International Symposium on Tsunamis and Tsunami Research, 1969.

16. Gutenberg, B. and Richter, C. F., Seismicity of the Earth and Associated Phenomena, 2d ed., Hafner Publishing Co., New York, 1965.

17. Wiegel, R., Earthquake Engineering, Chapter III, Prentice-Hall, Englewood Cliffs, 1970.

18. Adams, W. M., "Tsunami Effects and Risk at Kahuku Point, Oahu, Hawaii," Engineering Geology Case Histories, Geological Society of America, No. 8, 1970, pp 63-70.

19. Rascon, O. A. and Villarreal, A. G., "On a Stochastic Model to Estimate Tsunami Risk," Journal, Hydraulic Research, Vol 13, No. 4, 1975, pp 383-403.

20. Cox, D. C., "Proposed Oahu Tsunami: Hazard Zone, National Flood Insurance Program," Jan 1977, University of Hawaii, Environmental Center Review RR:0048.

21. Gumbel, E. J., "The Calculated Risk in Flood Control," Applied Scientific Research, Section A, Vol 5, 1955, pp 273-280.

22. Borgman, L. E. and Resio, D. T., "External Prediction in Wave Climatology," Ports 77, 4th Annual Symposium of the Waterway, Port, Coastal, and Ocean Division, American Society of Civil Engineers, Vol 1, Mar 1977, pp 394-412.

23. Chen, H. S. and Mei, C. C., "Oscillations and Wave Forces in an Offshore Harbor (Applications of the Hybrid Finite Element Method to Water-Wave Scattering)," Report No. 190, 1974, Massachusetts Institute of Technology, Cambridge, Mass.

24. Bernard, E. N., "Linearized Long Wave, Numerical Model of the Hawaiian Islands," HIG-75-13, Jun 1975, Hawaii Institute of Geophysics, University of Hawaii, Honolulu, Hawaii.

25. Houston, J. R. and Garcia, A. W., "Type 16 Flood Insurance Study: Tsunami Predictions for Pacific Coastal Communities," Technical Report H-74-3, May 1974, U. S. Engineers Waterways Experiment Station, CE, Vicksburg, Miss.

26. Garcia, A. W. and Houston, J. R., "Type 16 Flood Insurance Study: Tsunami Predictions for Monterey and San Francisco Bays and Puget Sound," Technical Report H-75-17, Nov 1975, U. S. Army Engineer Waterways Experiment Station, CE, Vicksburg, Miss.

27. Houston, J. R. et al., "Effect of Source Orientation and Location in the Aleutian Trench on Tsunami Amplitude Along the Pacific Coast of the Continental United States," Research Report H-75-4, Jul 1975, U. S. Army Engineer Waterways Experiment Station, CE, Vicksburg, Miss.

28. Tuck, E. O. and Hwang, L.-S., "Long Wave Generation on a Sloping Beach," Journal of Fluid Mechanics, Vol 51, Part 3, 1972, pp 449-461.

29. Plafker, G., "Tectronics of the March 27, 1964 Alaska Earthquake," U. S. Geological Survey Professional Paper 543-I, 1969, pp 11-174.

30. Plafker, G. and Savage, J. C., "Mechanism of the Chilean Earthquake of May 21 and 22, 1960," Bulletin, Geological Society of America, Vol 81, No. 4, 1970, pp 1001-1030.

31. Hwang, L.-S., Divoky, D., and Yuen, A., "Amchitka Tsunami Study," Report TC-177, Jun 1970, Tetra Tech, Inc., Pasadena, Calif.

32. Noye, B. J., "The Frequency Response of a Tide-Well," Proceedings, Third Australian Conference on Hydraulics and Fluid Mechanics, The Institution of Engineers, Australia, Sidney, 1970, pp 65-71.

33. Van Dorn, W. G., "Tsunami Response at Wake Island," Journal of Marine Research, Vol 28, No. 3, 1970, pp 336-344.

34. Hwang, L. S. and Divoky, D., "Numerical Investigations of Tsunami Behavior," Final Report, Mar 1975, Tetra Tech, Inc., Pasadena, Calif.

35. Symons, J. M. and Zetler, B. D., "The Tsunami of May 22, 1960 as Recorded at Tide Stations," Preliminary Report, U. S. Department of Commerce, Coast and Geodetic Survey, Washington, D. C.

36. Adams, W. M., "Conditional Expected Tsunami Inundation for Hawaii," Journal, Waterways, Harbors, and Coastal Engineering Division, American Society of Civil Engineers, Vol 101, WW4, Nov 1975, pp 319-329.

37. Newmark, N. M. and Rosenblueth, E., Fundamentals of Earthquake Engineering, Prentice-Hall, Englewood Cliffs, 1971.

38. Esteva, L., "Bases para la Formulacion de Decisiones de Diseno Sismico," Report 182, 1968, Instituto de Ingenieria, UNAM.

39. Wiegel, R. L., :Protection of Crescent City, California, from Tsunami Waves," Mar 1965, Redevelopment Agency of the City of Crescent City, Berkeley, Calif.

40. Bretschneider, C. L. and Wybro, P. G., "Tsunami Inundation Prediction," Proceedings of the 15th Coastal Engineering Conference, American Society of Civil Engineers, pp 1000-1024.

41. Butler, H. L. and Raney, D. C., "Finite Difference Schemes for Simulating Flow in an Inlet-Wetlands System," Proceedings, 1976 Numerical Analysis and Computers Conference, Report 76-3, Sep 1976, pp 393-411, Army Research Office, Research Triangle Park, N. C.

Table 1

1-in-10-Year Elevations for Hawaiian Coastline

Island	Location	Elevation, ft
Hawaii	1-74	1.5
	75-81	2.0
	82	2.5
	83-95	3.0
	96-100	3.5
	101-103	4.0
	104	6.0
	105	4.0
	106-111	3.5
	112-121	3.0
	122-135	2.5
	136-154	2.0
Oahu	1-5	3.0
	6	3.5
	7-12	4.0
	13-16	3.5
	17-26	3.0
	27	2.5
	28	2.0
	29	1.5
	30-39	0.5
	40	1.0
	41	2.0
	42-62	2.5
	63	2.0
	64-65	1.5
	66-72	1.0
	73-87	Negligible
	88	1.0
	89-91	1.5
	92	2.0
	93-94	2.5
	95-105	3.0
Maui	1-3	1.5
	4-6	2.0
	7-24	2.5
	25-33	2.0
	34	2.5
	35	3.0
	36	4.0
	37-41	5.5
	42	4.0
	43	3.0
	44	2.5
Maui (Continued)	45	2.0
	46	1.5
	47-81	1.0
Kauai	1-10	3.0
	11-15	2.5
	16-18	2.0
	19-55	1.5
	56	2.0
	57	2.5
	58	3.0
Molokai	1-2	2.5
	3-5	3.0
	6-7	3.5
	8	3.0
	9	2.5
	10	2.0
	11-12	1.5
	13-25	1.0
	26	0.5
	27-32	1.0
	33-52	0.5
	53	1.0
	54	1.5
	55	2.0
Lanai	1	1.0
	2	1.5
	3-5	2.0
	6-7	1.5
	8-14	2.0
	15	1.5
	16-17	1.0
	18-34	0.5
Niihau	1-2	1.0
	3-8	1.5
	9	2.0
	10	2.5
	11-14	3.0
	15	2.5
	16	2.0
	17	1.5
	18-19	1.0

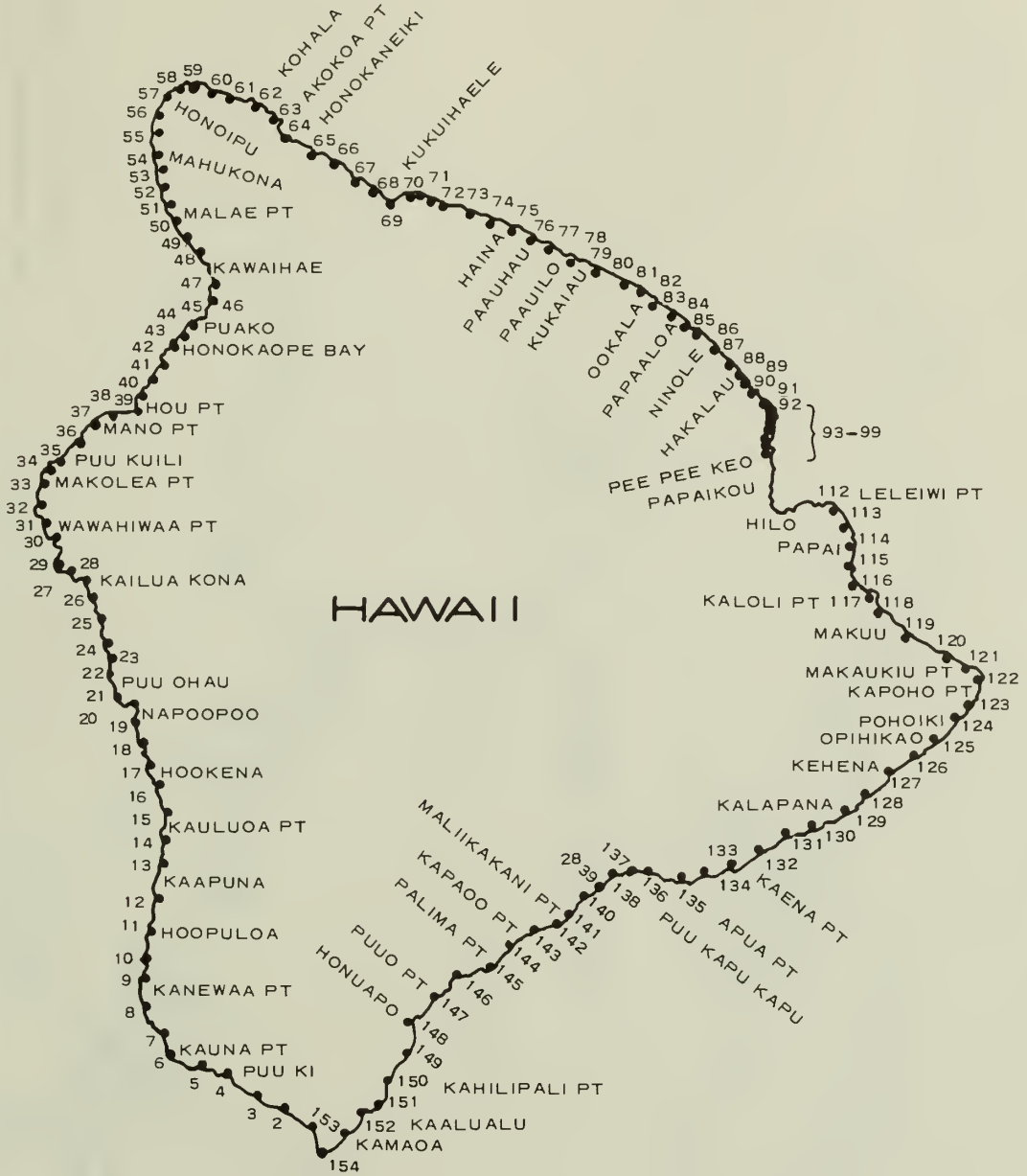

LOCATION MAP

HAWAII

PLATE 1

PLATE 2

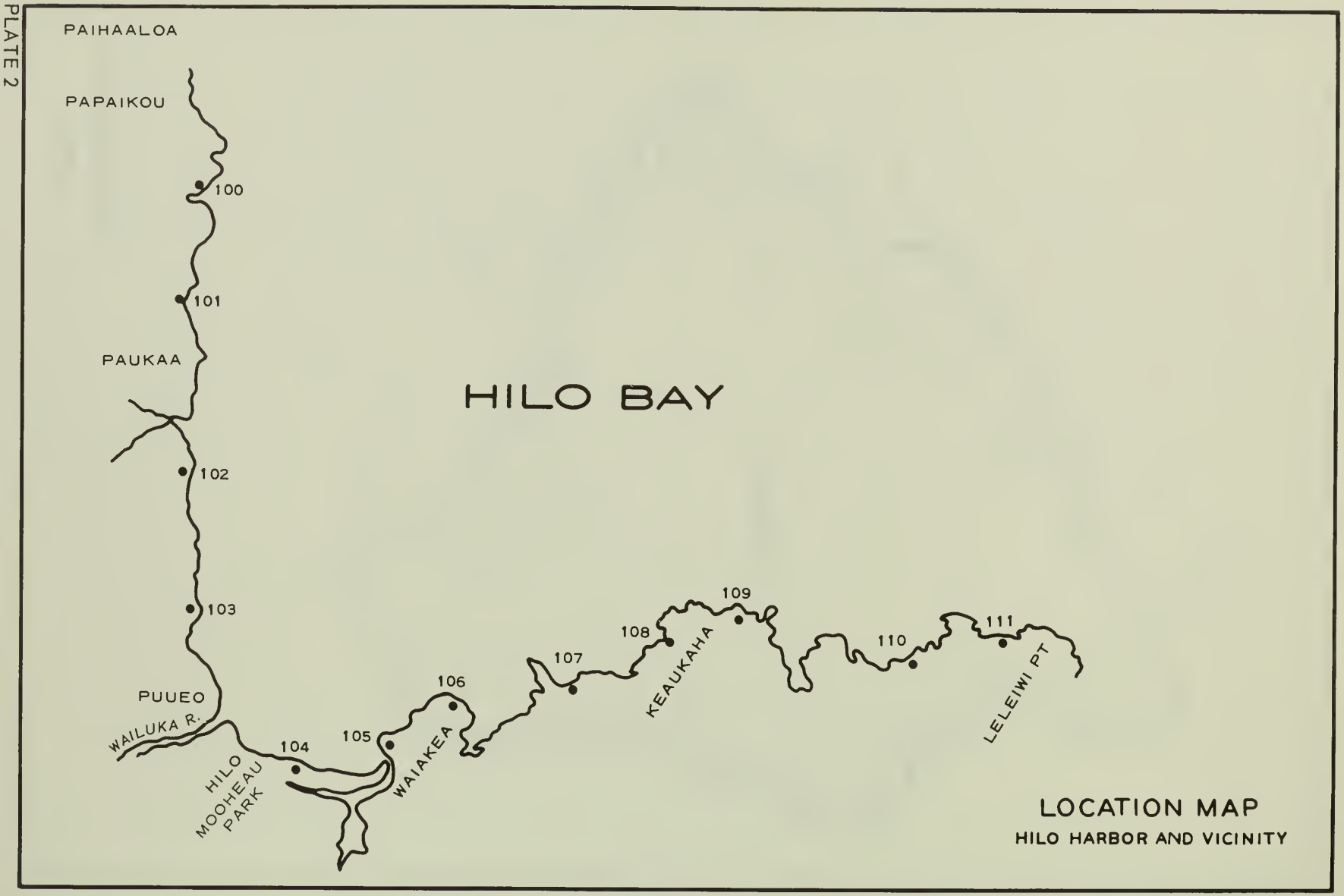

LOCATION MAP

HILO HARBOR AND VICINITY

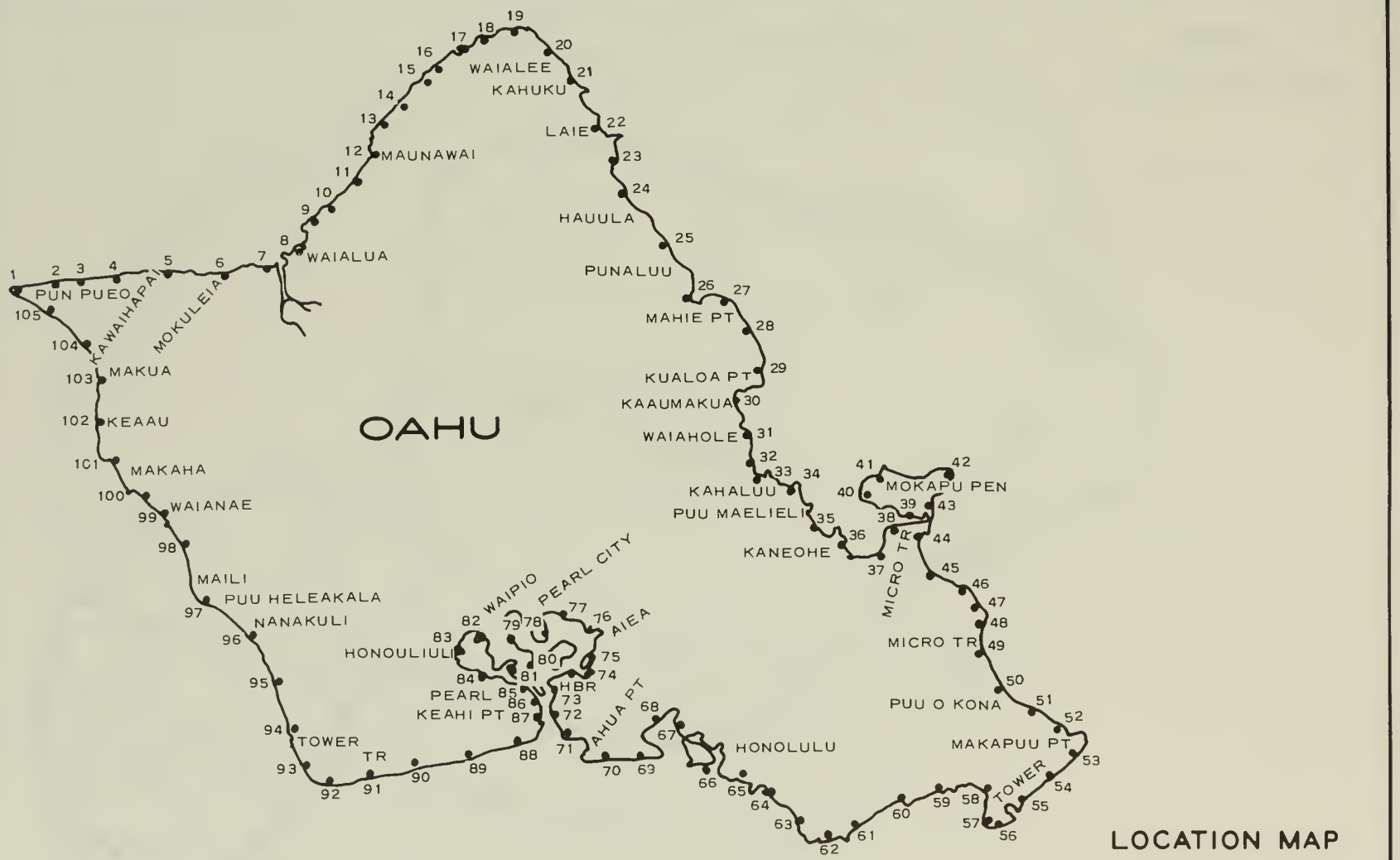

LOCATION MAP
OAHU

PLATE 3

PLATE 4

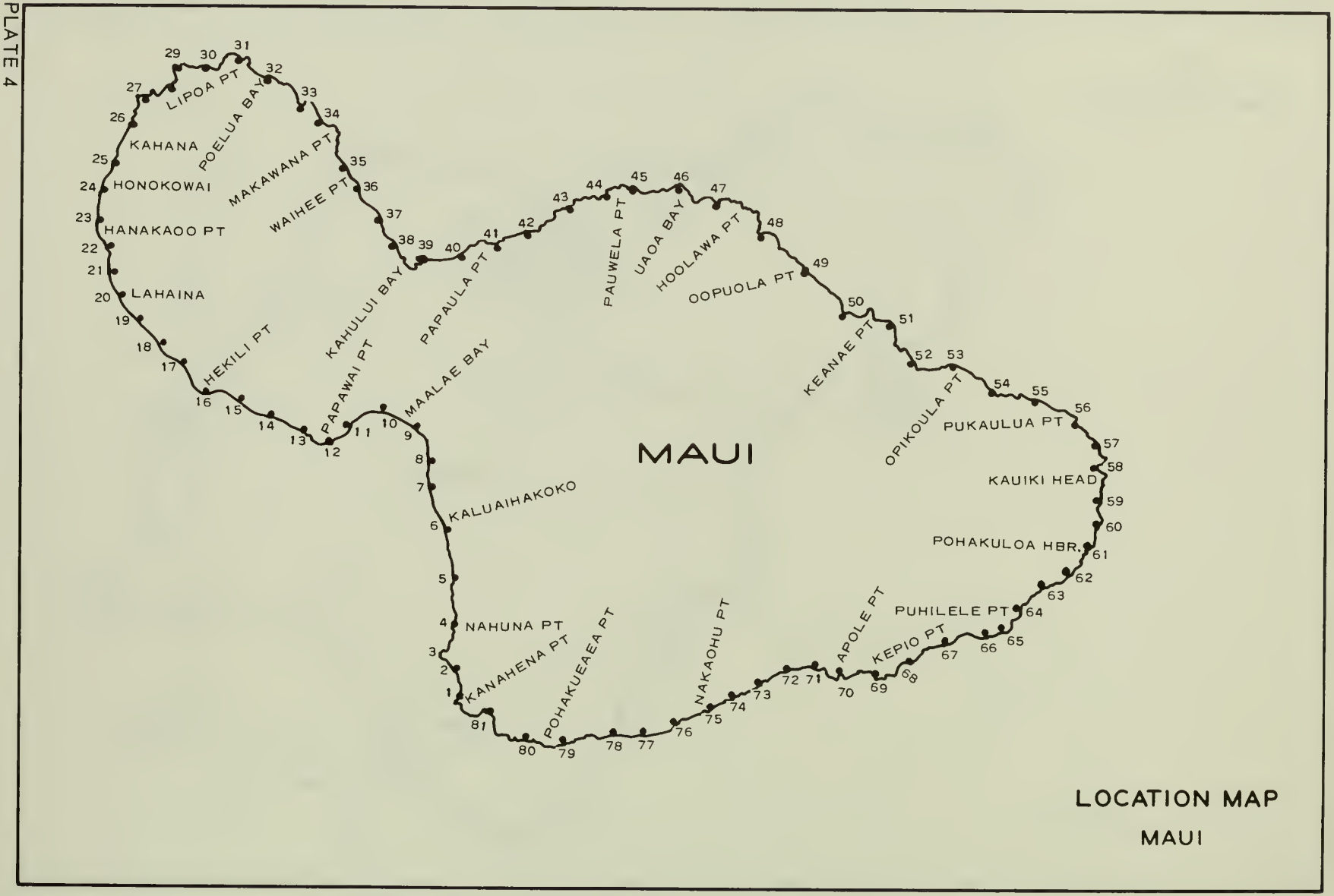

LOCATION MAP

MAUI

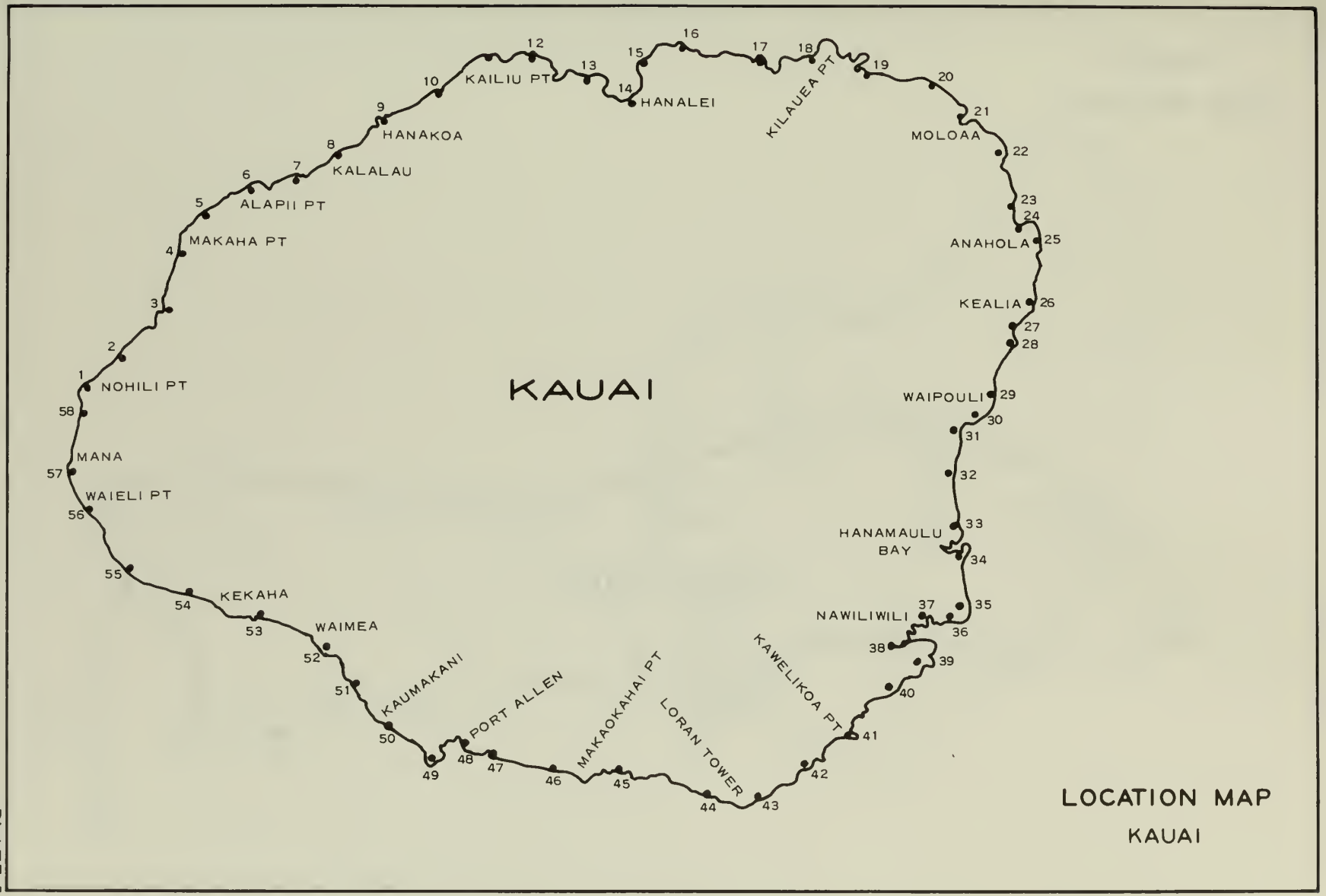

LOCATION MAP
KAUAI

PLATE 5

PLATE 6

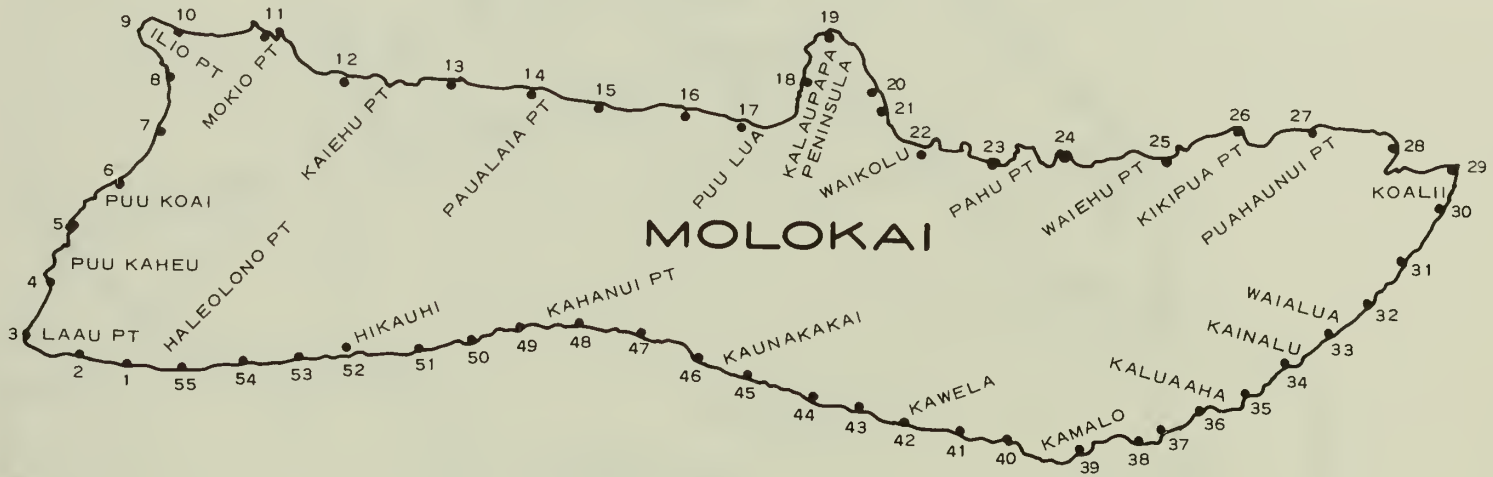

LOCATION MAP

MOLOKAI

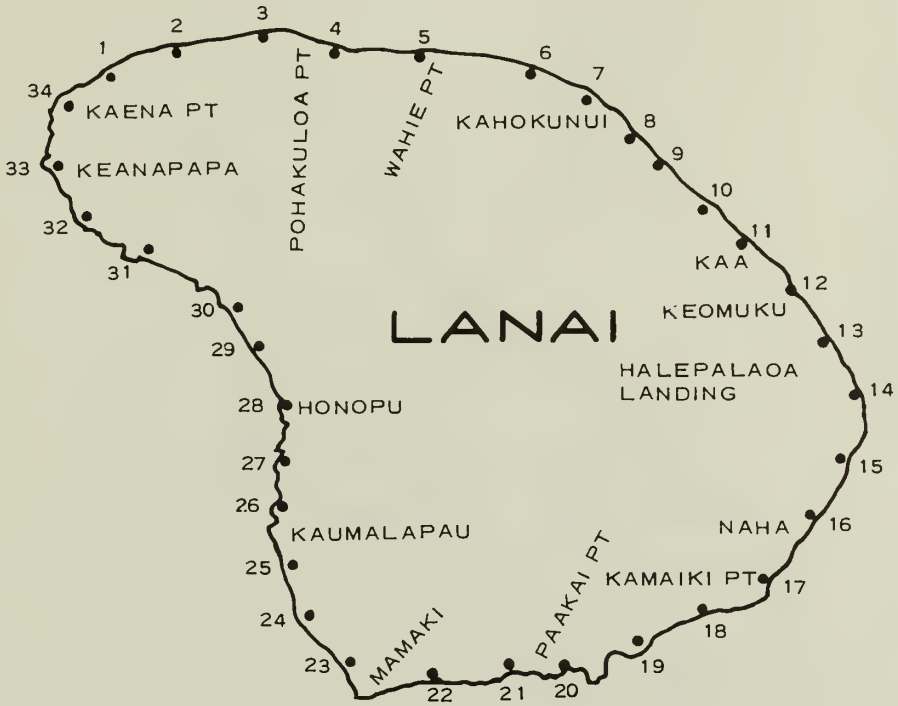

LOCATION MAP

LANAI

PLATE 7

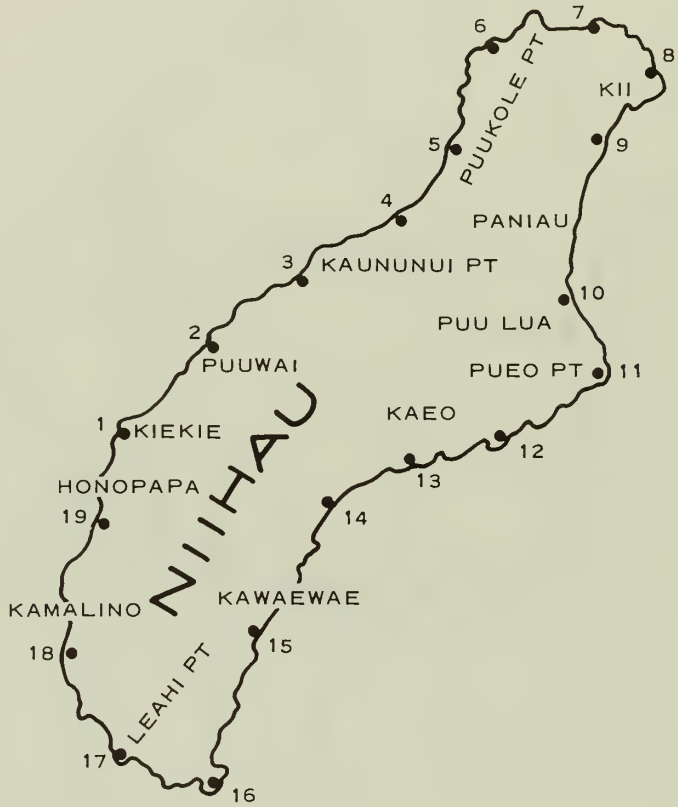

LOCATION MAP

NIIHAU

PLATE 8

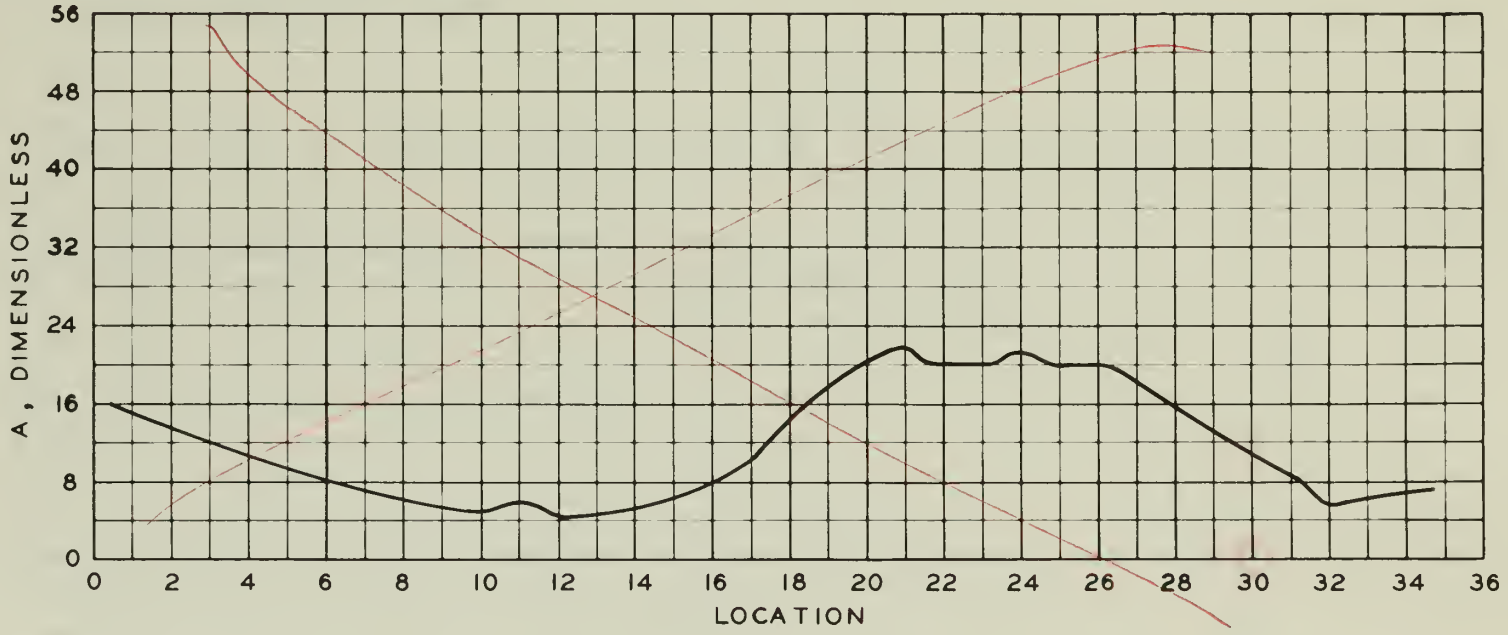

NOTE: LOCATIONS SHOWN IN PLATE 1

COEFFICIENT A VS LOCATION

HAWAII

LOCATIONS 1 - 34

PLATE 9

PLATES 9 THRU 44 HAVE BEEN REVISED

PLATE 10

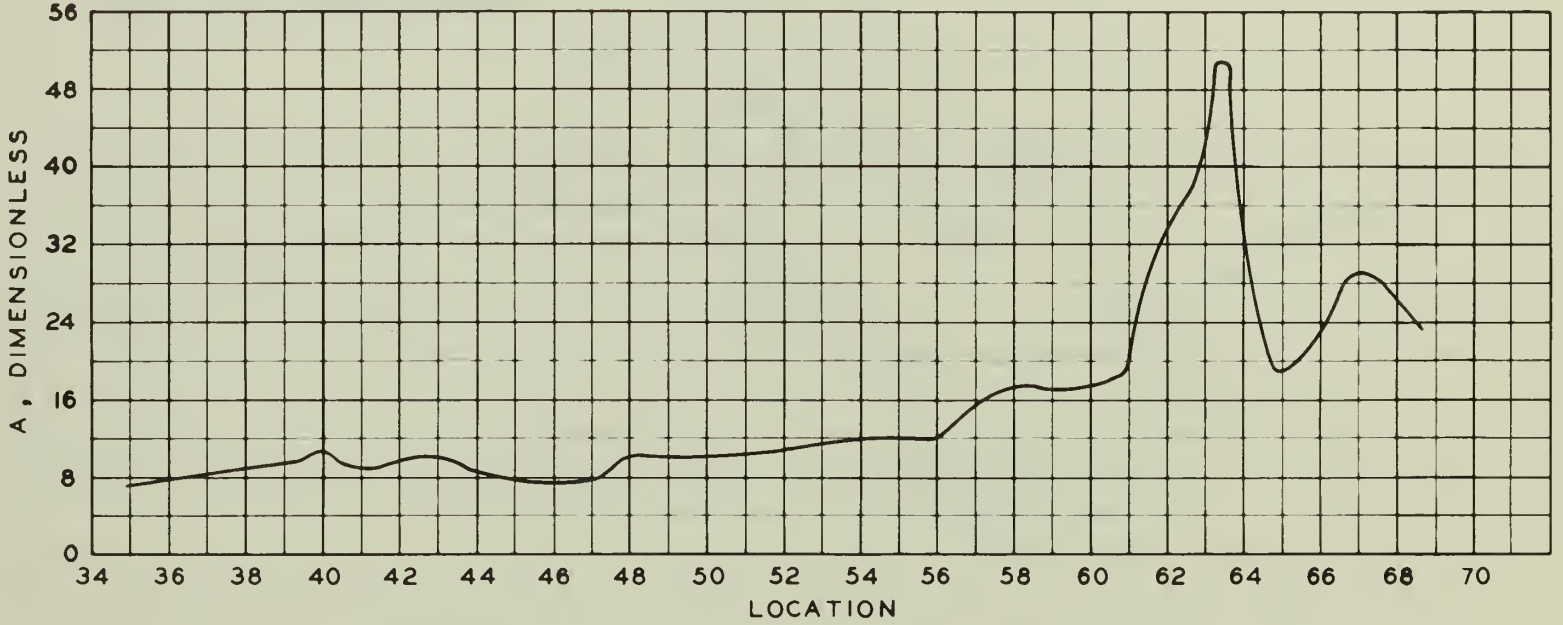

NOTE: LOCATIONS SHOWN
IN PLATE 1

COEFFICIENT A VS LOCATION

HAWAII

LOCATIONS 35-68

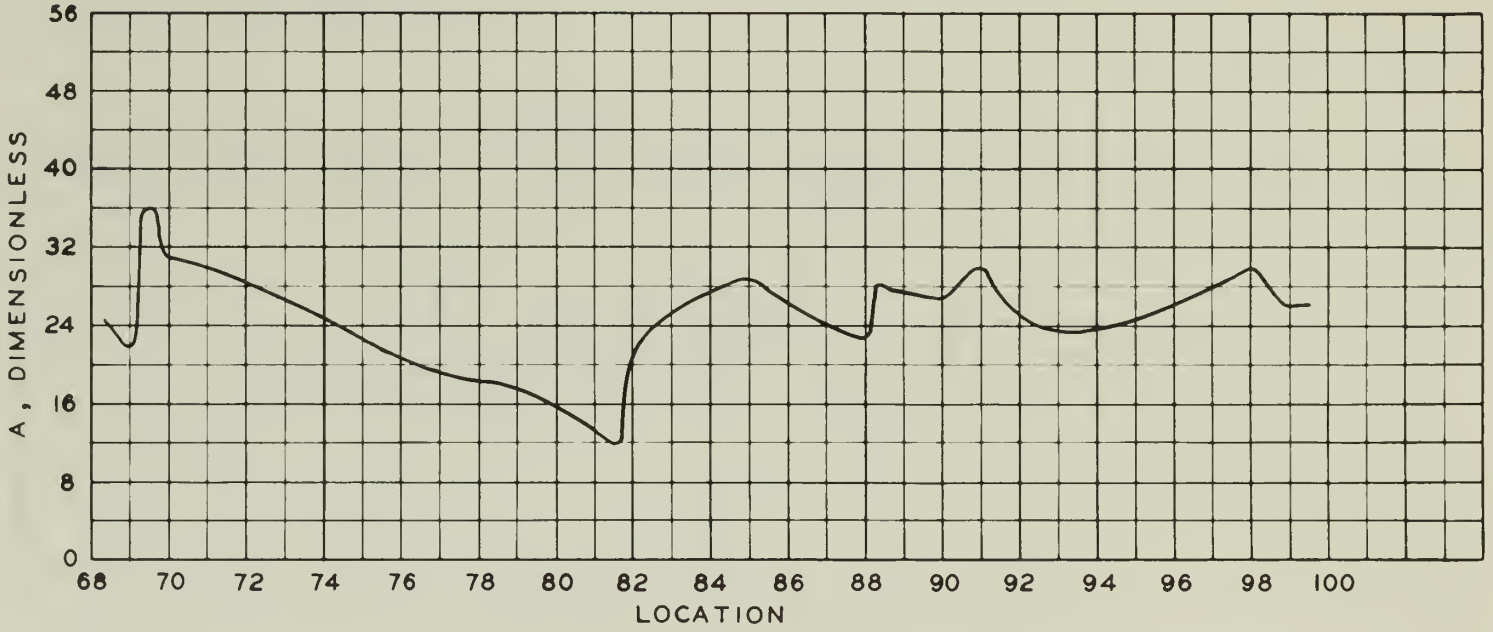

NOTE: LOCATIONS SHOWN
IN PLATE 1

COEFFICIENT A VS LOCATION

HAWAII
LOCATIONS 69-99

PLATE 11

PLATE 12

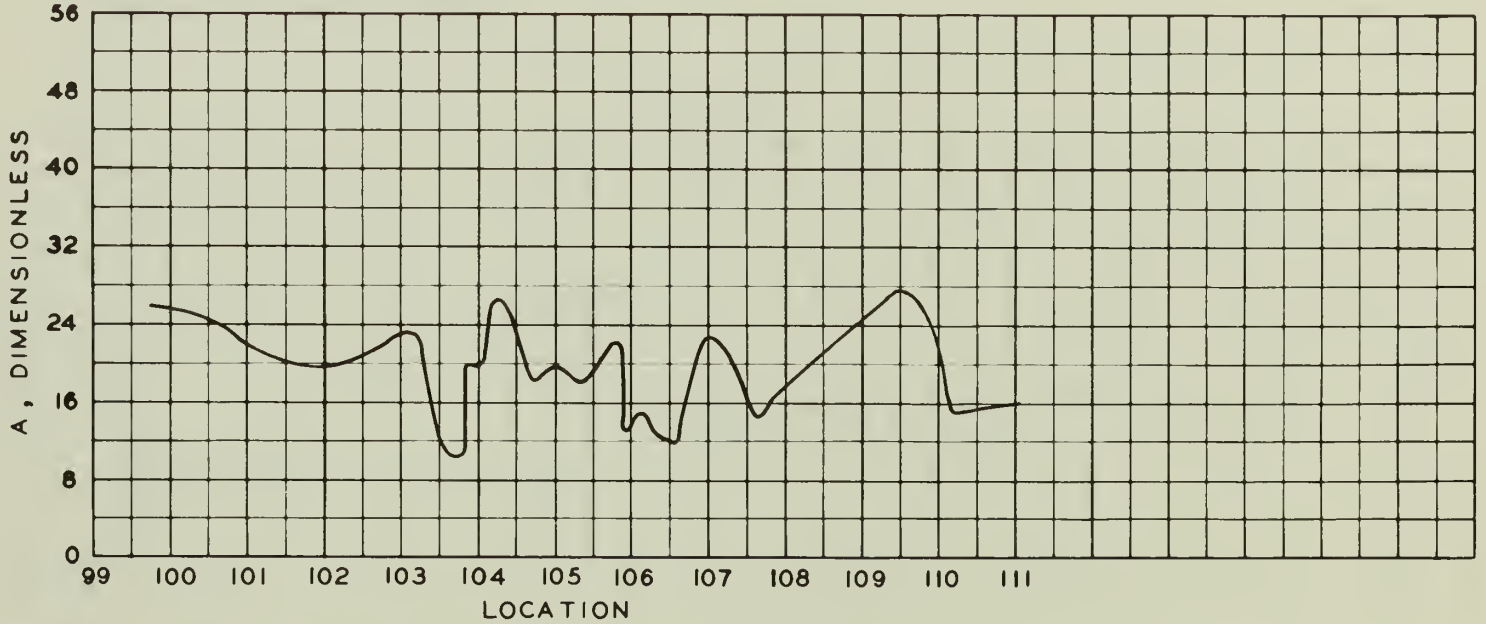

NOTE: LOCATIONS SHOWN
IN PLATE 2

COEFFICIENT A VS LOCATION

HILO HARBOR & VICINITY
LOCATIONS 100-111

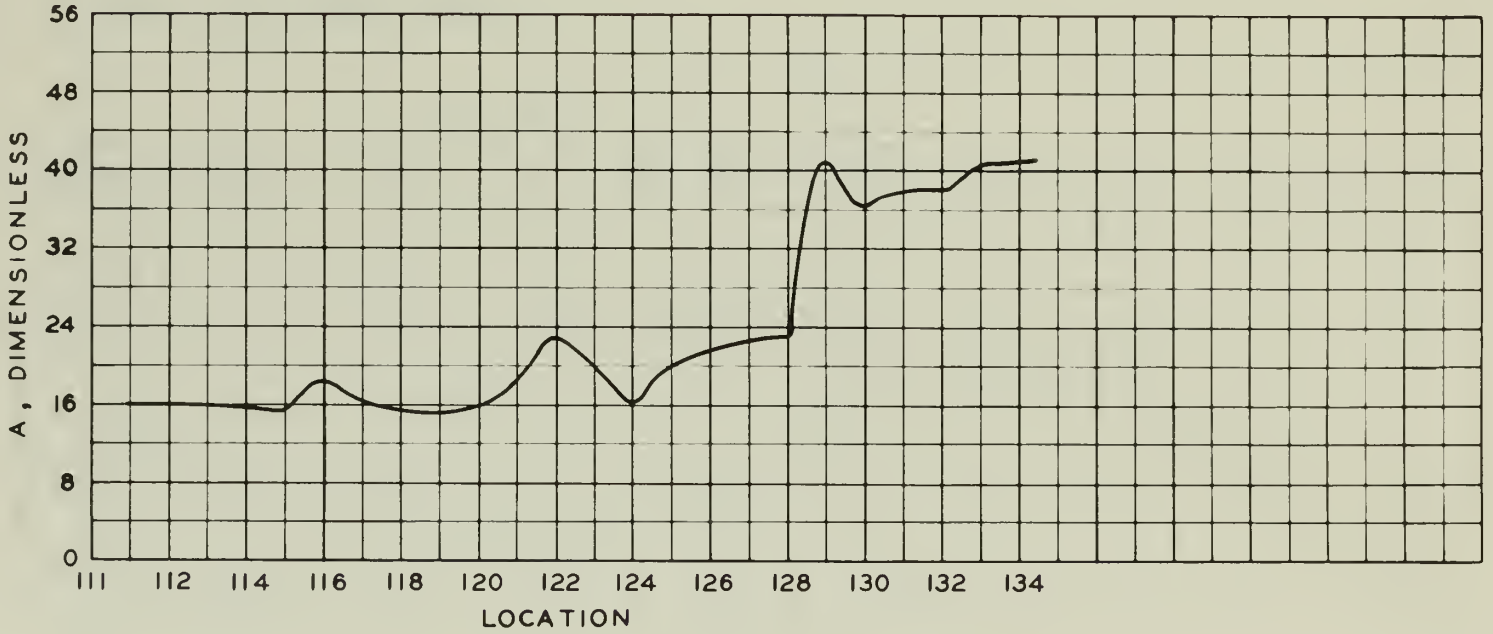

NOTE: LOCATIONS SHOWN
IN PLATE 1

COEFFICIENT A VS LOCATION

HAWAII
LOCATIONS 112-134

PLATE 13

PLATE 14

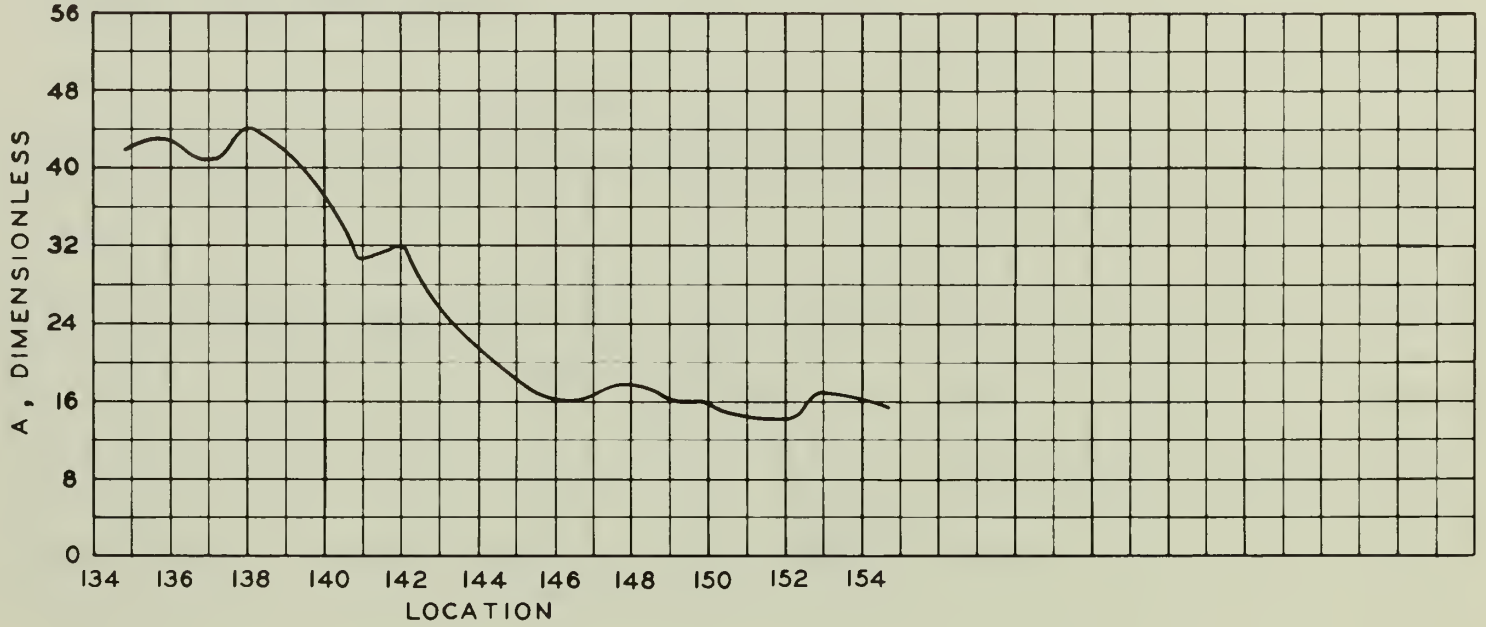

NOTE: LOCATIONS SHOWN
IN PLATE 1

COEFFICIENT A VS LOCATION

HAWAII

LOCATIONS 135-154

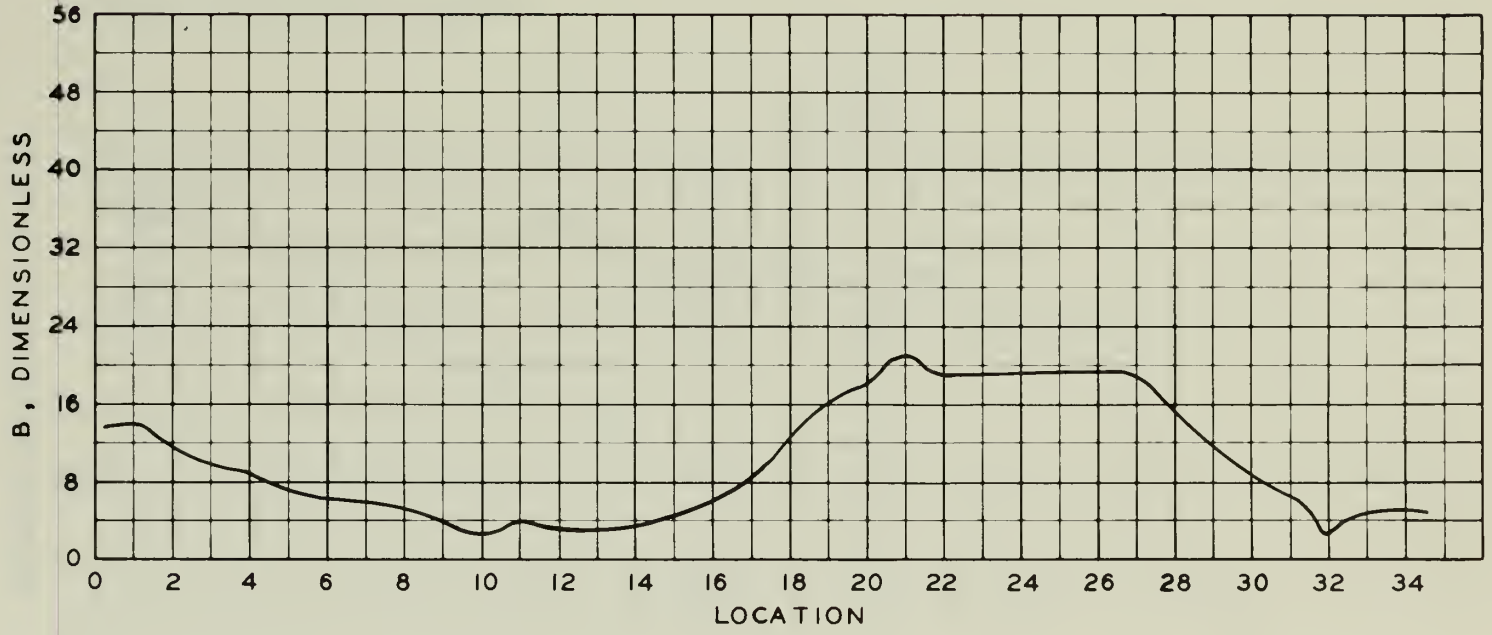

NOTE: LOCATIONS SHOWN
IN PLATE 1

COEFFICIENT B VS LOCATION

HAWAII
LOCATIONS 1 - 34

PLATE 15

PLATE 16

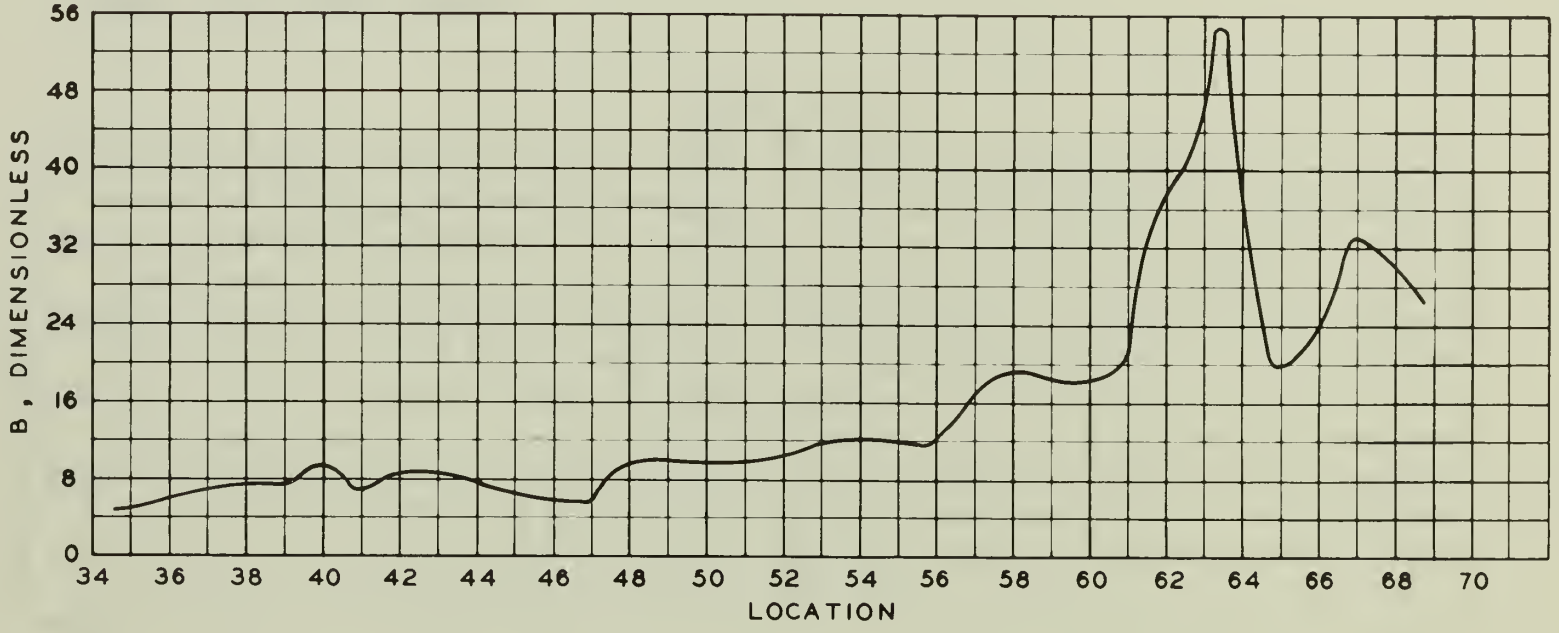

NOTE: LOCATIONS SHOWN
IN PLATE 1

COEFFICIENT B VS LOCATION

HAWAII
LOCATIONS 35-68

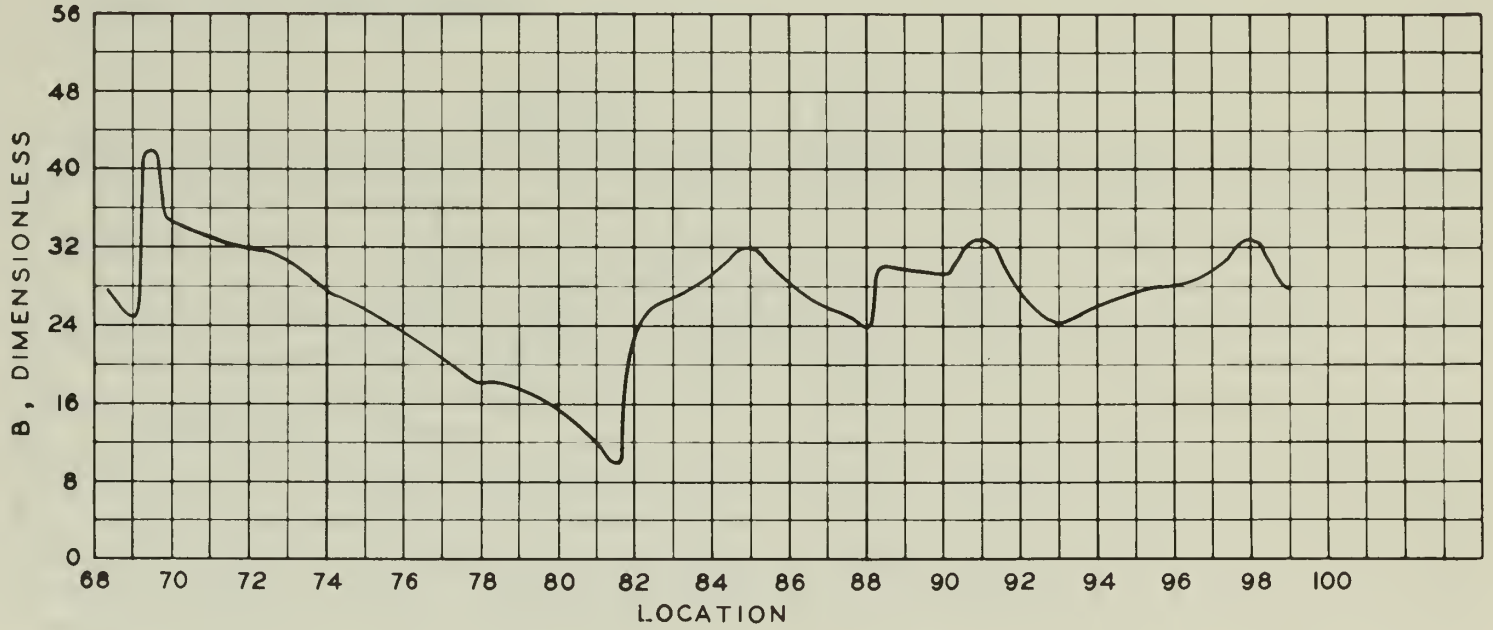

NOTE: LOCATIONS SHOWN
IN PLATE 1

COEFFICIENT B VS LOCATION

HAWAII
LOCATIONS 69-99

PLATE 17

PLATE 18

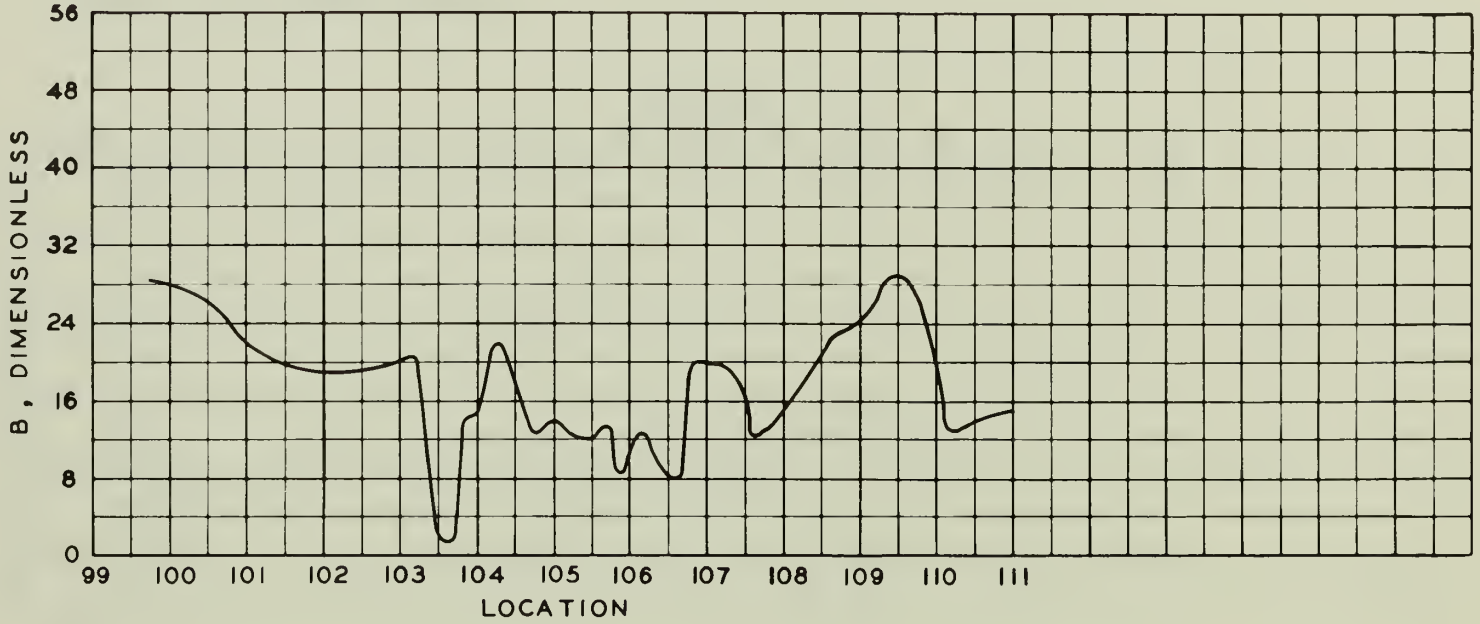

NOTE: LOCATIONS SHOWN
IN PLATE 2

COEFFICIENT B VS LOCATION

HILO HARBOR & VICINITY
LOCATIONS 100-111

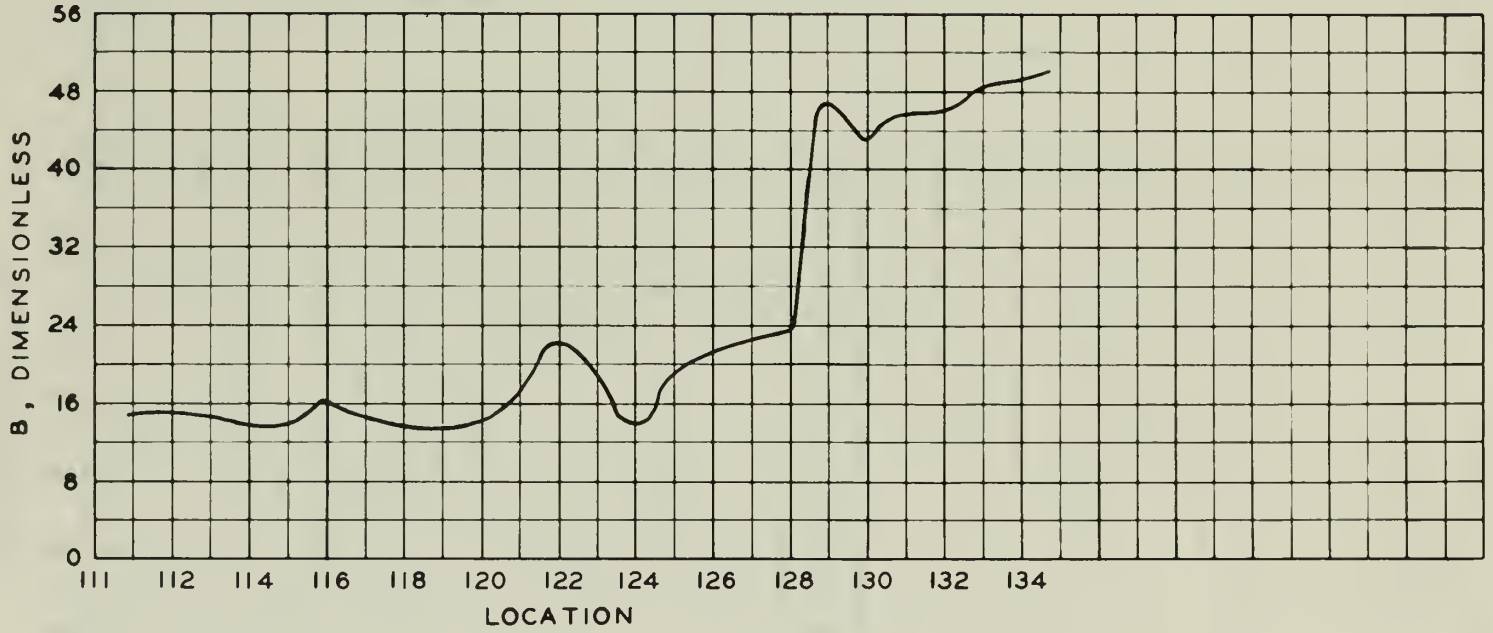

NOTE: LOCATIONS SHOWN
IN PLATE 1

COEFFICIENT B VS LOCATION

HAWAII
LOCATIONS 112-134

PLATE 19

PLATE 20

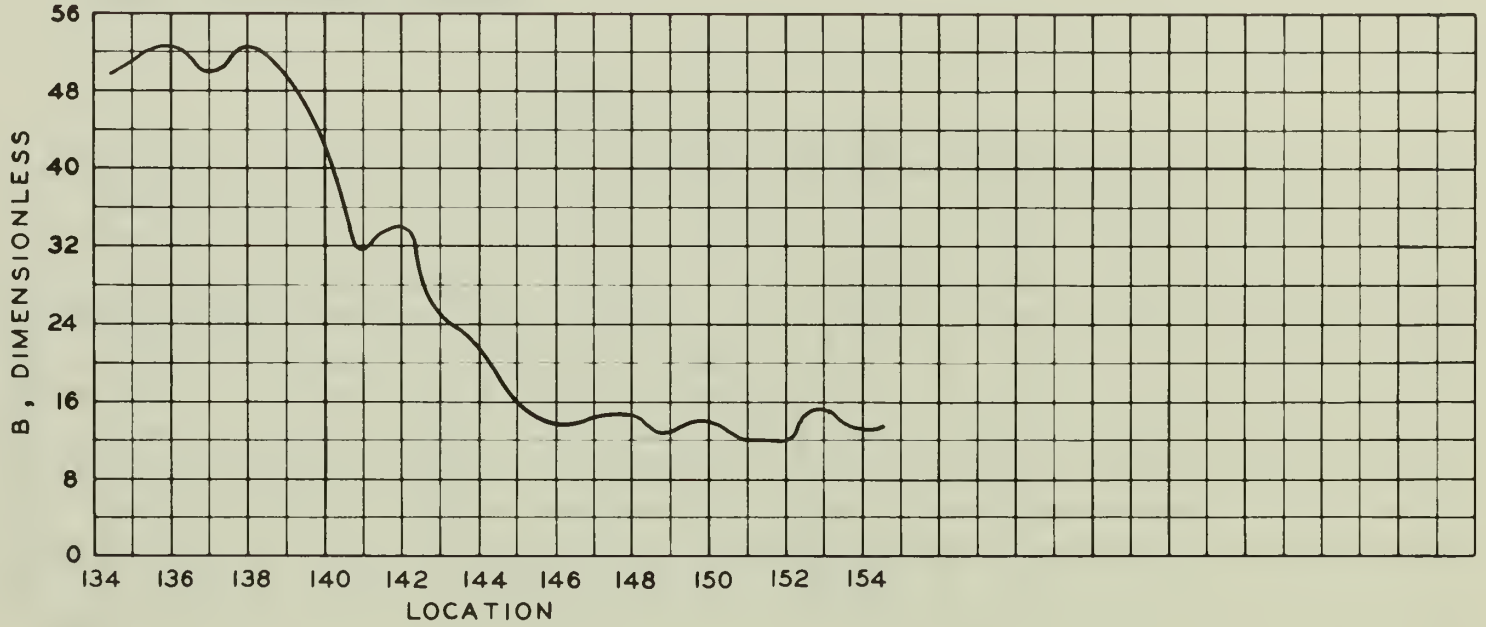

NOTE: LOCATIONS SHOWN
IN PLATE 1

COEFFICIENT B VS LOCATION

HAWAII
LOCATIONS 135-154

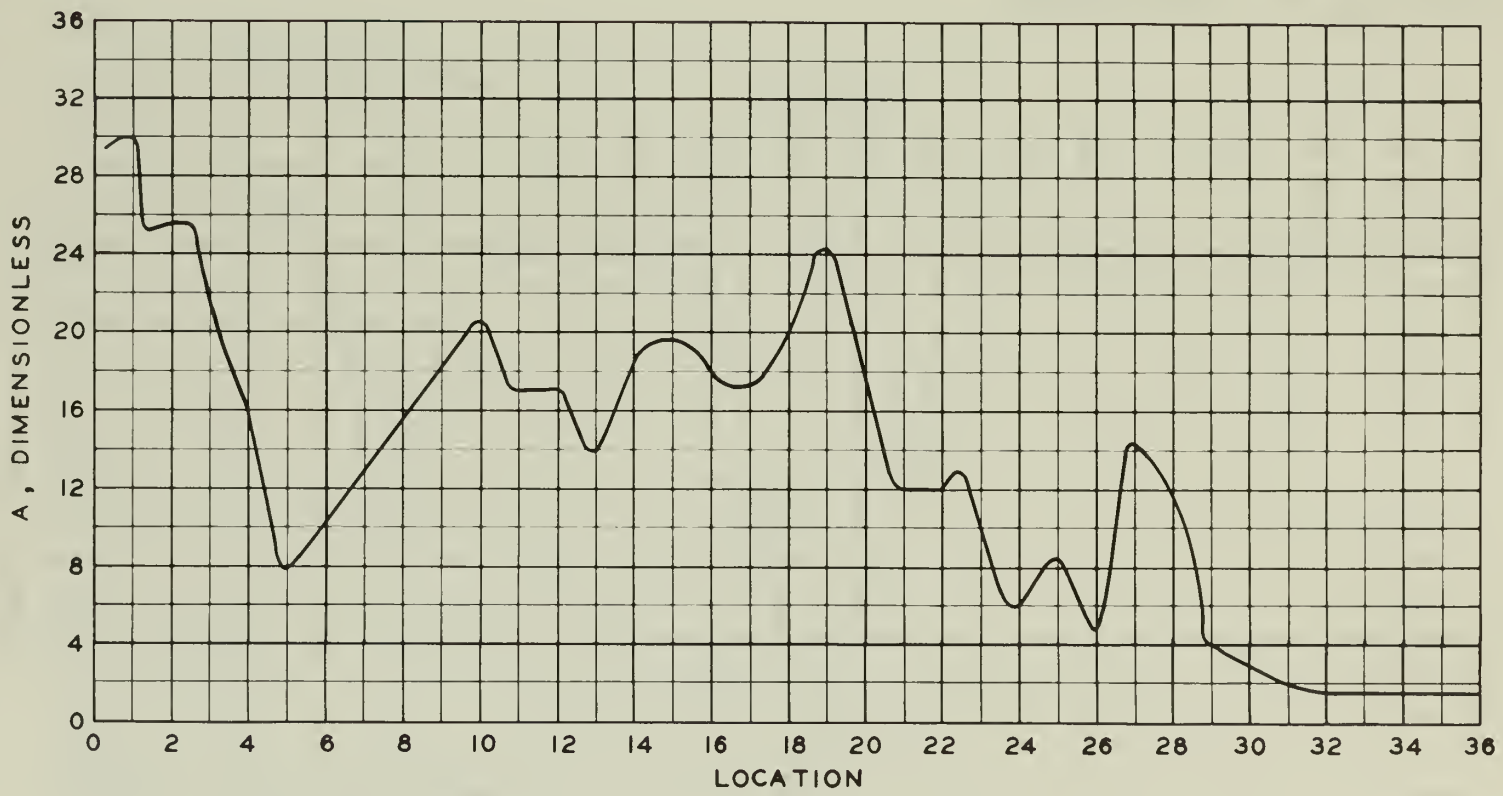

NOTE: LOCATIONS SHOWN IN PLATE 3

COEFFICIENT A VS LOCATION

OAHU

LOCATIONS 1-36

PLATE 21

PLATE 22

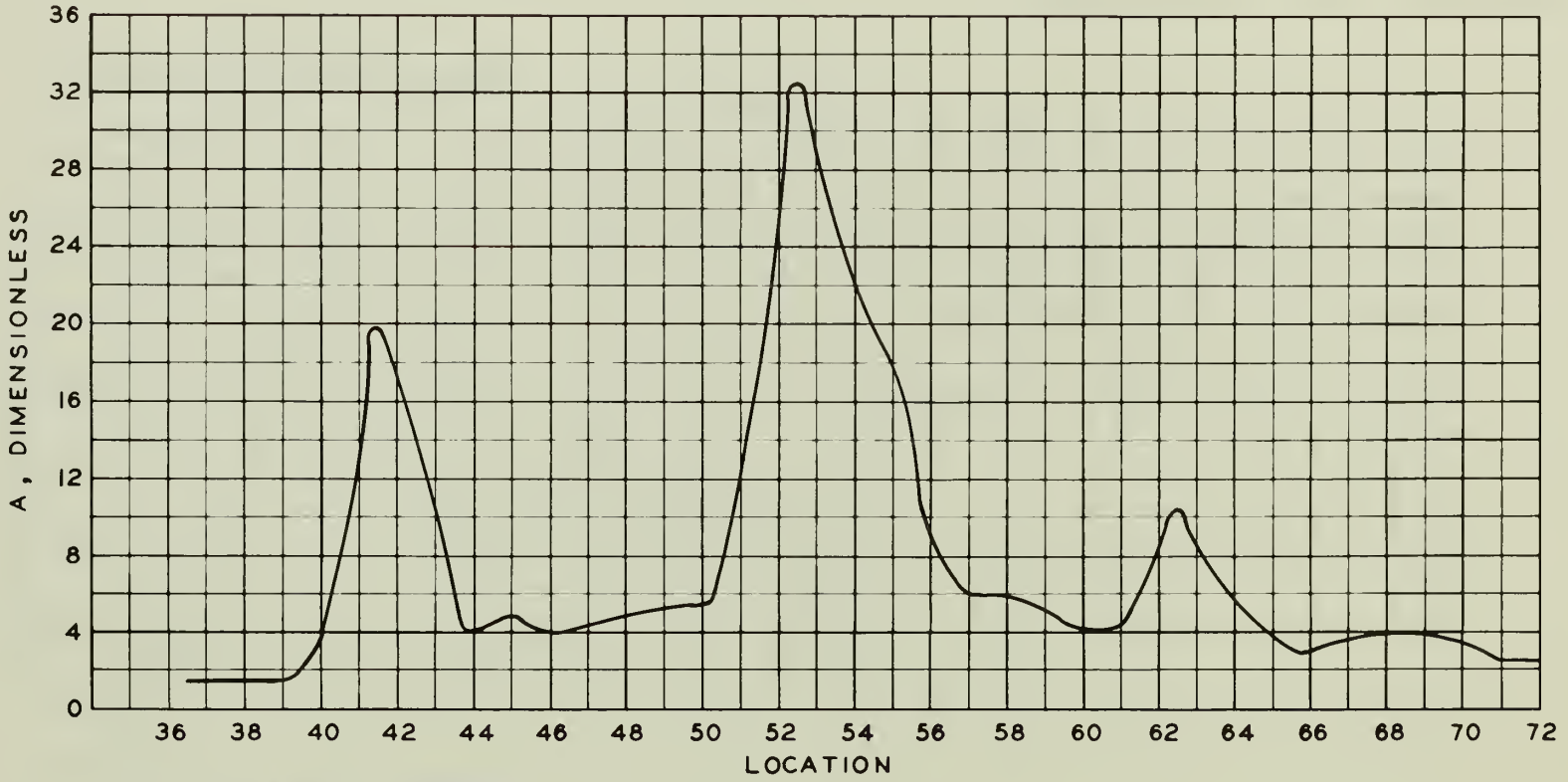

NOTE: LOCATIONS SHOWN IN PLATE 3

COEFFICIENT A VS LOCATION

OAHU

LOCATIONS 37-72

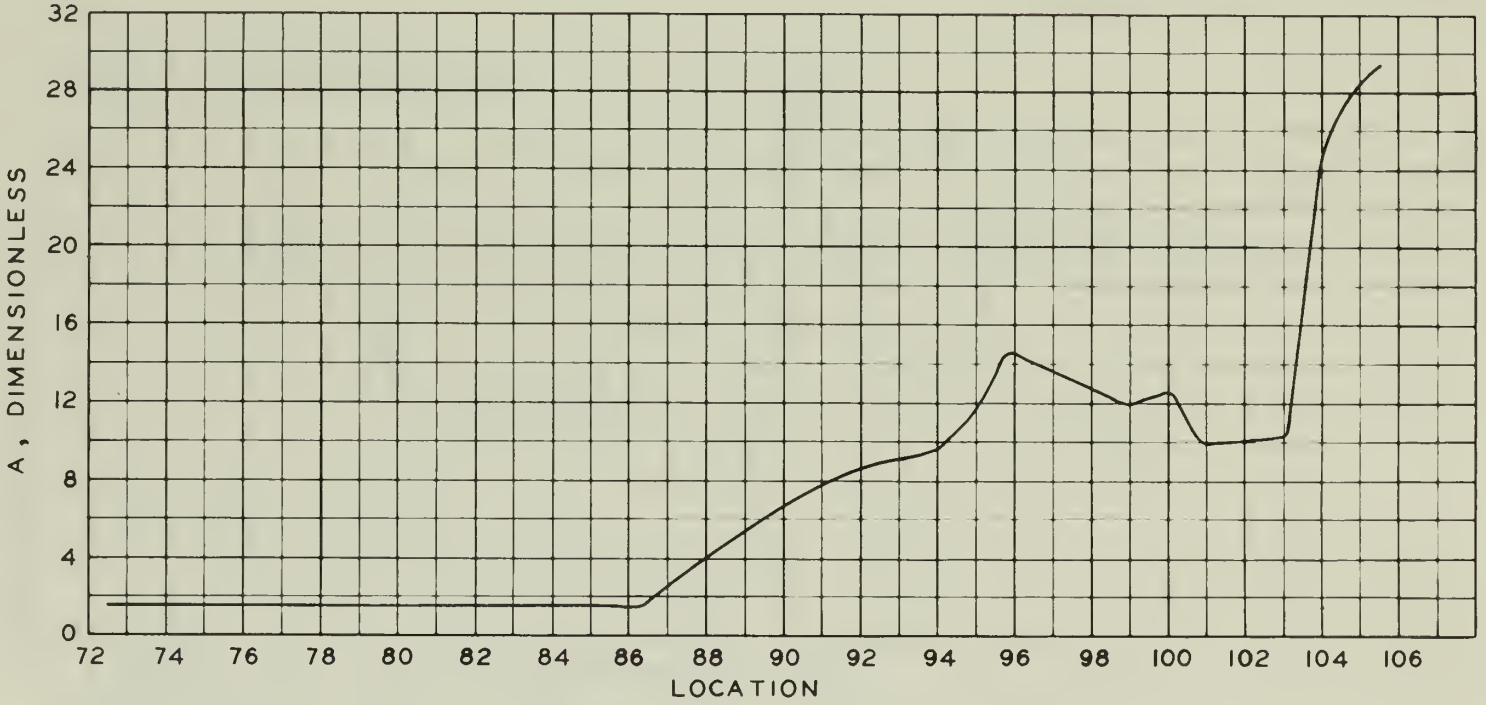

NOTE: LOCATIONS SHOWN
IN PLATE 3

COEFFICIENT A VS LOCATION

OAHU
LOCATIONS 73-105

PLATE 23

PLATE 24

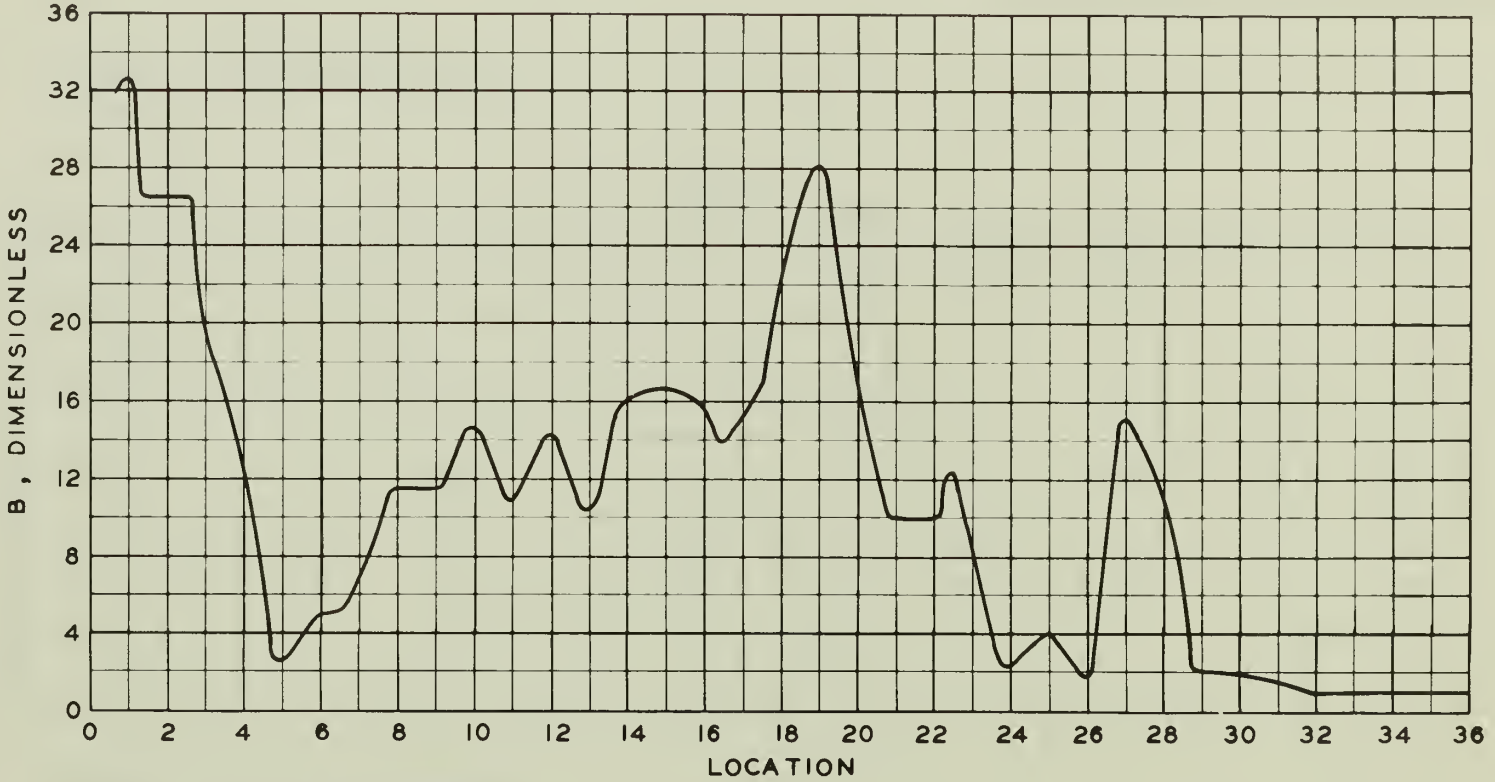

NOTE: LOCATIONS SHOWN IN PLATE 3

COEFFICIENT B VS LOCATION

OAHU

LOCATIONS 1-36

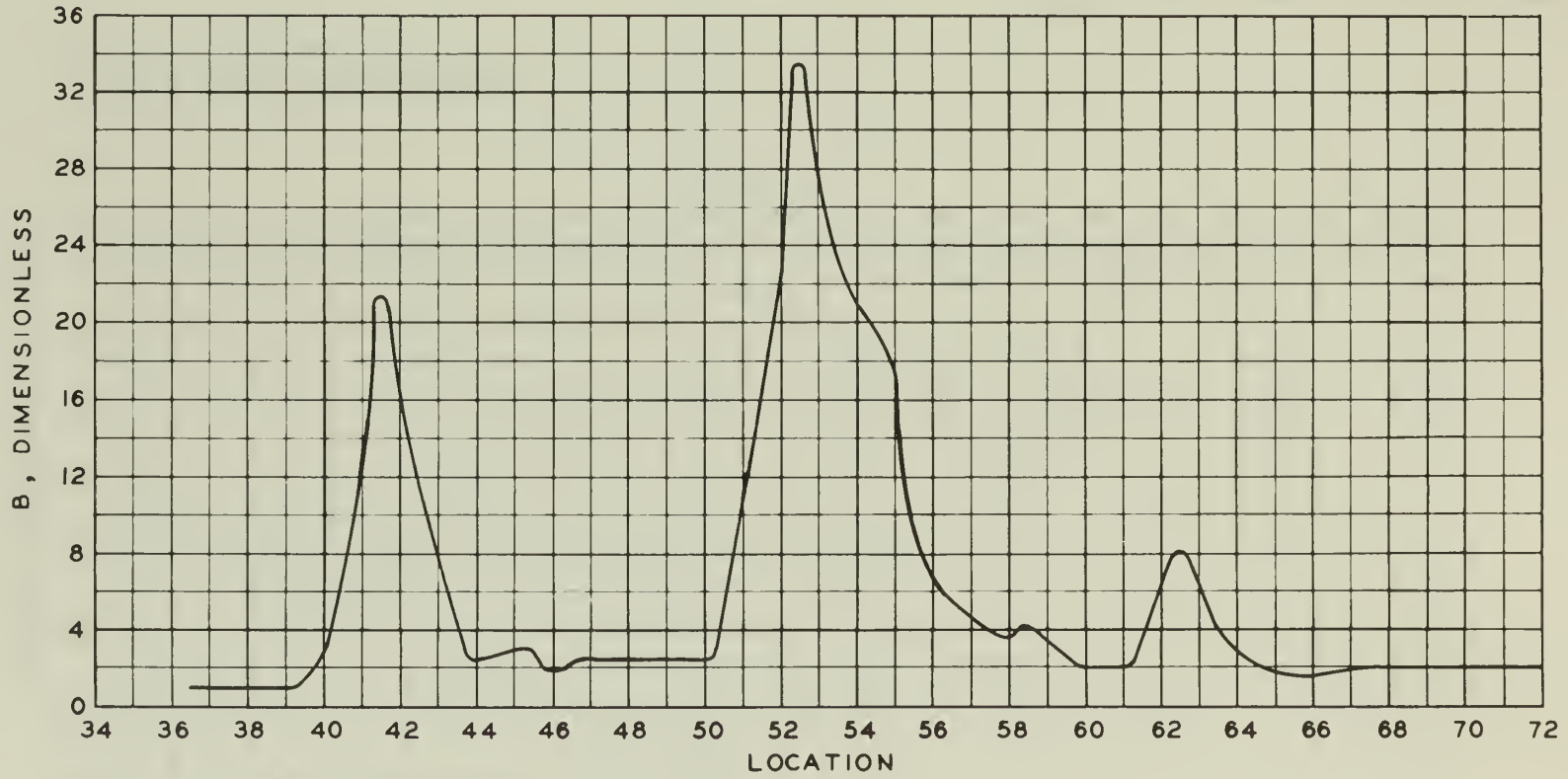

NOTE: LOCATIONS SHOWN IN PLATE 3

COEFFICIENT B VS LOCATION

OAHU

LOCATIONS 37-72

PLATE 25

PLATE 26

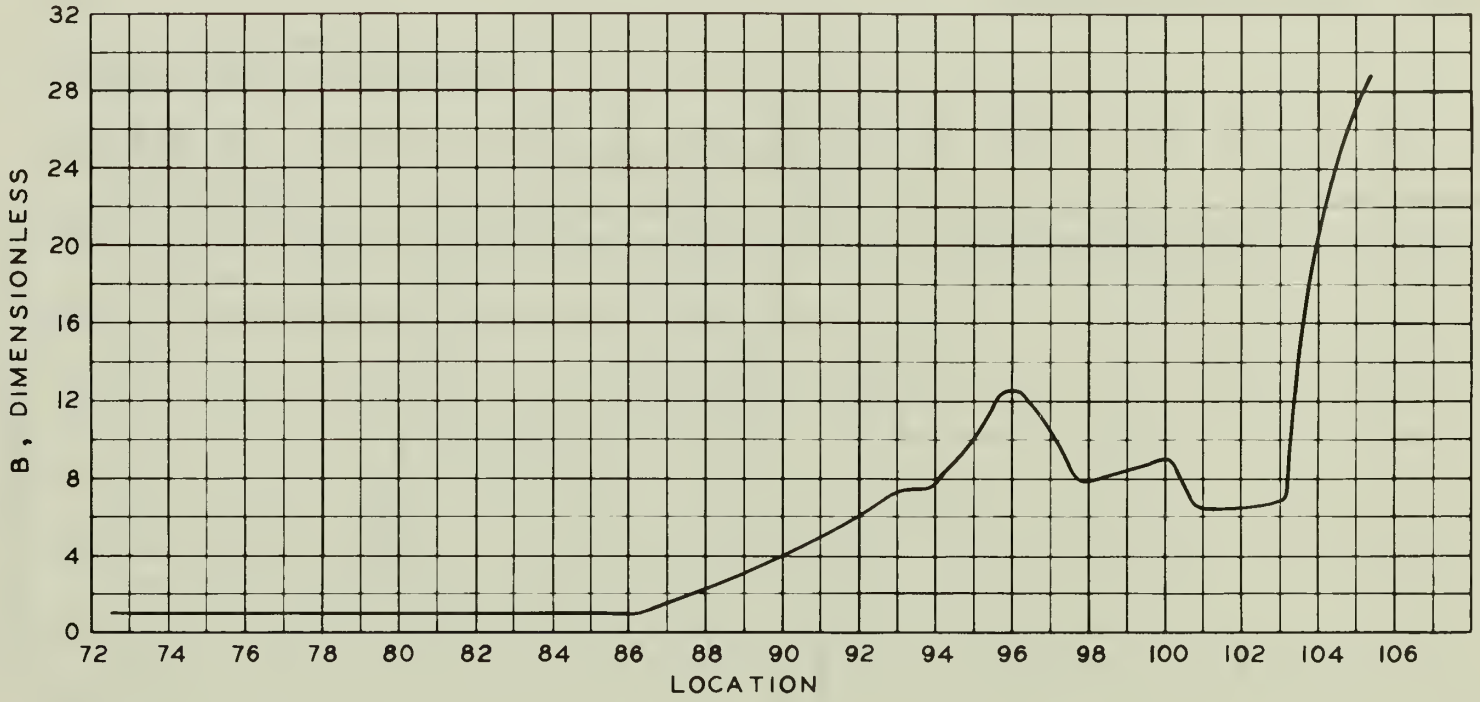

NOTE: LOCATIONS SHOWN
IN PLATE 3

COEFFICIENT B VS LOCATION

OAHU
LOCATIONS 73-105

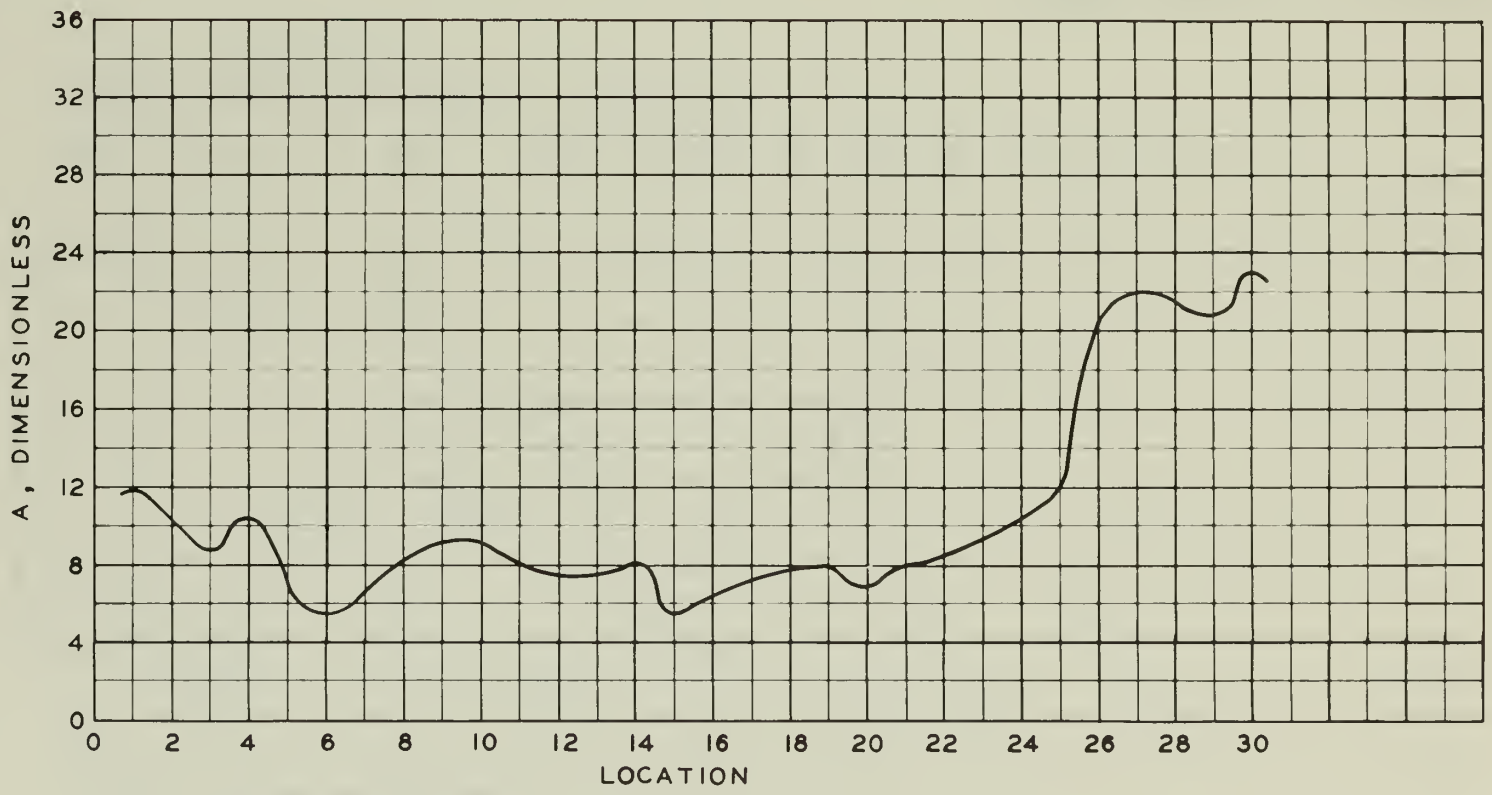

NOTE: LOCATIONS SHOWN IN PLATE 4

COEFFICIENT A VS LOCATION

MAUI

LOCATIONS 1 - 30

PLATE 27

PLATE 28

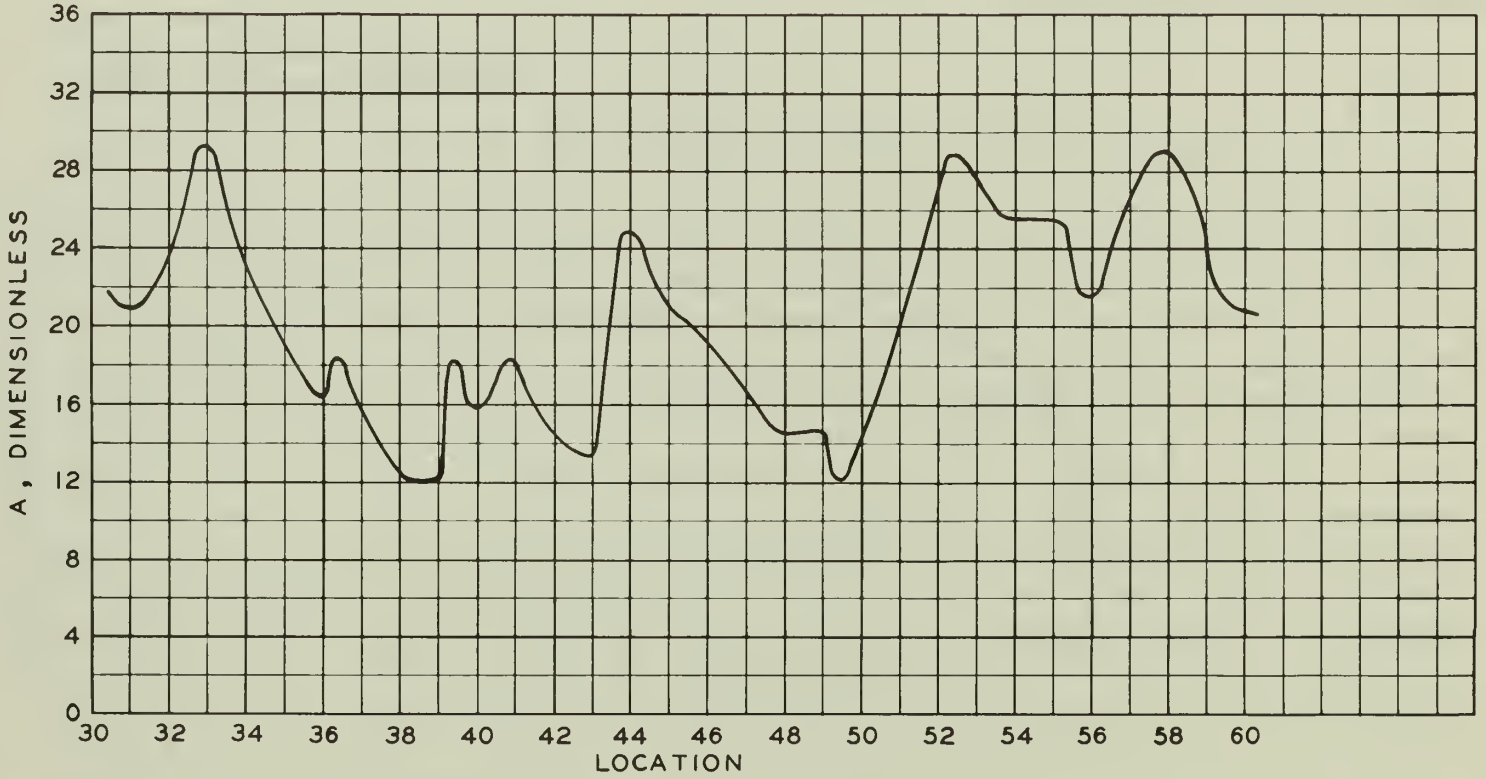

NOTE: LOCATIONS SHOWN IN PLATE 4

COEFFICIENT A VS LOCATION

MAUI
LOCATIONS 31-60

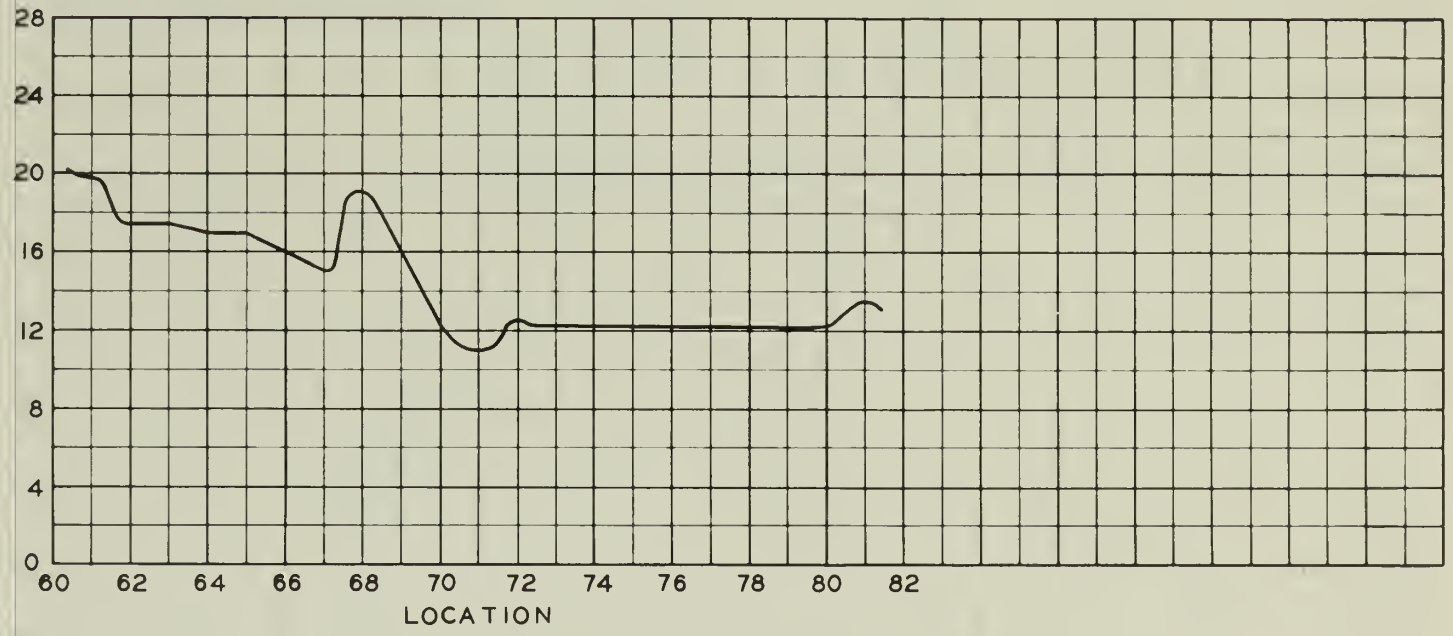

NOTE: LOCATIONS SHOWN
IN PLATE 4

COEFFICIENT A VS LOCATION

MAUI
LOCATIONS 61-81

PLATE 29

PLATE 30

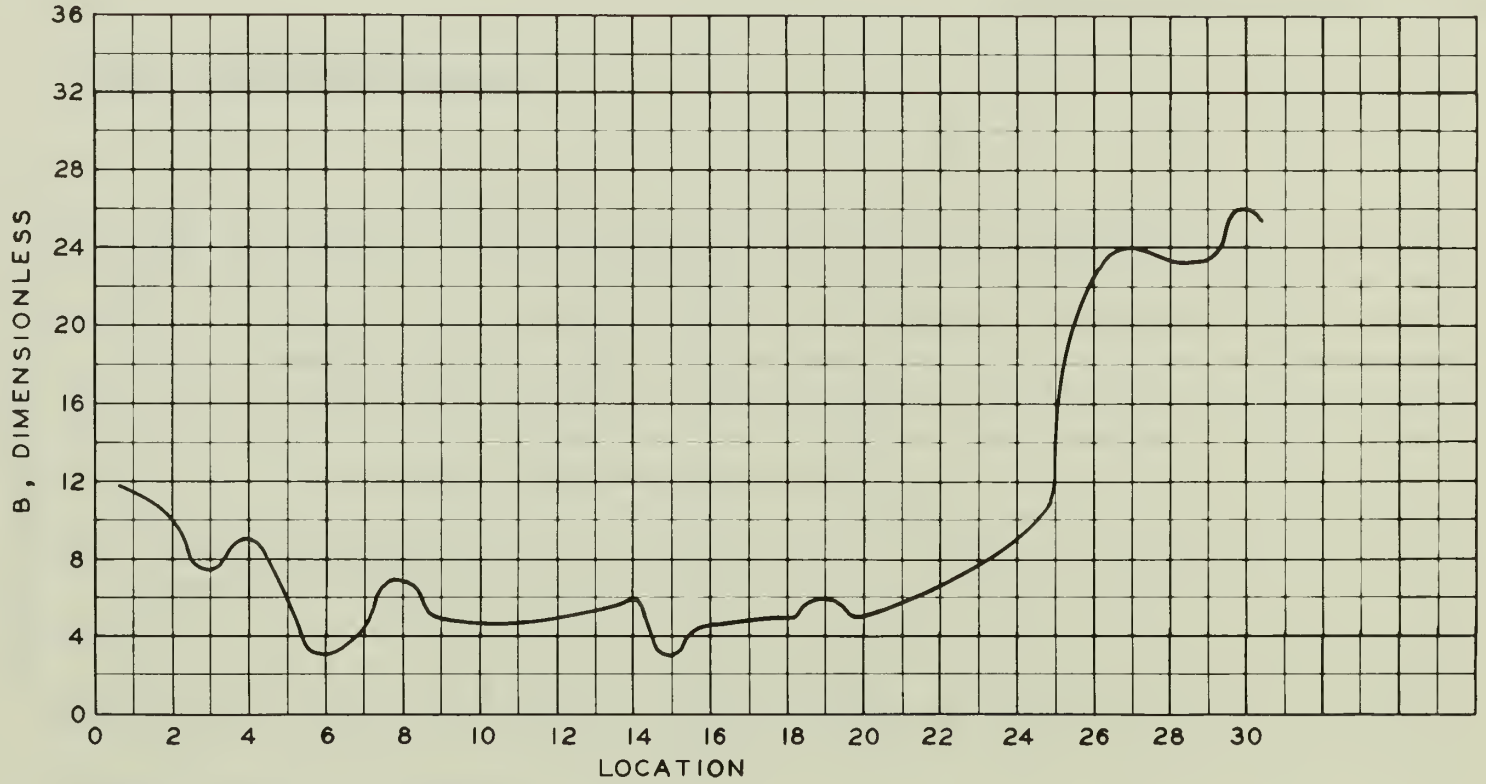

NOTE: LOCATIONS SHOWN IN PLATE 4

COEFFICIENT B VS LOCATION

MAUI
LOCATIONS 1-30

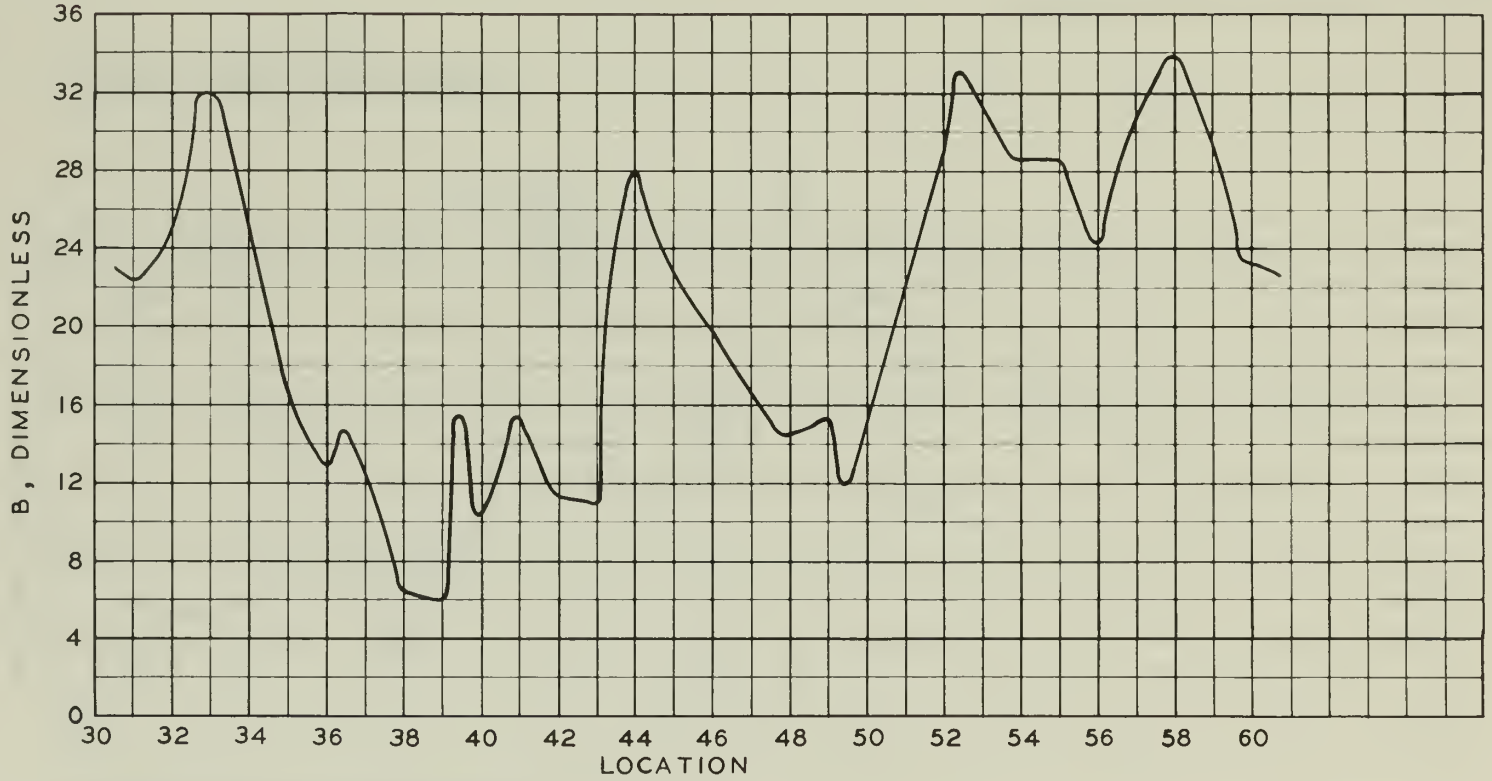

NOTE: LOCATIONS SHOWN IN PLATE 4

COEFFICIENT B VS LOCATION

MAUI
LOCATIONS 31-60

PLATE 31

PLATE 32

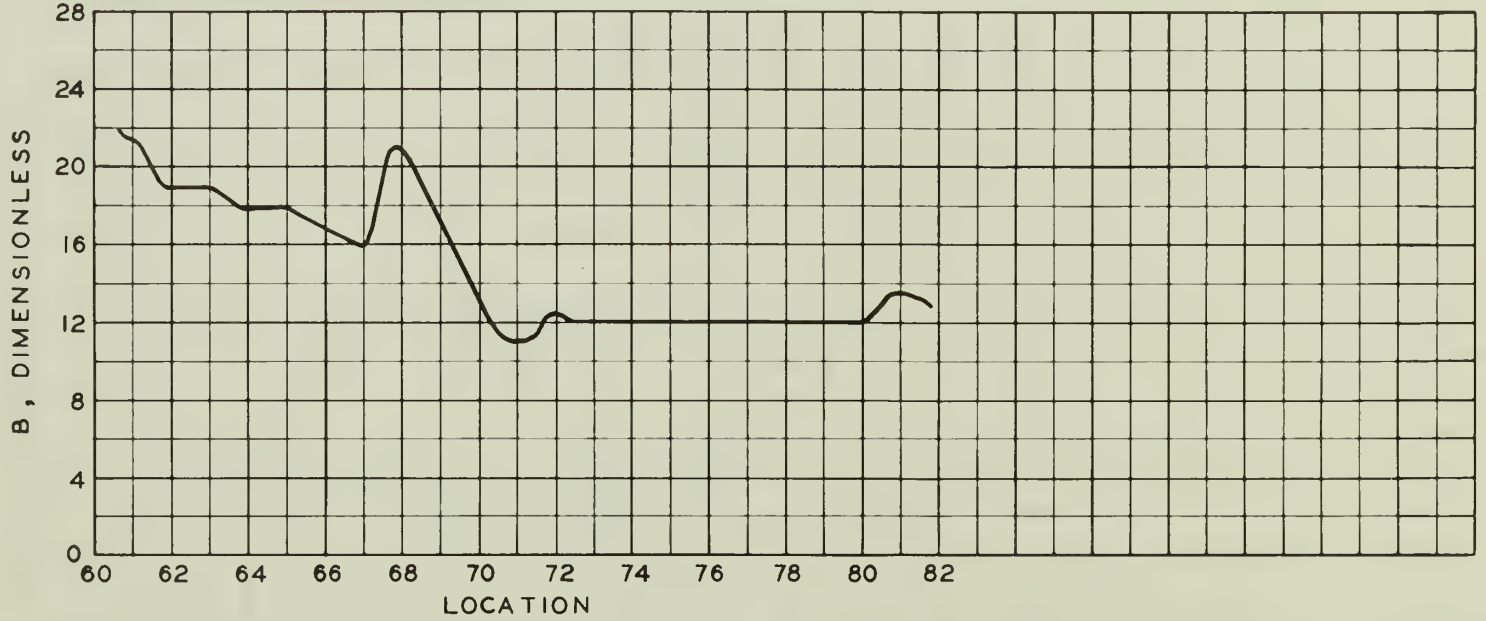

NOTE: LOCATIONS SHOWN
IN PLATE 4

COEFFICIENT B VS LOCATION
MAUI
LOCATIONS 61-81

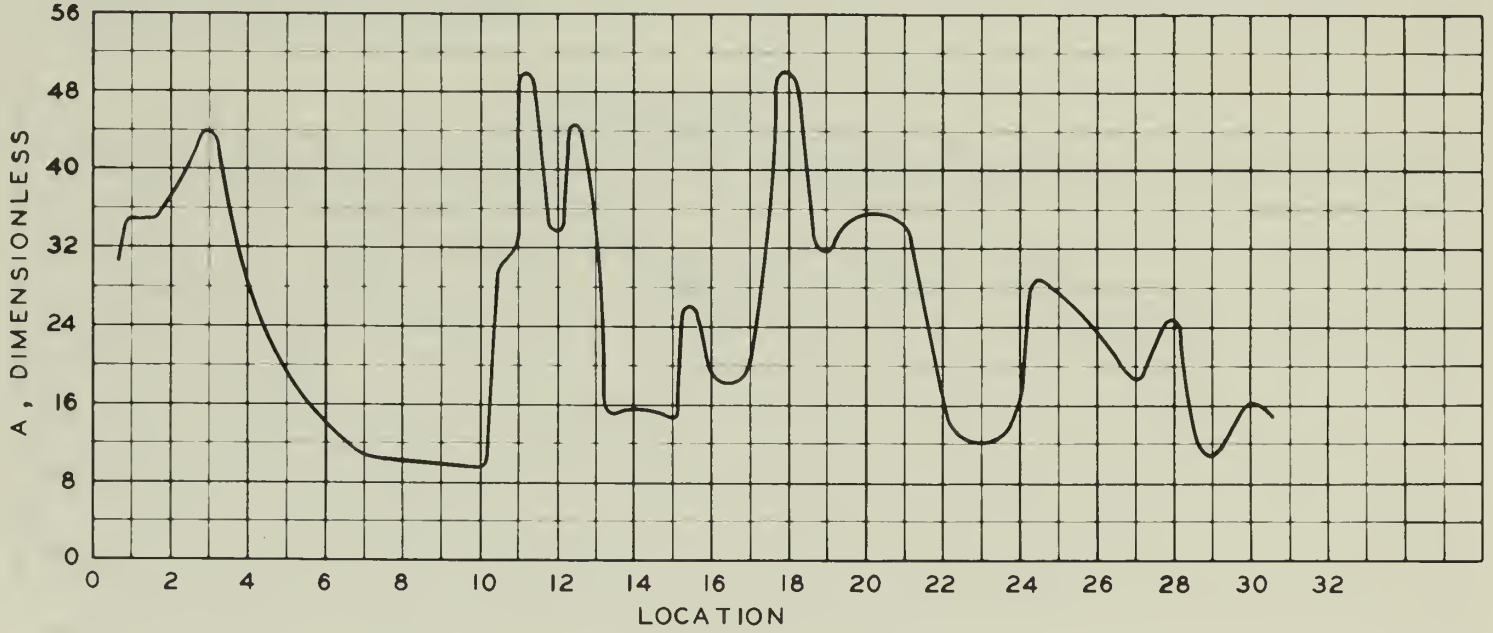

NOTE: LOCATIONS SHOWN
IN PLATE 5

COEFFICIENT A VS LOCATION

KAUAI
LOCATIONS 1 - 30

PLATE 33

PLATE 34

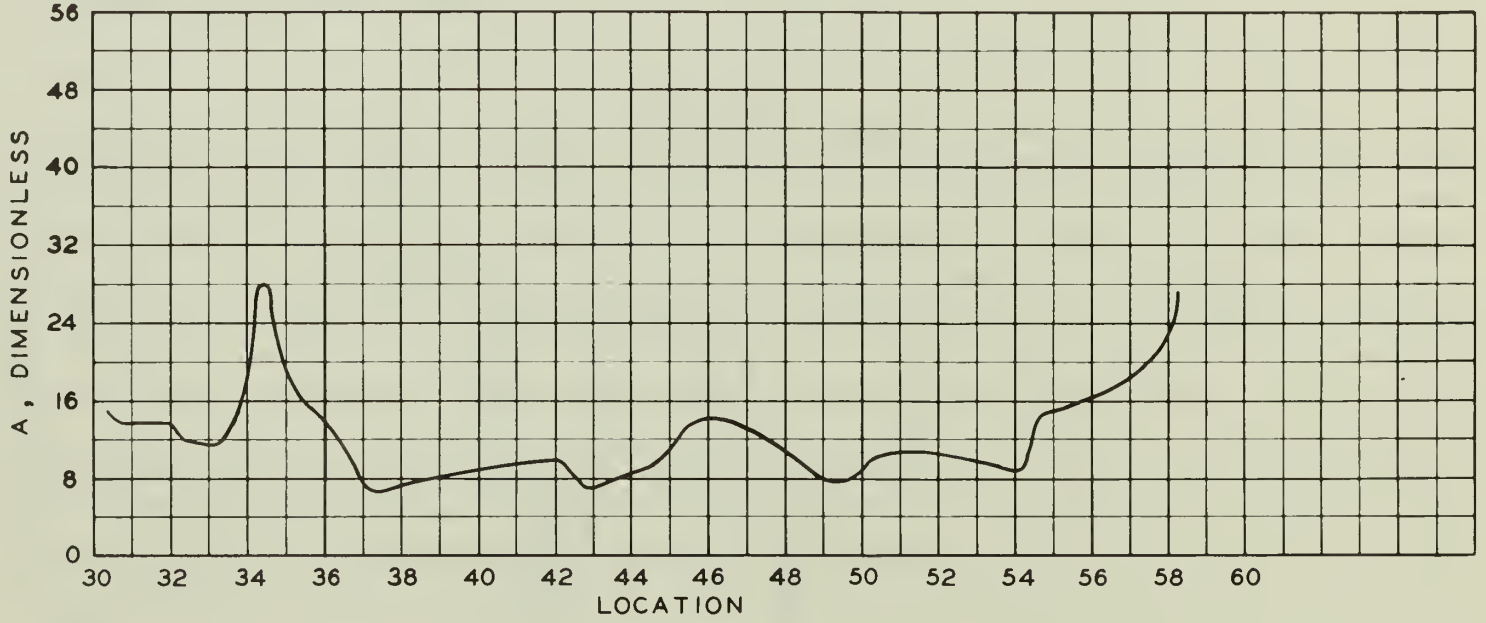

NOTE: LOCATIONS SHOWN
IN PLATE 5

COEFFICIENT A VS LOCATION

KAUAI

LOCATIONS 31-58

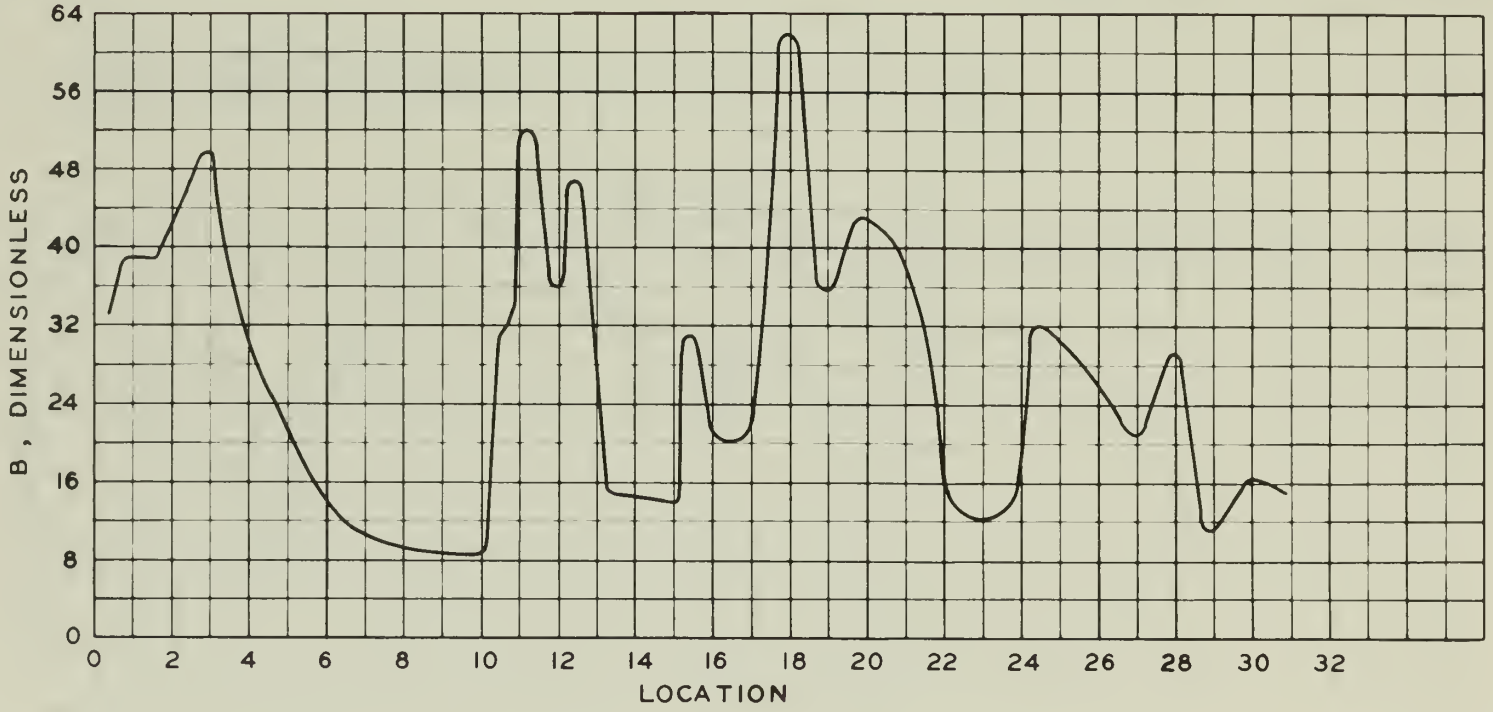

NOTE: LOCATIONS SHOWN
IN PLATE 5

COEFFICIENT B VS LOCATION

KAUAI
LOCATIONS 1 - 30

PLATE 35

PLATE 36

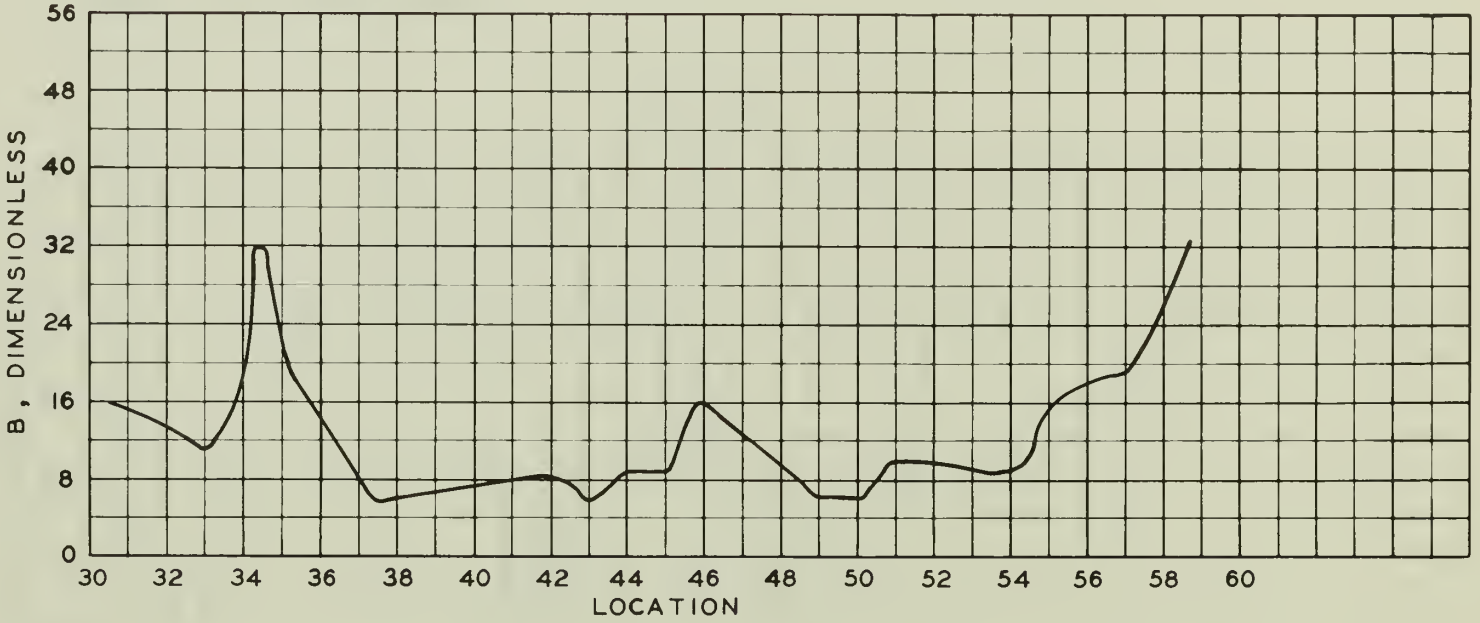

NOTE: LOCATIONS SHOWN
IN PLATE 5

COEFFICIENT B VS LOCATION

KAUAI
LOCATIONS 31-58

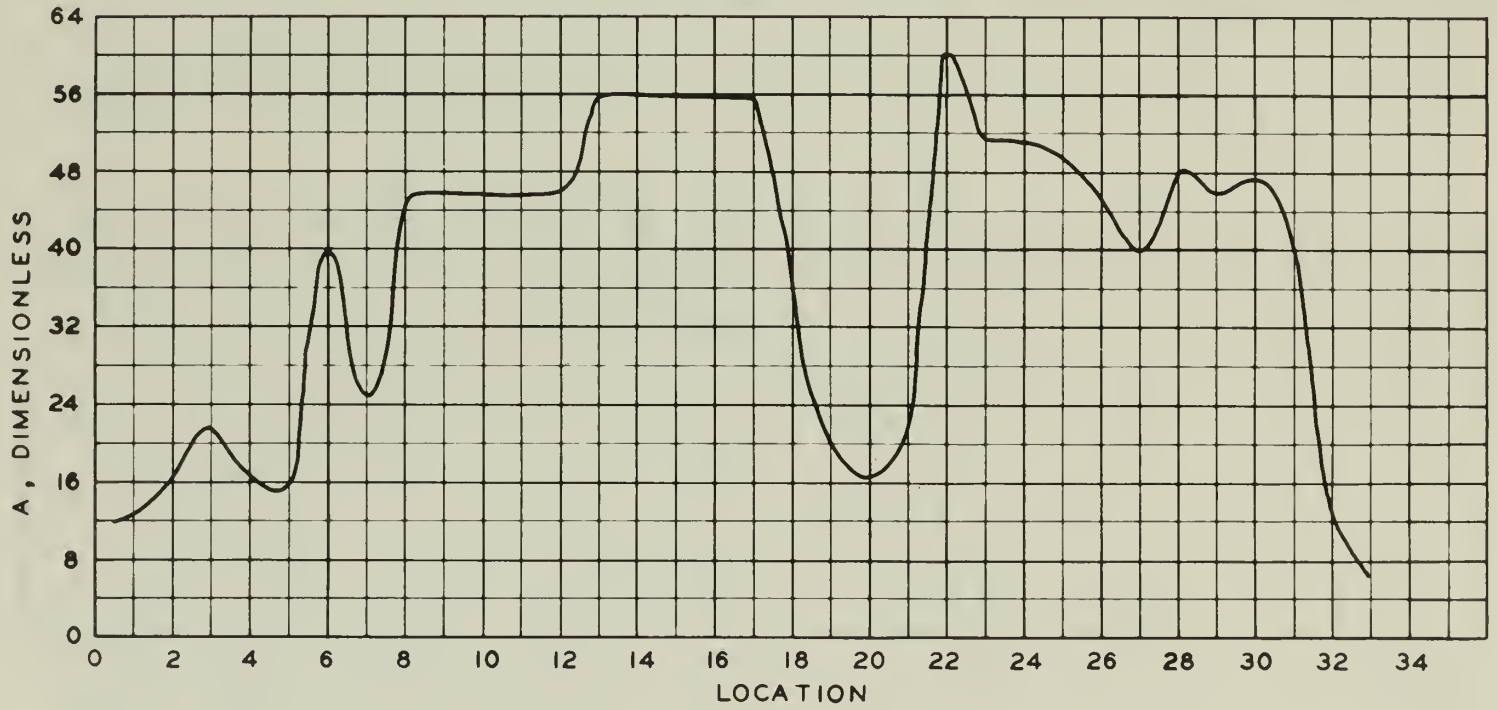

NOTE: LOCATIONS SHOWN
IN PLATE 6

COEFFICIENT A VS LOCATION

MOLOKAI
LOCATIONS 1 - 32

PLATE 37

PLATE 38

NOTE: LOCATIONS SHOWN
IN PLATE 6

COEFFICIENT A VS LOCATION

MOLOKAI
LOCATIONS 33-55

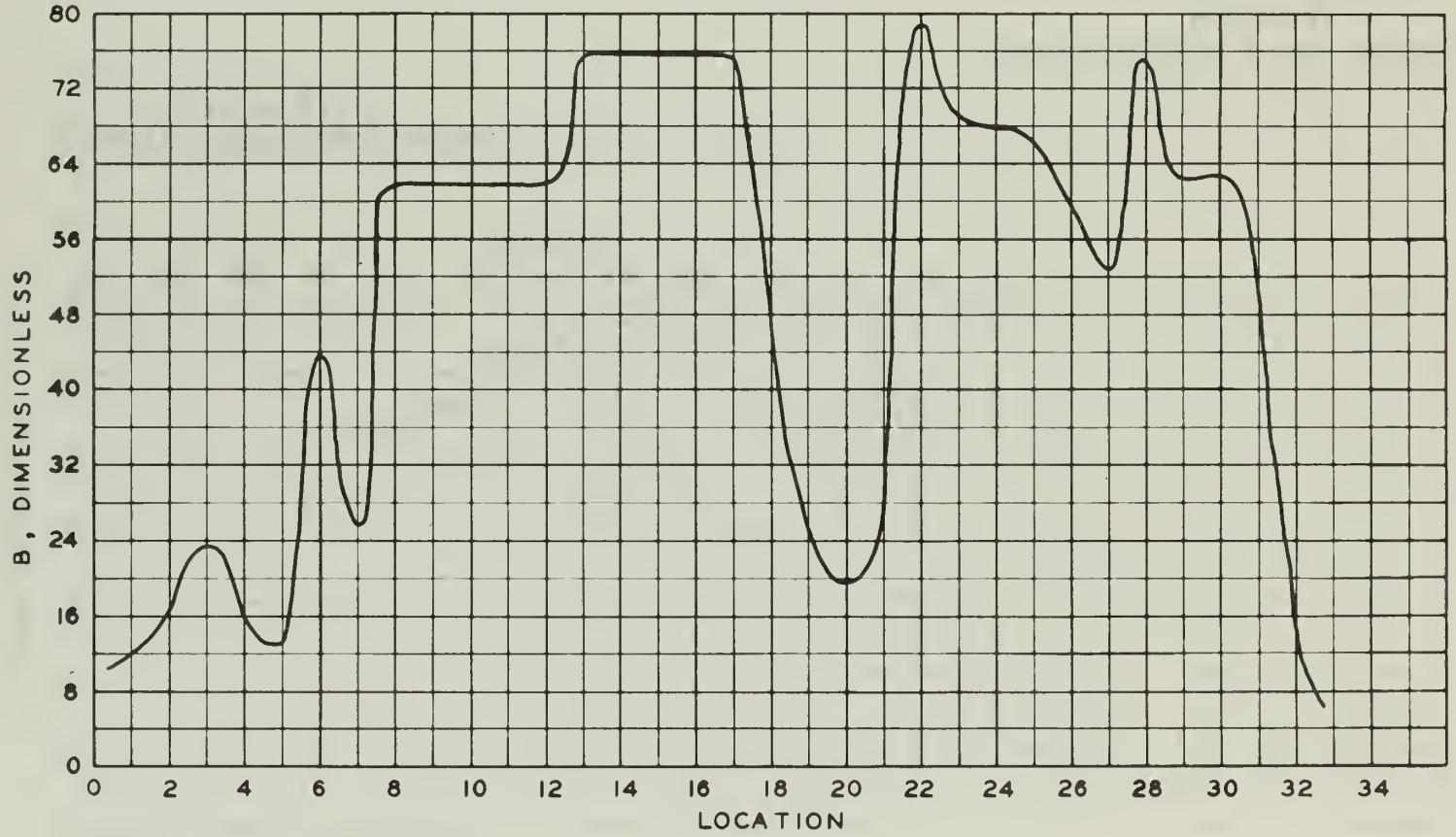

NOTE: LOCATIONS SHOWN IN PLATE 6

COEFFICIENT B VS LOCATION

MOLOKAI
LOCATIONS 1 - 32

PLATE 39

PLATE 40

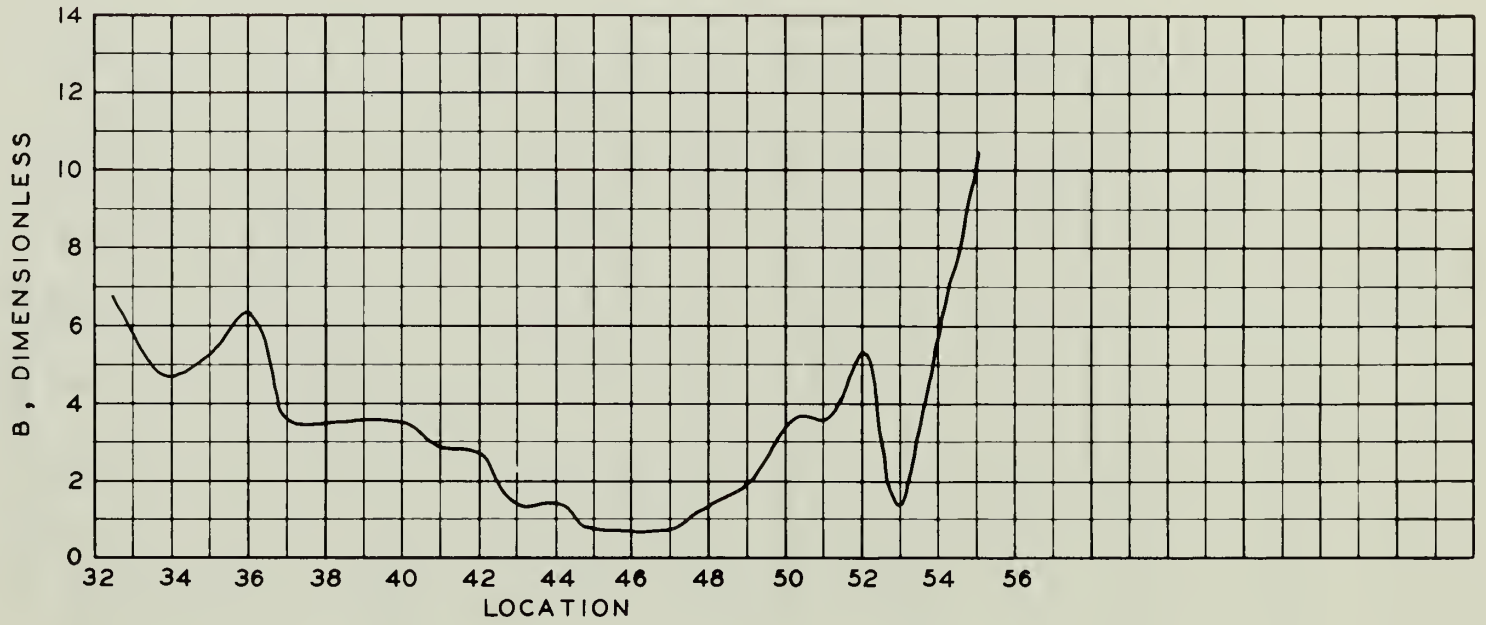

NOTE: LOCATIONS SHOWN
IN PLATE 6

COEFFICIENT B VS LOCATION
MOLOKAI
LOCATIONS 33-55

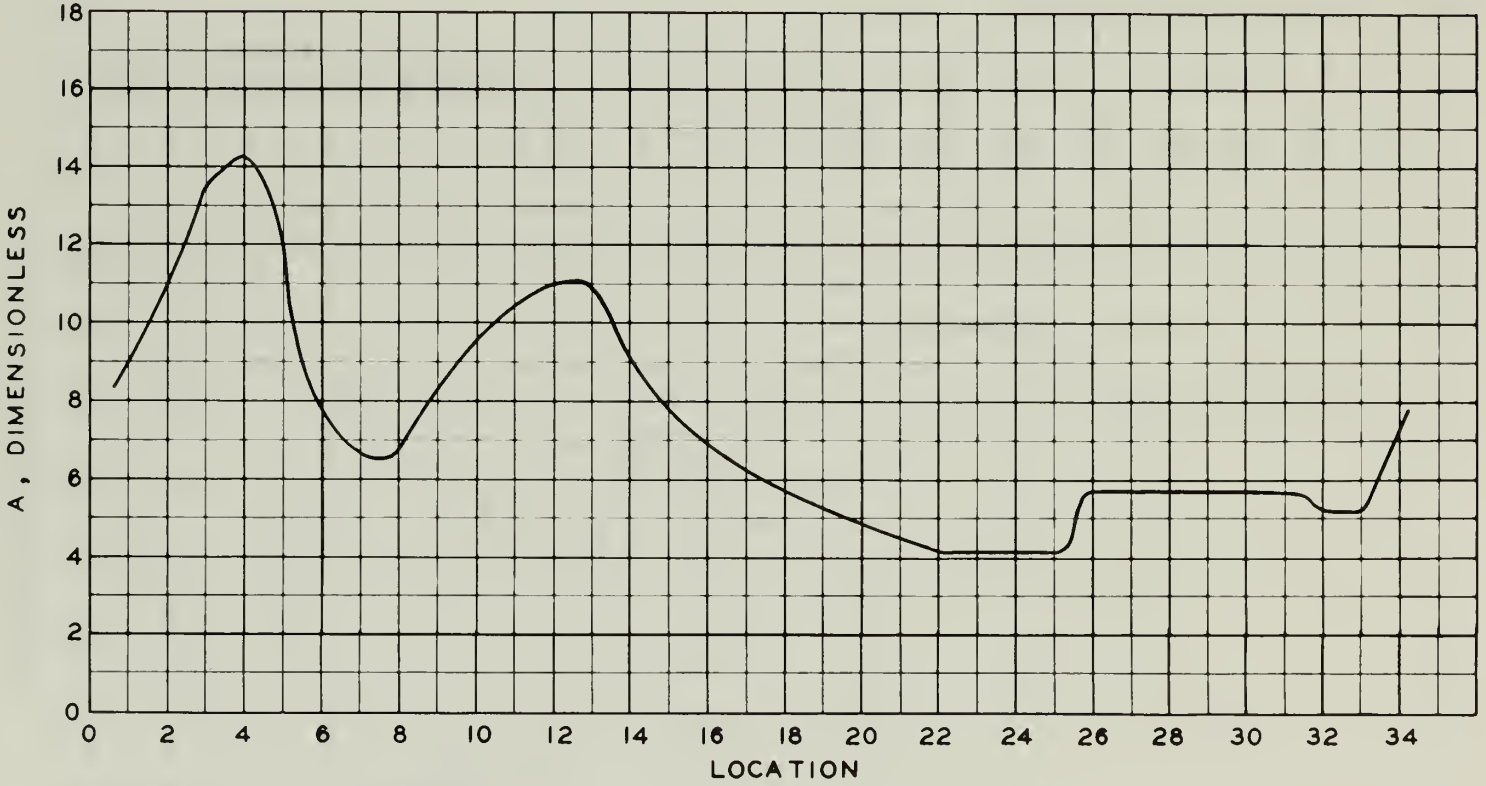

NOTE: LOCATIONS SHOWN IN PLATE 7

COEFFICIENT A VS LOCATION

LANAI
LOCATIONS 1-34

PLATE 41

PLATE 42

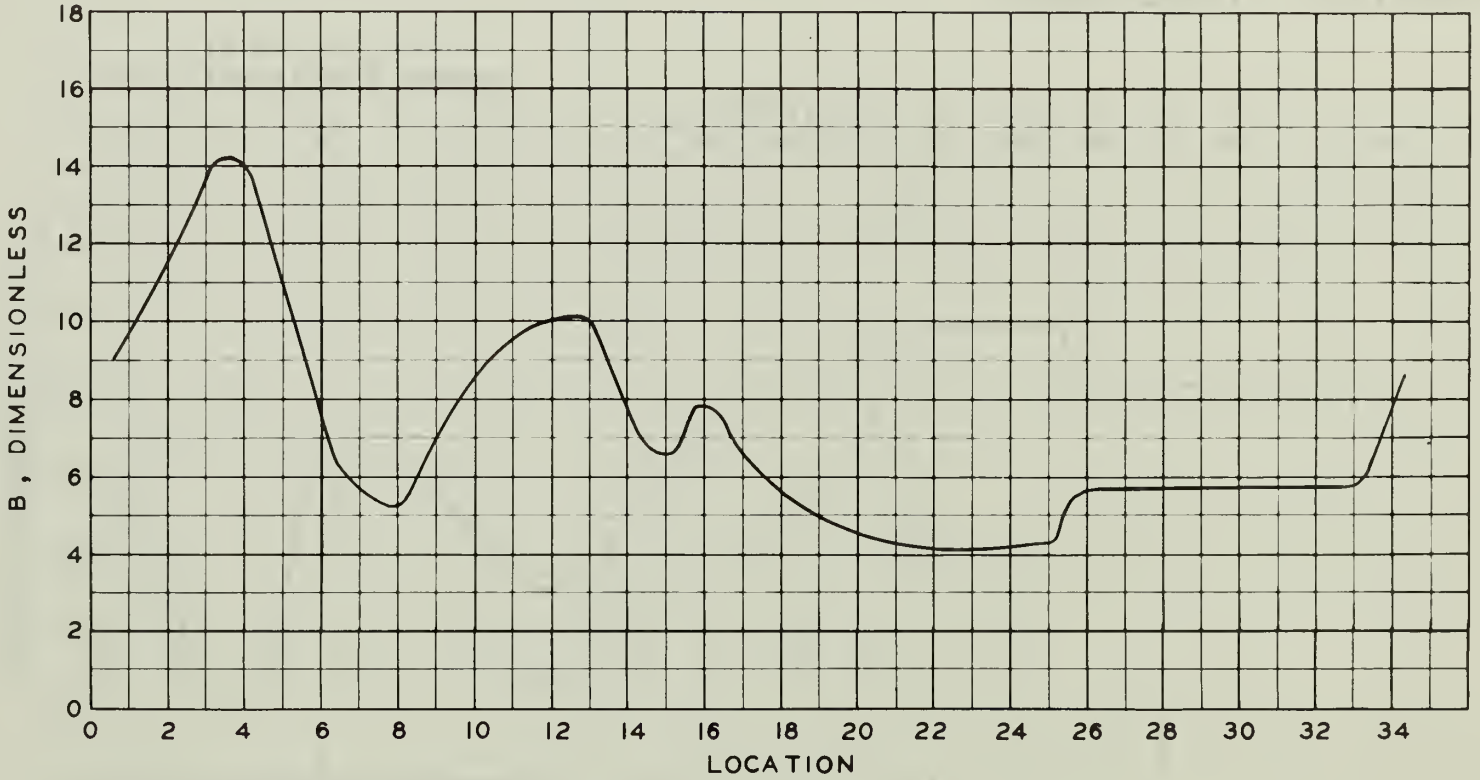

NOTE: LOCATIONS SHOWN IN PLATE 7

COEFFICIENT B VS LOCATION

LANAI

LOCATIONS 1 - 34

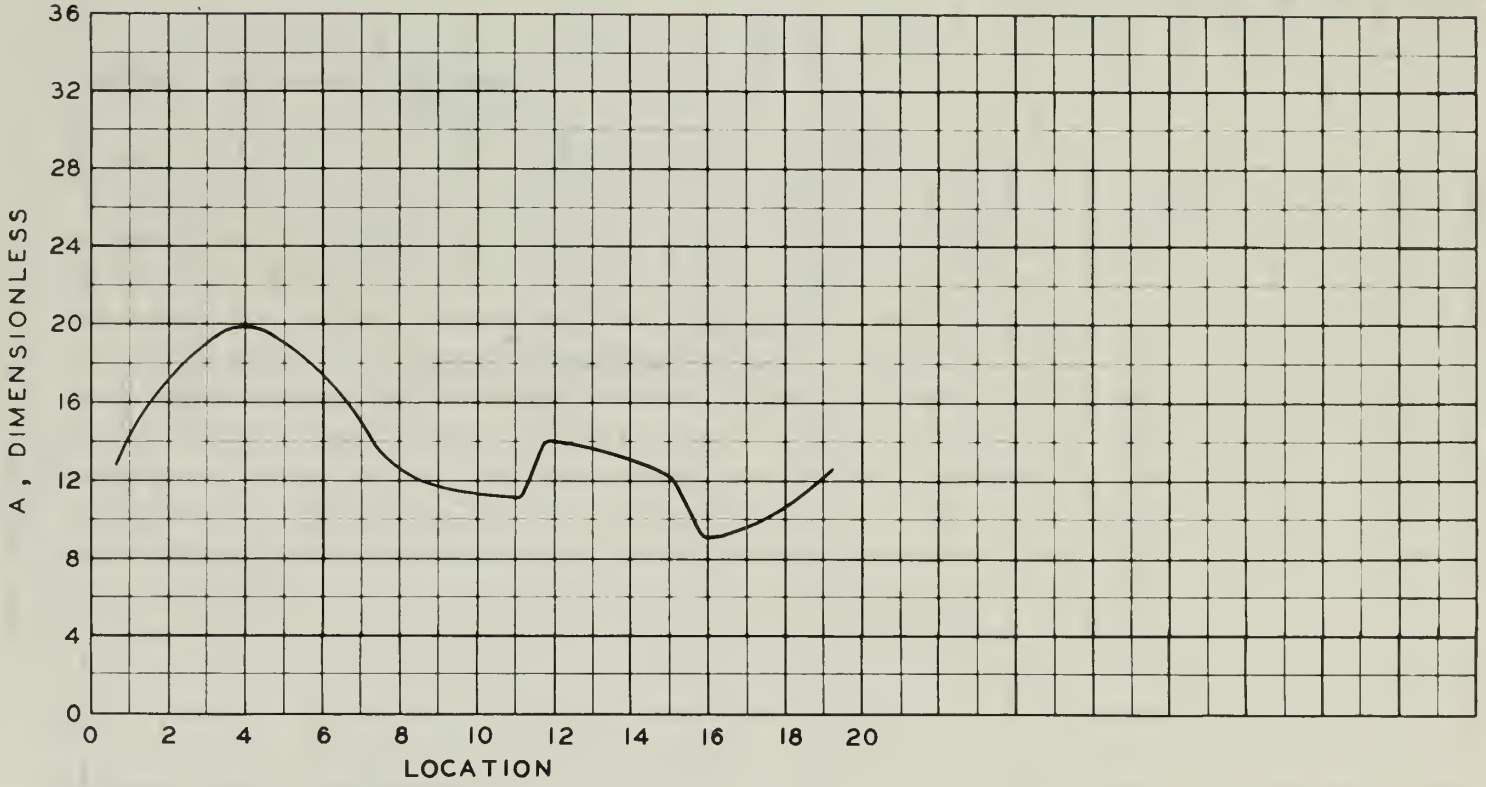

NOTE: LOCATIONS SHOWN IN PLATE 8

COEFFICIENT A VS LOCATION

NIIHAU

LOCATIONS 1 - 19

PLATE 43

PLATE 44

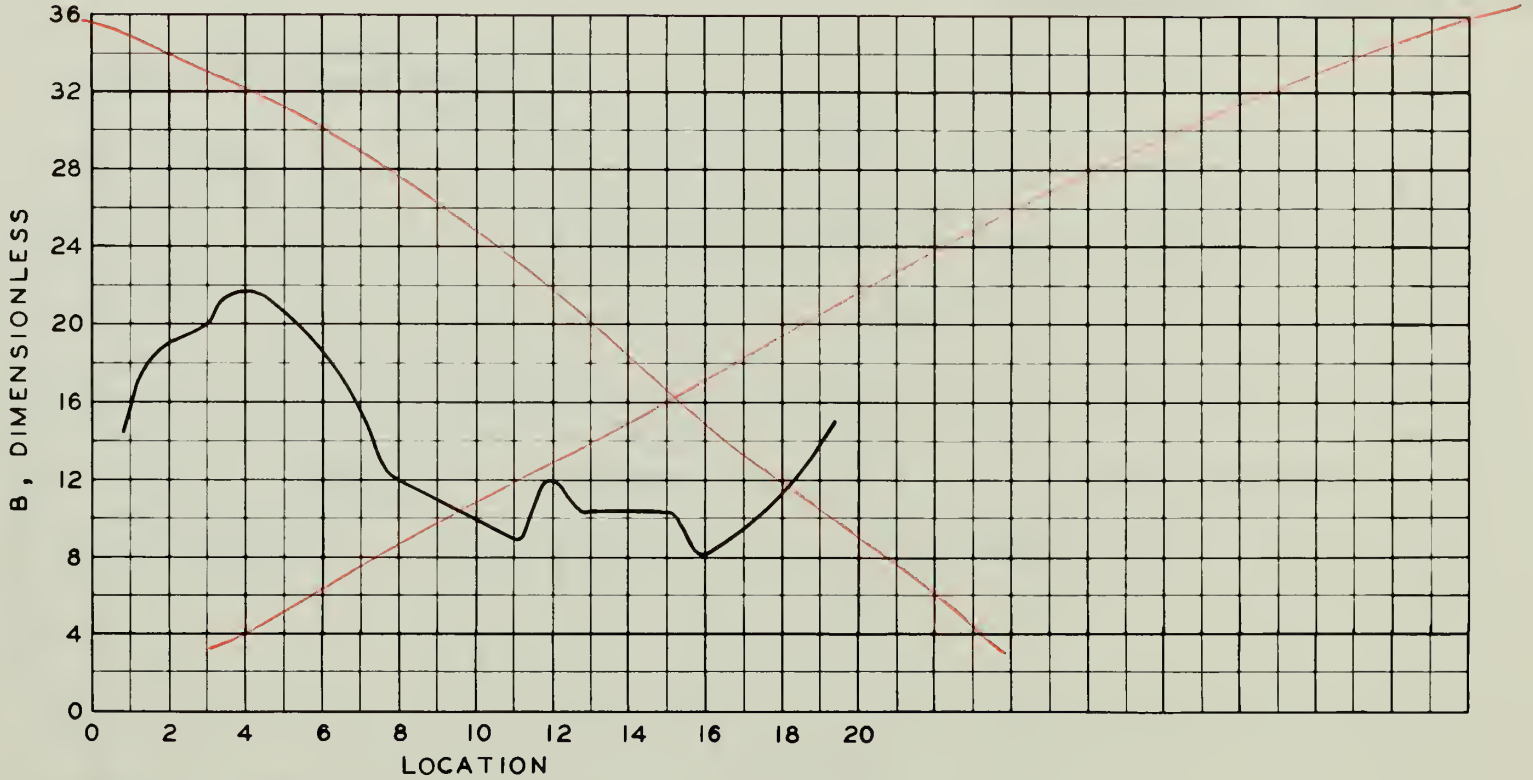

NOTE: LOCATIONS SHOWN IN PLATE 8

COEFFICIENT B VS LOCATION

NIIHAU

LOCATIONS 1 - 19

APPENDIX A: NOTATION

a	Boundary of region
a_o	Radius of vertical circular cylinder
A	Coefficient in wave height equation
$b(\omega)$	Amplitude of frequency component ω
b_o	Incident wave amplitude
B	Coefficient in wave height equation
d	Water depth, ft
D	Number of years
F	Frequency per year of tsunami occurrence
g	Acceleration due to gravity, 32.2 ft/sec^2
h	Elevation of the maximum tsunami wave crest above mean sea level at the shoreline
H_n	Hankel function of the first kind of order n
i	$\sqrt{-1}$
k	Wave number
m	Number of components
n	Integer
n_a	Unit normal vector outward from region R
P	Probability
r	Spherical coordinate, ft
R	Region containing the islands
R_e	Real number
t	Time, sec
x	Cartesian coordinate, ft
y	Cartesian coordinate, ft
α_n	Unknown coefficient
β_n	Unknown coefficient
η	Wave amplitude
Θ	Spherical coordinate, radian
ξ	Response of harbor
$\rho(\omega)$	Phase angle
ϕ	Total velocity potential, ft^2/sec

ϕ_a	Total velocity potential evaluated on boundary a , ft^2/sec
ϕ_I	Velocity potential of incident wave, ft^2/sec
ϕ_R	Far-field velocity potential, ft^2/sec
ω	Angular frequency, radians/sec
∇	Gradient operator, ft^{-1}
§	Line integral

In accordance with letter from DAEN-RDC, DAEN-ASI dated 22 July 1977, Subject: Facsimile Catalog Cards for Laboratory Technical Publications, a facsimile catalog card in Library of Congress MARC format is reproduced below.

Houston, James R
Tsunami-wave elevation frequency of occurrence for the Hawaiian Islands / by James R. Houston, Robert D. Carver, Dennis G. Markle. Vicksburg, Miss. : U. S. Waterways Experiment Station, 1977.
62, [1] , 2 p., 44 leaves of plates : ill. ; 27 cm.
(Technical report - U. S. Army Engineer Waterways Experiment Station ; H-77-16)
Prepared for U. S. Army Engineer Division, Pacific Ocean, San Francisco, California.
References: p. 60-62.

1. Finite element method. 2. Flood frequencies. 3. Hawaiian Islands. 4. Mathematical models. 5. Tsunamis. I. Carver, Robert D., joint author. II. Markle, Dennis G., joint author. III. United States. Army. Corps of Engineers. Pacific Ocean Division. IV. Series: United States. Waterways Experiment Station, Vicksburg, Miss. Technical report ; H-77-16.
TA7.W34 no.H-77-16